Chapter 1

Introduction

Lorenz studied the strange changes in the atmosphere which is the first example to study chaos in 1963. In the past four decades, a large number of studies have shown that chaotic phenomena are observed in many physical systems that possess non-linearity [1, 2]. It was also reported that the chaotic motion occurred in many non-linear control systems [3].

Chaos and chaotic systems have received a flurry of research effort in the past few decades. Such systems are nonlinear by nature, can occur in various natural and man-made systems, and are characterized by great sensitivity to initial conditions [4]. Besides the theoretical interest in the analysis of such nonlinear systems, there is another dimension to that interest; namely, utilizing such systems for useful practical applications [5-12]. Many researchers have devoted themselves to finding new ways to control chaos more efficiently [13-16]. Chaotic phenomena are quite useful in many applications such as fluid mixing [17], human brain dynamics [18], and heart beat regulation [19], information processing, etc. Therefore, making a periodic dynamical system chaotic, or preserving chaos of a chaotic dynamical system, is very meaningful and worthy to be investigated [20, 21].

Fractional calculus is a 300-year-old mathematical topic [22-25]. Although it has a long history, for many years it was not used in physics and engineering. However, during the last 10 years or so, fractional calculus starts to attract increasing attention of physicists and engineers from an application point of view [26, 27]. It was found that many systems in interdisciplinary fields can be elegantly described with the help of fractional derivatives. Many systems are known to display fractional-order dynamics, such as viscoelastic systems [28], dielectric polarization [29],

electrode–electrolyte polarization [30], electromagnetic waves [31], quantitative finance [32], and quantum evolution of complex systems [33].

It is well known that chaos cannot occur in autonomous continuous time systems of integer-order less than three according to the Poincare–Bendixon theorem [34, 35]. A recent example of a continuous time third order system that exhibits chaos is the Chen system [36]. The order of a system can be defined as the sum of the orders of all involved derivatives. However, in autonomous fractional order systems, it is not the case. For example, it has been shown that the fractional order Chua's circuit with an appropriate cubic nonlinearity and with order as low as 2.7 can produce a chaotic attractor [37]. In [38, 39], the bifurcation and the chaotic dynamics of fractional order cellular neural networks are studied. In [40], chaotic behaviors of a fractional order ''jerk'' model is studied, in which a chaotic attractor can be generated with the system order as low as 2.1 and a conjecture is presented that third order chaotic systems can still produce chaotic behavior with a total system order of $2 + e$, $0 < e < 1$. In [41], chaotic behavior of the fractional order Lorenz system is studied, but unfortunately, the results presented in this thesis are not correct as pointed out by [42]. Also in [42], chaos and hyperchaos in fractional order Rössler equations are discussed, in which it is shown that chaos can exist in the fractional order Rössler equation with order as low as 2.4, and hyperchaos can also exist in the fractional order Rössler hyperchaotic system with order as low as 3.8. In [43-46], chaotic behaviors in the fractional order Chen system are studied and the lowest order to have chaos in this fractional order Chen system is shown to be 2.1 and 2.92, respectively.

Chaos synchronization [47-55] is a very important topic in the nonlinear [56-58] science and it has been developed extensively. Recently many scientists in various fields have been attracted to investigate chaos synchronization due to its application in a variety of fields including secure communications, chemical, physical, and

biological systems, neural networks and so on. So various synchronization schemes, such as variable structure control [59], parameters adaptive control [60-67], observer based control [68, 69], active control [70-76], nonlinear control [77, 78], anti-control [79-85] and so on, have been successfully applied to the chaos synchronization.

Furthermore, the problem of anti-controlling chaos (from periodic to chaotic) is interesting, non-traditional, and indeed very challenging. More importantly, within the biological context, anti-control of chaos suggests great potential for future applications. Recently, there have been many successful thesiss towards the goal of anti-control, which are essentially experimental or semi-analytical [86]. Sometimes chaotic behavior and chaos synchronization are beneficial and desirable in many applications. For example, chaos is important in secure communication, information processing, liquid mixing, biological systems, etc. [87–89]. For this purpose, making a nonchaotic dynamical system chaotic or retaining (or enhancing) the chaos of a chaotic system is called "anti-control of chaos or chaotification [90, 91]". Therefore, the anti-control of chaos is meaningful topic and worth to be investigated.

Mechanical resonance is widely applied in high-precision oscillators for a multitude of time-keeping and frequency reference applications. The extraordinary small size and high level of integration that can be achieved with nano resonators appear to open exceptional possibilities for creating miniature-scale precision oscillators to be used in e.g. mobile communication and navigation devices.

The chaos, chaos synchronization and anti-control of integral and fractional order nano parameter resonator system are studied in this thesis. Linear approximation of a fractional order integrator to analyze nano parameter resonator system can be obtained by utilizing frequency domain techniques based in Bode diagrams. By applying numerical analyses such as phase portraits, Poincaré maps and bifurcation diagrams, the periodic and chaotic motions are observed. The chaos synchronizations

of two uncoupled integral and fractional order identical chaotic nano resonator systems are obtained by replacing their corresponding parameters by the same function of chaotic state variables of a third identical chaotic system. Anti-control of chaos are obtained by addition of an external constant term or nonlinear term. Replacing a system parameter by a function of chaotic state variables of a modified van der Pol system, we can obtain anti-control of chaos.

This thesis is organized as follows. In Chapter 2, a method for the approximation of the fractional derivative is given. The nano resonator system and its fractional order form are presented. Numerical simulations, phase portraits, Poincaré maps and bifurcation diagrams, for various different fractional order nano resonator systems are studied. In Chapter 3, numerical simulations for integral and fractional order nano resonator systems based on driving the corresponding parameters of two chaotic systems by a chaotic signal of a third system are given for order 1 ~ 0.1. In Chapter 4, anticontrols of chaos are obtained by addition of a constant term and by adition of a nonlinear term. In Chapter 5, anticontrols of chaos are obtained by replacing a system parameter by a function of a state variable of modified van der Pol system. Anticontrol of chaos can be successfully obtained for total order 1.8 ~ 0.2. In Chapter 6, conclusions are drawn.

Chapter 2

Chaos in a Nonlinear Damped Mathieu System, in a Nano Resonator System and in Its Fractional Order Systems

In this Chapter, the chaotic behaviors of a nonlinear nano resonator system with integral orders and with fractional orders are studied. By applying numerical analyses such as phase portraits, Poincaré maps and bifurcation diagrams, the periodic and chaotic motions are observed. It is found that chaos exists both in the integral order and in the fractional order nano resonator systems.

2.1 Method for the approximation of the fractional derivative

The idea of fractional integrals and derivatives has been known since the development of the regular calculus, with the first reference probably being associated with Leibniz in 1695 [92].

Two commonly used definitions for the general fractional differintegral are the Grunwald definition and the Riemann-Liouville definition. The latter is given here

$$\frac{d^q f(t)}{dt^q} = \frac{1}{\Gamma(n-q)} \frac{d^n}{dt^n} \int_0^t \frac{f(\tau)}{(t-\tau)^{q-n+1}} d\tau \tag{2.1}$$

where $n-1 \leq q < n$ and $\Gamma(\cdot)$ is an Euler's gamma function.

The Laplace transformation of the Riemann-Liouville fractional derivative (1) is

$$L\left\{\frac{d^q f(t)}{dt^q}\right\} = s^q L\{f(t)\} - \sum_{k=0}^{n-1} s^k \left[\frac{d^{q-1-k} f(t)}{dt^{q-1-k}}\right]_{t=0}, \text{ for } n-1 \leq q < n \tag{2.2}$$

By considering the initial conditions to be zero, this formula reduces to the more expected and comforting form

$$L\left\{\frac{d^q f(t)}{dt^q}\right\} = s^q L\{f(t)\} \tag{2.3}$$

and the fractional integral of order q can be described as $F(s) = \dfrac{1}{s^q}$ in the frequency domain.

The standard definitions of the fractional differintegral do not allow direct implementation of the operator in time domain simulations of complicated systems with fractional elements. Using the standard integer order operators to approximate the fractional operators is an effective method to analyze such systems.

The approximation approach taken here is to approximate the system behavior in the frequency domain [93]. By utilizing frequency domain techniques based in Bode diagrams, one can obtain a linear approximation of a fractional order integrator. Thus an approximation of any desired accuracy over any frequency band can be achieved.

Table in Appendix from Ref. [94] gives approximations for $\dfrac{1}{s^q}$ with $q = 0.1 \sim 0.9$ in steps of 0.1 with errors of approximately 2 dB from $\omega = 10^{-2}$ to 10^2 rad/s. These approximations will be used in the following numerical simulations.

2.2 The Chaos of the Nonlinear Damped Mathieu System and of the Nano Resonator System with Its Fractional Order Form

Mechanical resonance is widely applied in high-precision oscillators for a multitude of time-keeping and frequency reference applications. In all such cases, the high-precision resonating element consists of an off-chip passive component, such as a quartz crystal. Major drawback of these off-chip resonator technologies is that they are bulky and must interface with transistor chips at the boards, posing a bottleneck against the ultimate miniaturization of e.g. wireless devices. The extraordinary small size and high level of integration that can be achieved with nano resonators appear to

open exceptional possibilities for creating miniature-scale precision oscillators to be used in e.g. mobile communication and navigation devices.

Nano resonator system studied in this thesis is a modified form of nonlinear damped Mathieu system which is obtained when the nano Mathieu oscillator has nonlinear time-dependent spring constant [91]. The nonlinear damped Mathieu system is a nonautonomous system with two states x and y:

$$\begin{cases} \dfrac{dx}{dt} = y \\ \dfrac{dy}{dt} = -(a + b\sin\omega_1 t)x - (a + b\sin\omega_1 t)x^3 - cy + d\sin\omega_2 t \end{cases} \tag{2.4}$$

where a, b, c, d are constant parameters, and ω_1, ω_2 are circular frequencies. The phase portraits, Poincaré maps, bifurcation diagram and the Lyapunov exponent for system (2.4) are showed in Fig. 2.1 where $a = 0.2$, $b = 0.2$, $c = 0.4$, $\omega_1 = \omega_2 = \omega = 1$. Let $\omega_1 = \omega_2 = \omega$, and replace $\sin\omega t$ by z which is the periodic time function solution of the nonlinear oscillator

$$\begin{cases} \dfrac{dz}{dt} = w \\ \dfrac{dw}{dt} = -ez - fz^3 \end{cases} \tag{2.5}$$

where e, f are constant parameters. Then we have the modified nonlinear damped Mathieu system, i.e. the nano resonator system:

$$\begin{cases} \dfrac{dx}{dt} = y \\ \dfrac{dy}{dt} = -(a + bz)x - (a + bz)x^3 - cy + dz \\ \dfrac{dz}{dt} = w \\ \dfrac{dw}{dt} = -ez - fz^3 \end{cases} \tag{2.6}$$

It becomes an autonomous system with four states where a, b, c, d, e and f are constant parameters of the system. System (2.4) consists of two parts:

$$\begin{cases} \dfrac{dx}{dt} = y \\ \dfrac{dy}{dt} = -(a+bz)x - (a+bz)x^3 - cy + dz \end{cases} \qquad (2.7)$$

and

$$\begin{cases} \dfrac{dz}{dt} = w \\ \dfrac{dw}{dt} = -ez - fz^3 \end{cases} \qquad (2.8)$$

Eq. (2.8) affords the periodic time function solution to system (2.7) as an excitation which induces the chaos in system (2.7). As a result, Eq. (2.7) can be considered as a nonautonomous system with two states, while Eq. (2.7) and Eq. (2.8) together can be considered as an autonomous system with four states. Our main interest devotes to Eq. (2.6), while Eq. (2.8) remains an integral order system. The phase portraits, Poincaré maps, bifurcation diagram and the Lyapunov exponent for (2.6) are showed in Fig. 2.2. The corresponding modified nonlinear fractional order damped Mathieu system, the fractional order nano resonator system, is:

$$\begin{cases} \dfrac{d^\alpha x_1}{dt^\alpha} = y_1 \\ \dfrac{d^\beta y_1}{dt^\beta} = -(a+bz_1)x_1 - (a+bz_1)x_1^3 - cy_1 + dz_1 \\ \dfrac{dz_1}{dt} = w_1 \\ \dfrac{dw_1}{dt} = -ez_1 - fz_1 \end{cases} \qquad (2.9)$$

where α and β are the fractional orders.

2.3 Numerical Simulations for the Integral and Fractional Order Systems

We vary the derivative orders α, β and the system parameter d, the other system parameters are fixed. Simulations are performed under $\alpha + \beta = 2$,
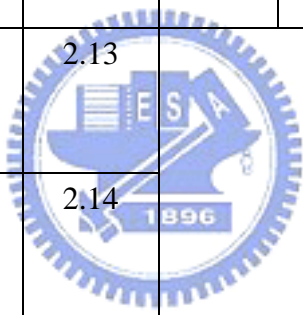
$\alpha + \beta = 1.9$ where α, β are not integers. In our numerical simulations, five parameters $a = 0.2$, $b = 0.2$, $c = 0.4$, $e = 1$ and $f = 0.3$ are fixed and d is varied. The initial states of the nano resonator system are $x(0) = 3$, $y(0) = 4$, $z(0) = 1$ and $w(0) = 0$. The numerical simulations are carried out by MATLAB, and are summarized in Table 1..

The phase portraits, Poincaré maps and the bifurcation diagrams of Case 1, 2, 3, 4, 10, 11, 12, 13, 15, 16, 17, 18, 19, 23, 25, 31, 33 and 34 for nano resonator system are showed in Fig. 2.3, 2.4, 2.5, 2.6, 2.10, 2.7, 2.8, 2.9, 2.11, 2.12, 2.13, 2.14, 2.2, 2.16, 2.17, 2.18, 2.19 and 2.15 respectively. Case 1, 2, 3 and 19 have similar shapes in their phase portraits and Poincaré maps, chaos in Case 3 is only distributed over the parameter $d = 40\sim50$, relatively, chaos in Case 1, 2 and 19 are distributed more wide than that of Case 3. Case 4, 23 and 25 have similar shapes in their phase portraits. Case 11, 13, 15, 17 and 34 have similar shapes in their phase portraits. Case 17 has the largest range of y among case 11, 13, 15, 17 and 34, even beyond 3000, chaos in case 13 and 17 are distributed over all varied parameter region, but in case 15, chaos is distributed over about the parameter $d > 50$. Case 10, 12, 16, 18, 31 and 33 have similar shapes in their phase portraits.

The results from simulation verified that chaos indeed exists in the system with total fractional orders $\alpha + \beta = 2$ and $\alpha + \beta = 1.9$, which are summarized in Table 2.1.

Table 2.1 Relation between orders of derivatives and existence of chaos.

Total order 2				Total order 1.9			
Cases	Orders	Existence of chaos	Fig. No.	Cases	Orders	Existence of chaos	Fig. No.
1	$\alpha = 1.1$, $\beta = 0.9$	Yes	2.3	20	$\alpha = 1.1$, $\beta = 0.8$	No	
2	$\alpha = 0.9$, $\beta = 1.1$	Yes	2.4	21	$\alpha = 0.8$, $\beta = 1.1$	No	
3	$\alpha = 1.2$, $\beta = 0.8$	Yes	2.5	22	$\alpha = 1.2$, $\beta = 0.7$	No	
4	$\alpha = 0.8$, $\beta = 1.2$	Yes	2.6	23	$\alpha = 0.7$, $\beta = 1.2$	Yes	2.16
5	$\alpha = 1.3$, $\beta = 0.7$	No		24	$\alpha = 1.3$, $\beta = 0.6$	No	
6	$\alpha = 0.7$, $\beta = 1.3$	No		25	$\alpha = 0.6$, $\beta = 1.3$	Yes	2.17
7	$\alpha = 1.4$, $\beta = 0.6$	No		26	$\alpha = 1.4$, $\beta = 0.5$	No	
8	$\alpha = 0.6$, $\beta = 1.4$	No		27	$\alpha = 0.5$, $\beta = 1.4$	No	
9	$\alpha = 1.5$, $\beta = 0.5$	No		28	$\alpha = 1.5$, $\beta = 0.4$	No	
10	$\alpha = 0.5$, $\beta = 1.5$	Yes	2.10	29	$\alpha = 0.4$, $\beta = 1.5$	No	
11	$\alpha = 1.6$,	Yes	2.7	30	$\alpha = 1.6$,	No	

	$\beta = 0.4$				$\beta = 0.3$		
12	$\alpha = 0.4$, $\beta = 1.6$	Yes	2.8	31	$\alpha = 0.3$, $\beta = 1.6$	Yes	2.18
13	$\alpha = 1.7$, $\beta = 0.3$	Yes	2.9	32	$\alpha = 1.7$, $\beta = 0.2$	No	
14	$\alpha = 0.3$, $\beta = 1.7$	No		33	$\alpha = 0.2$, $\beta = 1.7$	Yes	2.19
15	$\alpha = 1.8$, $\beta = 0.2$	Yes	2.11	34	$\alpha = 1.8$, $\beta = 0.1$	Yes	2.15
16	$\alpha = 0.2$, $\beta = 1.8$	Yes	2.12	35	$\alpha = 0.1$, $\beta = 1.8$	No	
17	$\alpha = 1.9$, $\beta = 0.1$	Yes	2.13				
18	$\alpha = 0.1$, $\beta = 1.9$	Yes	2.14				
19	$\alpha = 1$, $\beta = 1$	Yes	2.2				
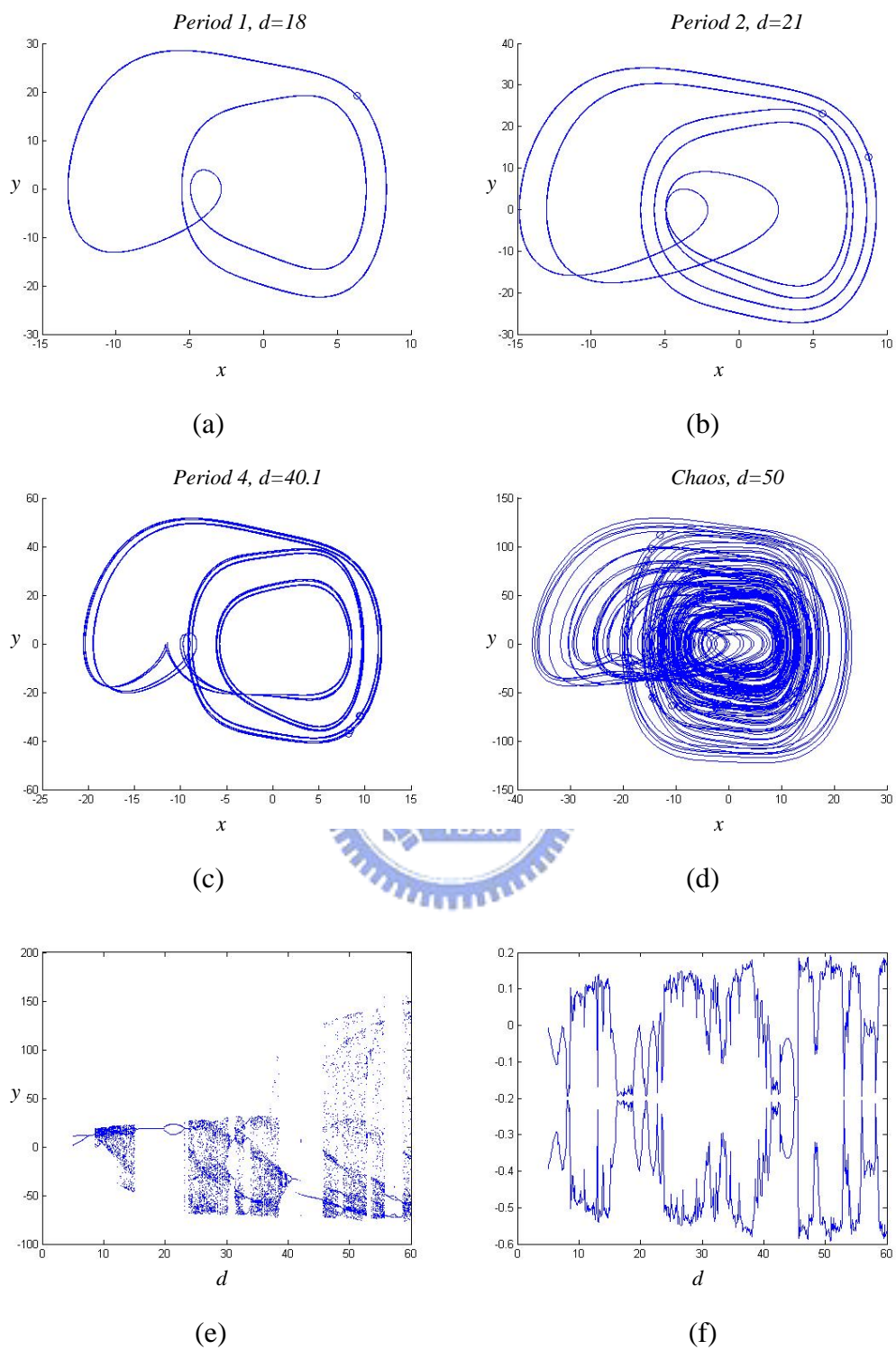
Fig. 2.1 The phase portraits, bifurcation diagram and the Lyapunov exponent for the

damped Mathieu system.
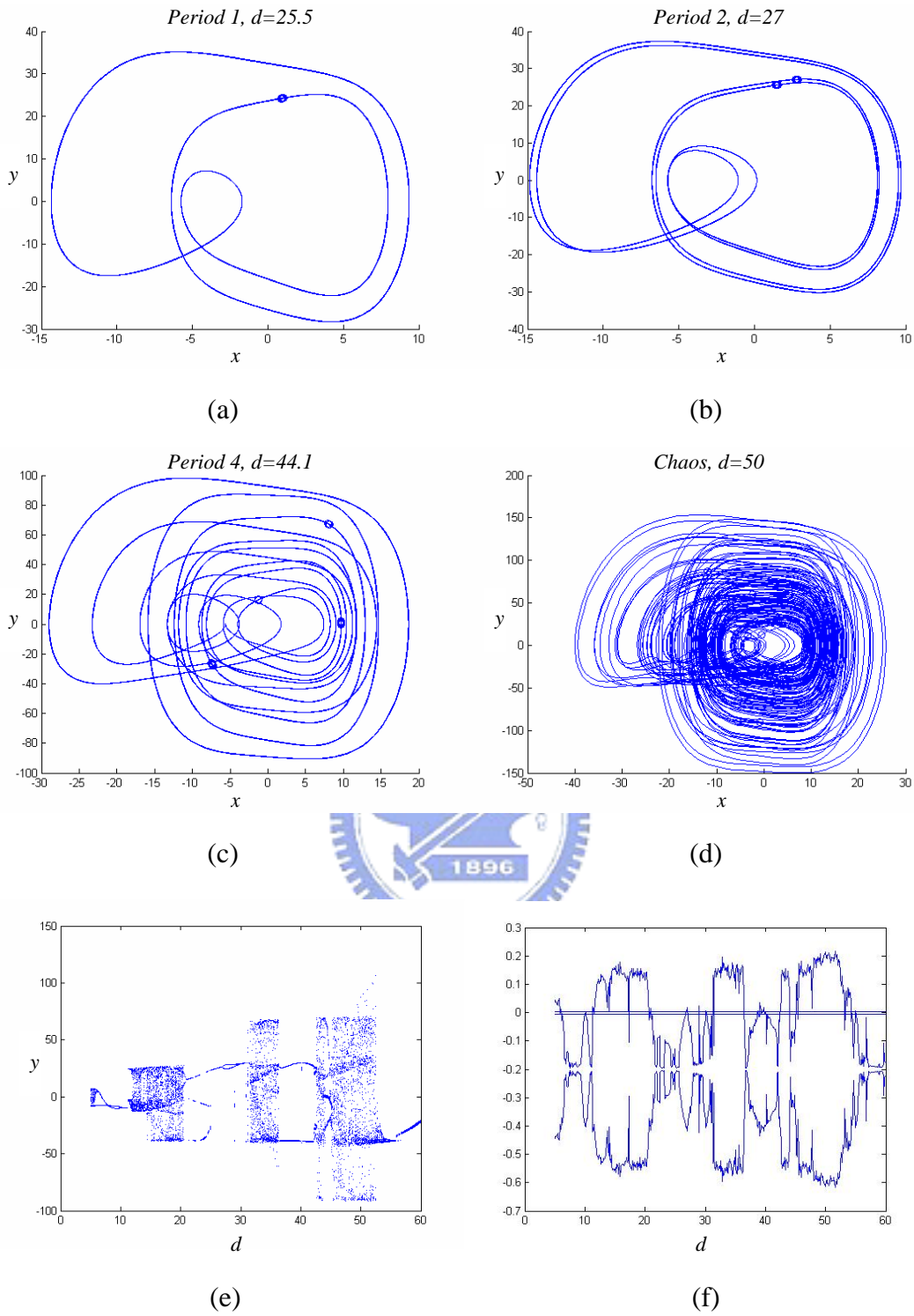
Fig. 2.2 The phase portraits, bifurcation diagram and the Lyapunov exponent for the

nano resonator system with order $\alpha = 1$ and $\beta = 1$.

(a)

(b)

(c)

(d)

(e)
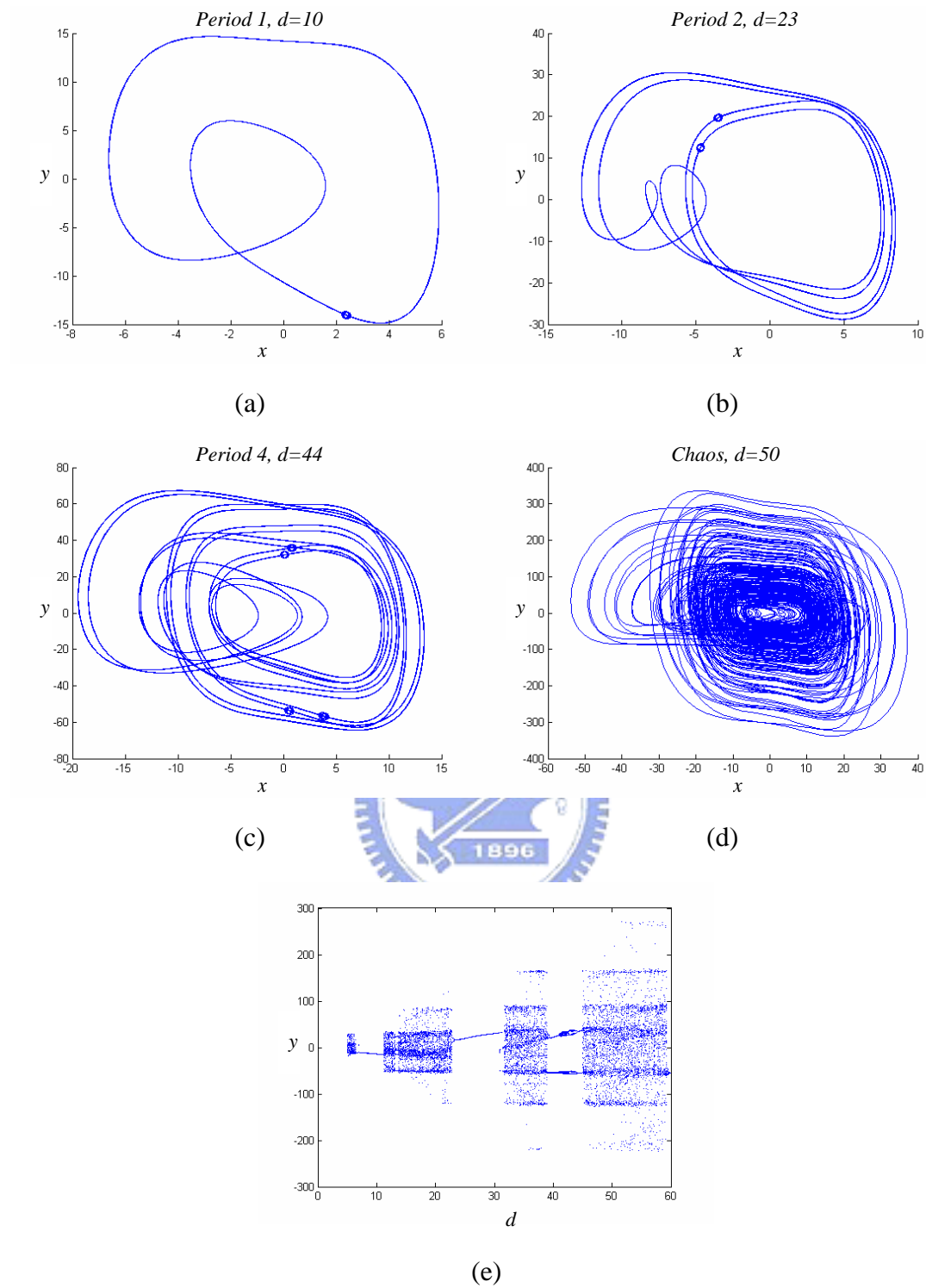
Fig. 2.3 The phase portraits and the bifurcation diagram for the nano resonator system
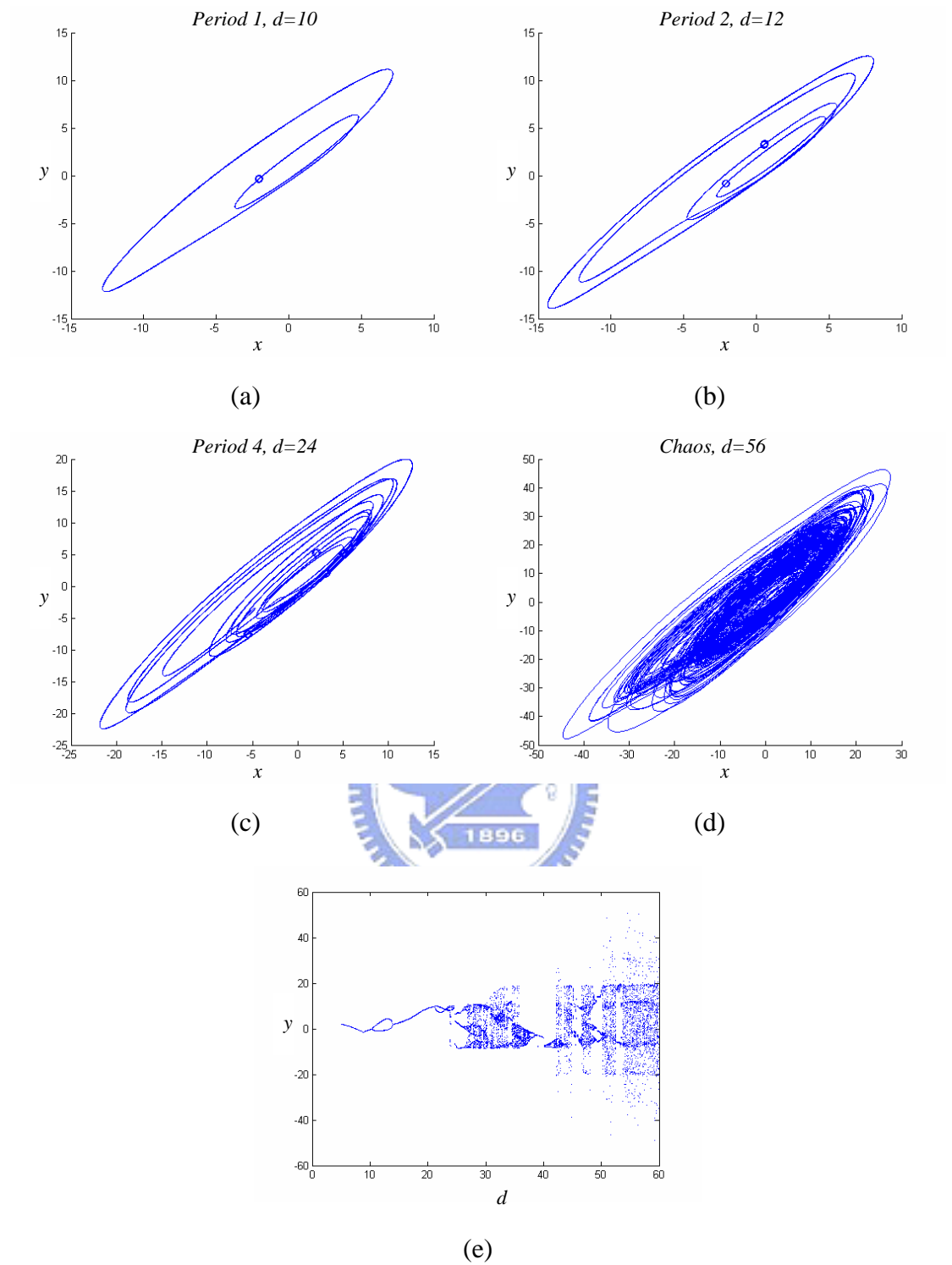
with order $\alpha = 1.1$ and $\beta = 0.9$.

14
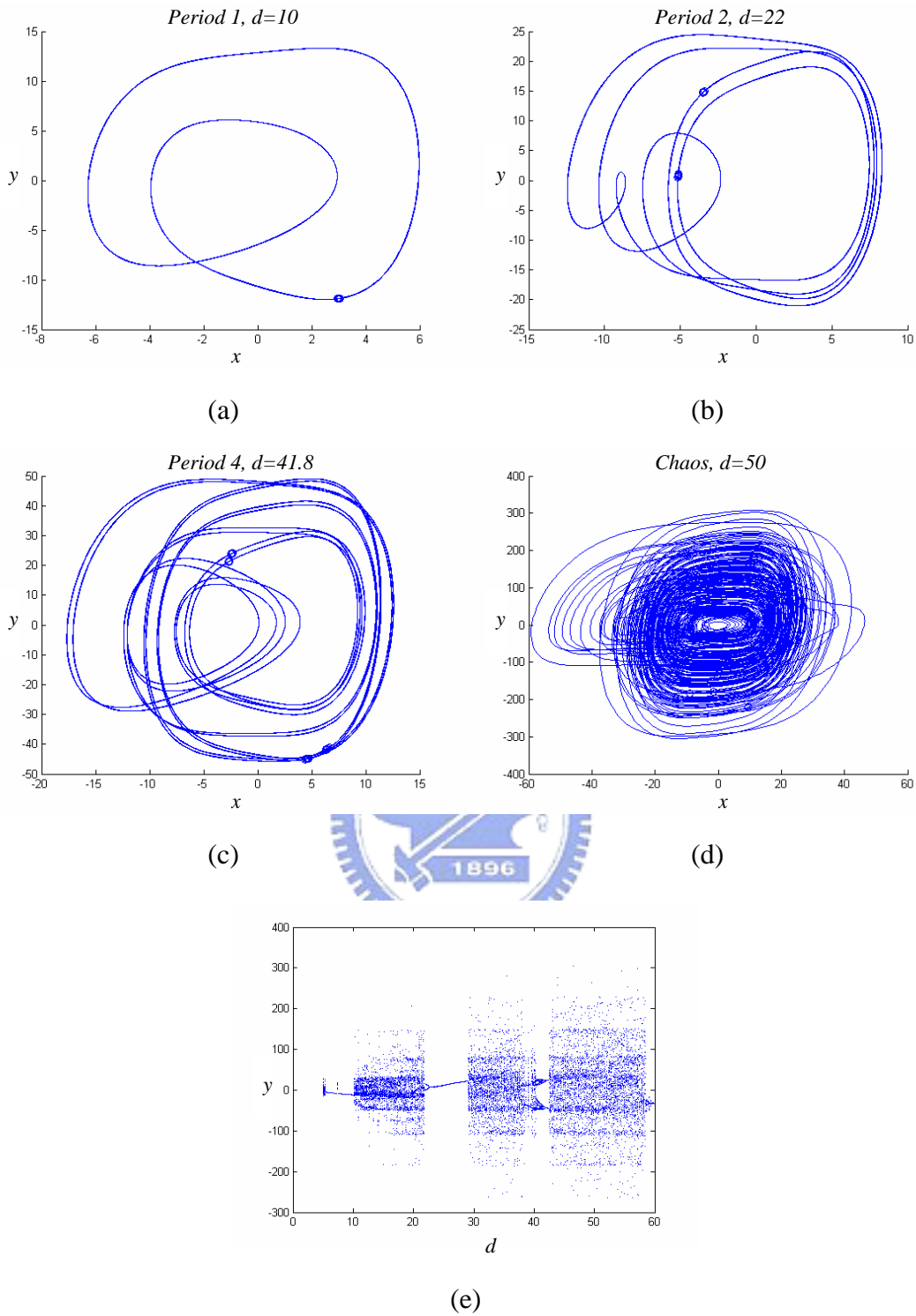
Fig. 2.4 The phase portraits and the bifurcation diagram for the nano resonator system

with order $\alpha = 0.9$ and $\beta = 1.1$.
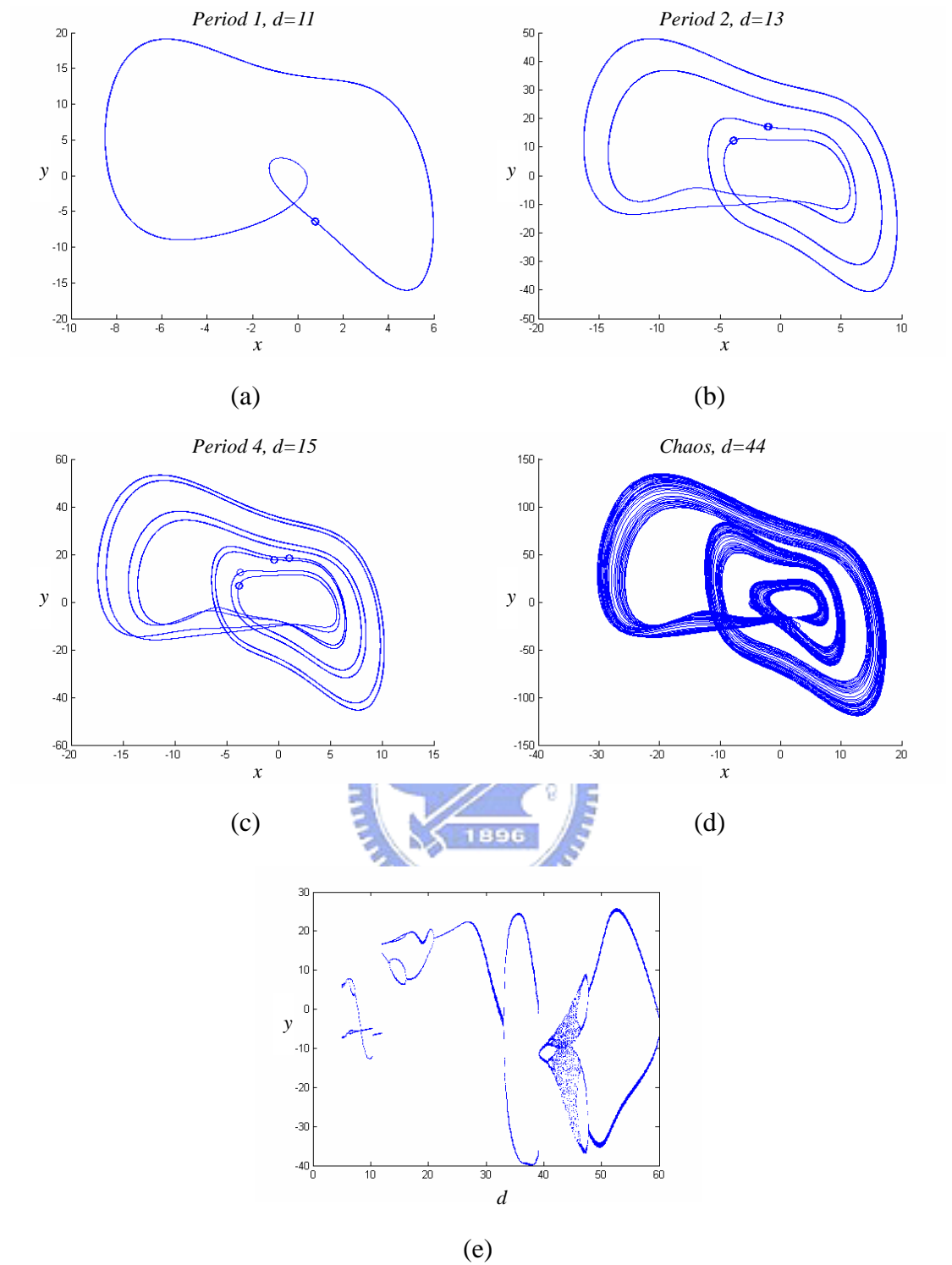
Fig. 2.5 The phase portraits and the bifurcation diagram for the nano resonator system

with order $\alpha = 1.2$ and $\beta = 0.8$.
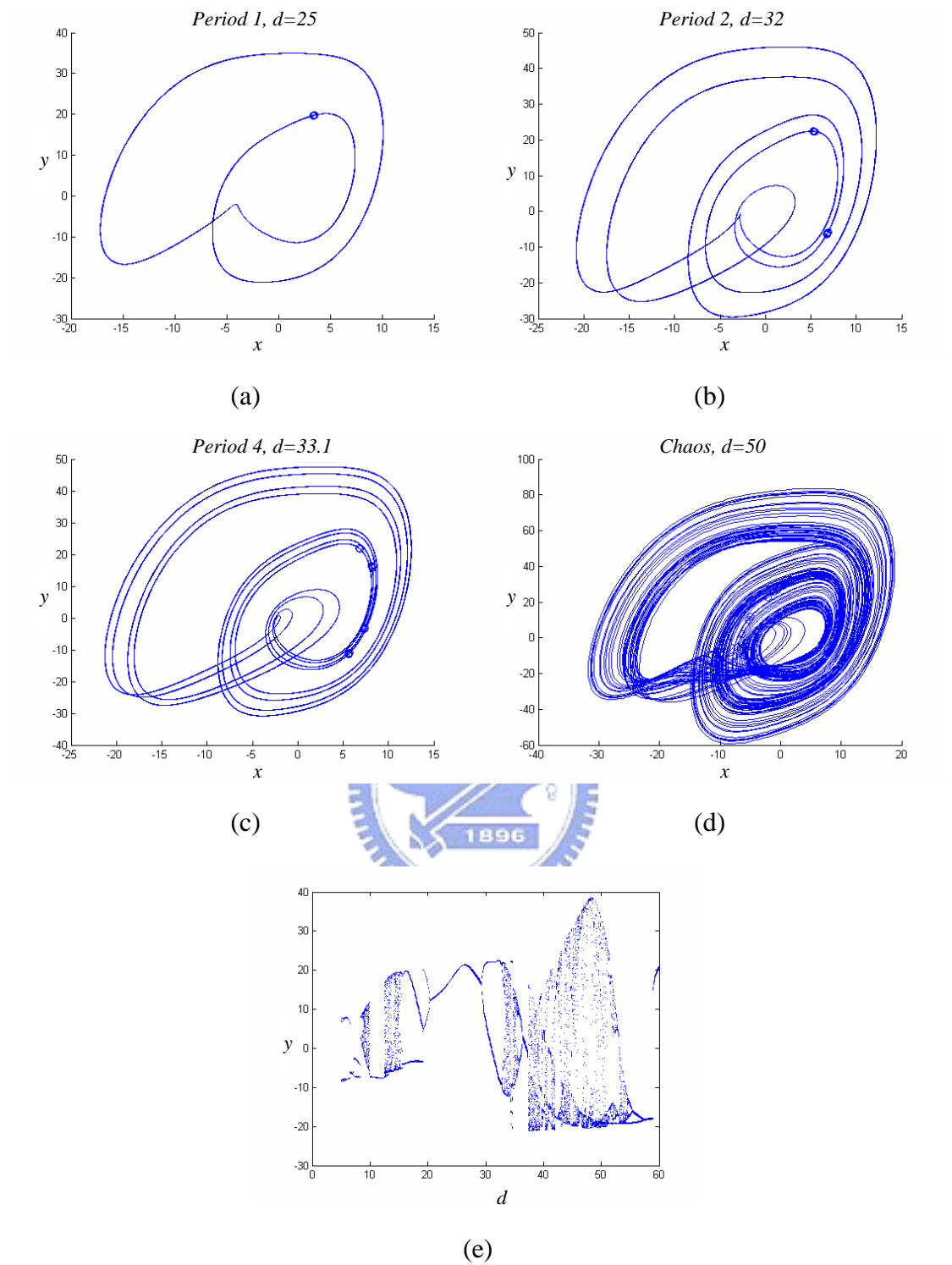
Fig. 2.6 The phase portraits and the bifurcation diagram for the nano resonator system

with order $\alpha = 0.8$ and $\beta = 1.2$.
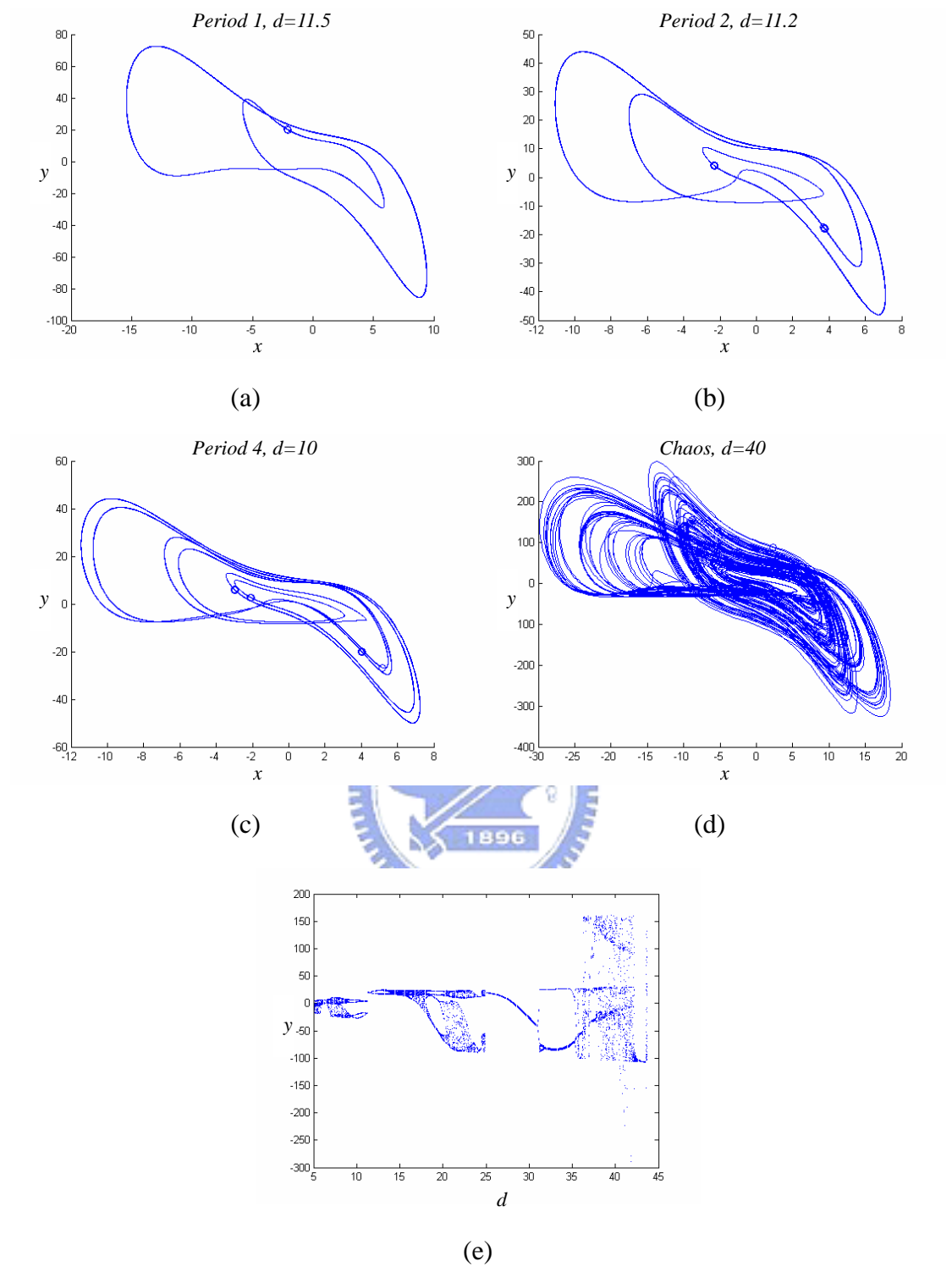
Fig.2.7 The phase portraits and the bifurcation diagram for the nano resonator system

with order $\alpha = 1.6$ and $\beta = 0.4$.
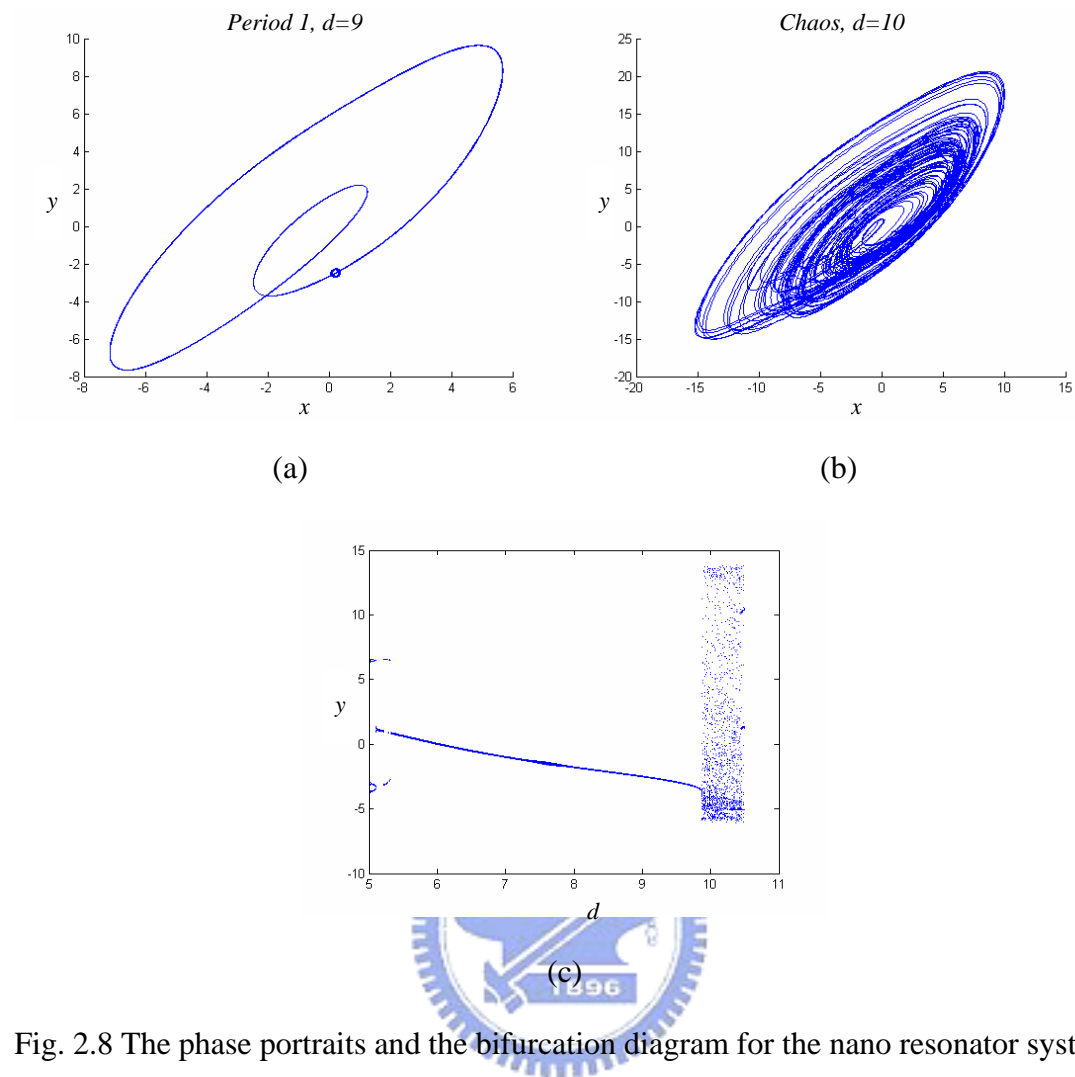
Fig. 2.8 The phase portraits and the bifurcation diagram for the nano resonator system

with order $\alpha = 0.4$ and $\beta = 1.6$.
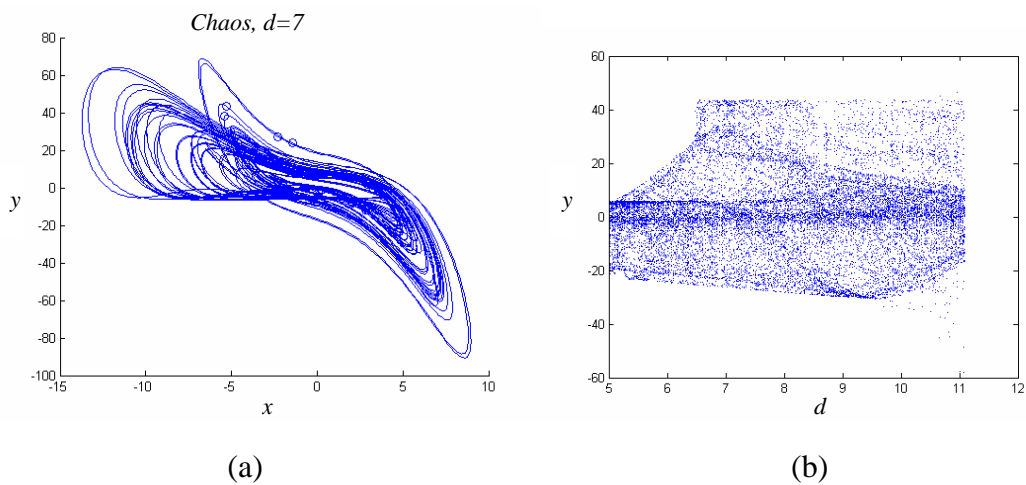
Fig. 2.9 The phase portraits and the bifurcation diagram for the nano resonator system

with order $\alpha = 1.7$ and $\beta = 0.3$.
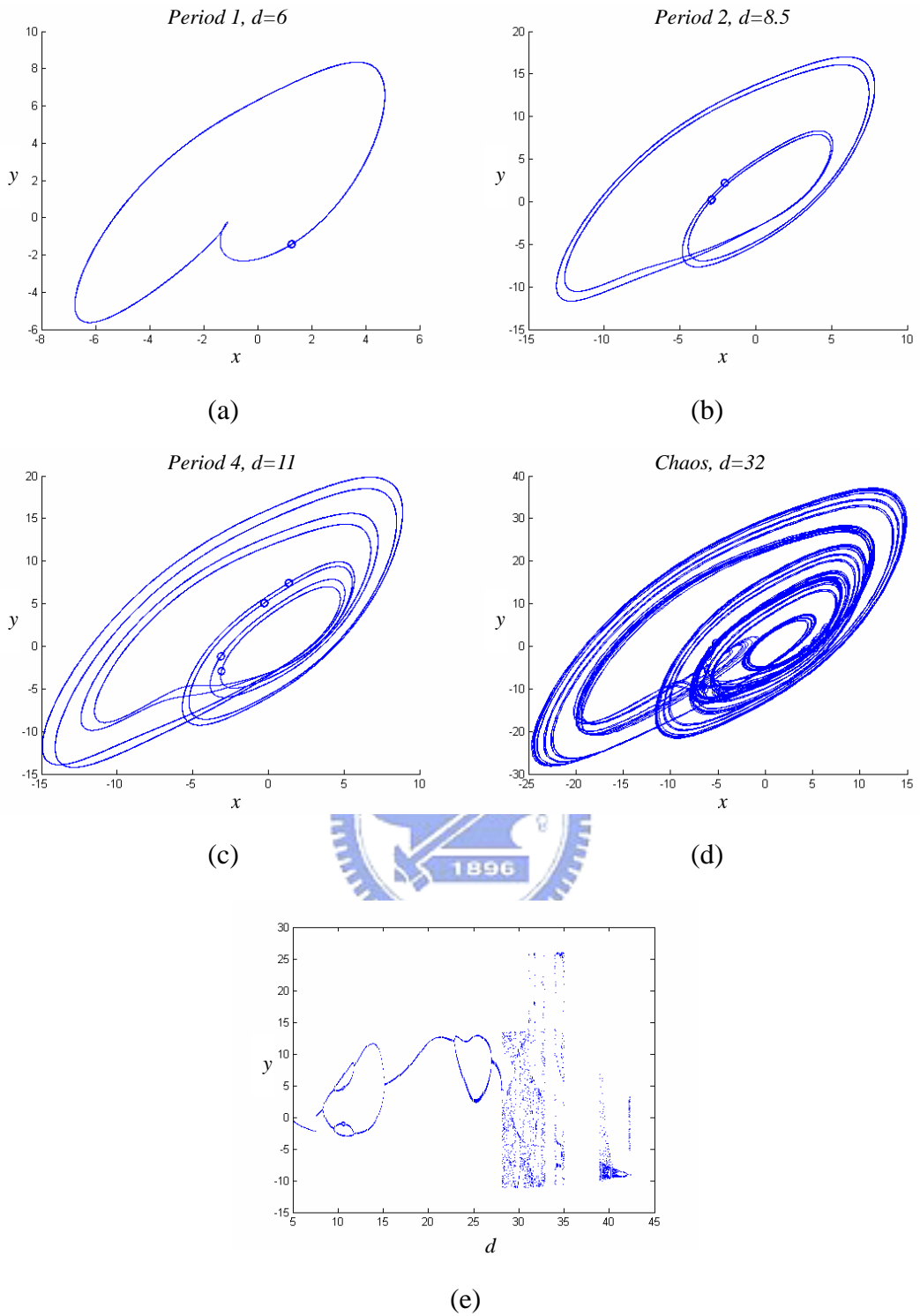
Fig. 2.10 The phase portraits and the bifurcation diagram for the nano resonator

system with order $\alpha = 0.5$ and $\beta = 1.5$.

Period 1, d=18.5

(a)

Period 2, d=17.5

(b)

Period 4, d=17

(c)

Chaos, d=10

(d)

(e)
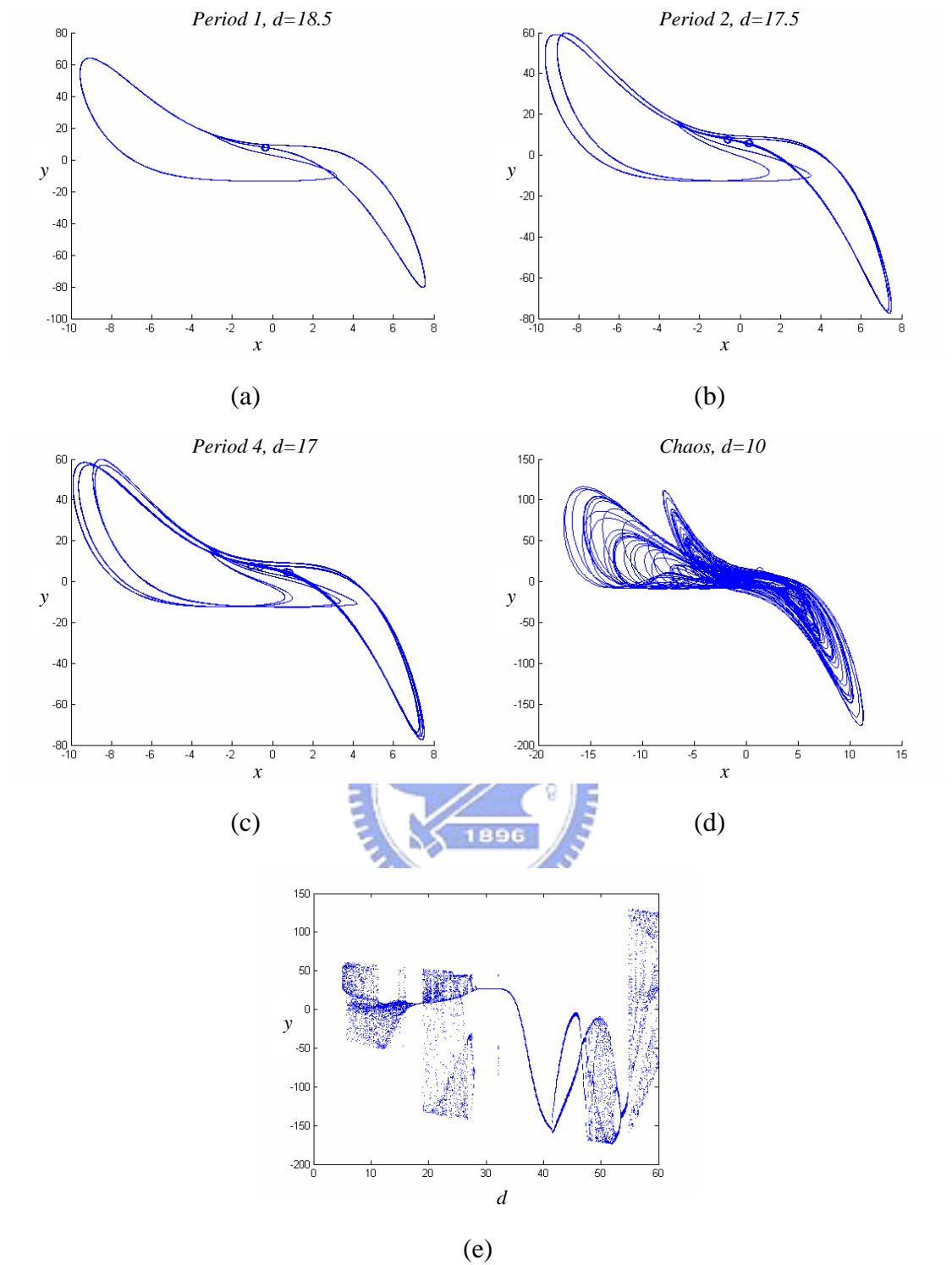
Fig. 2.11 The phase portraits and the bifurcation diagram for the nano resonator

system with order $\alpha = 1.8$ and $\beta = 0.2$.

21
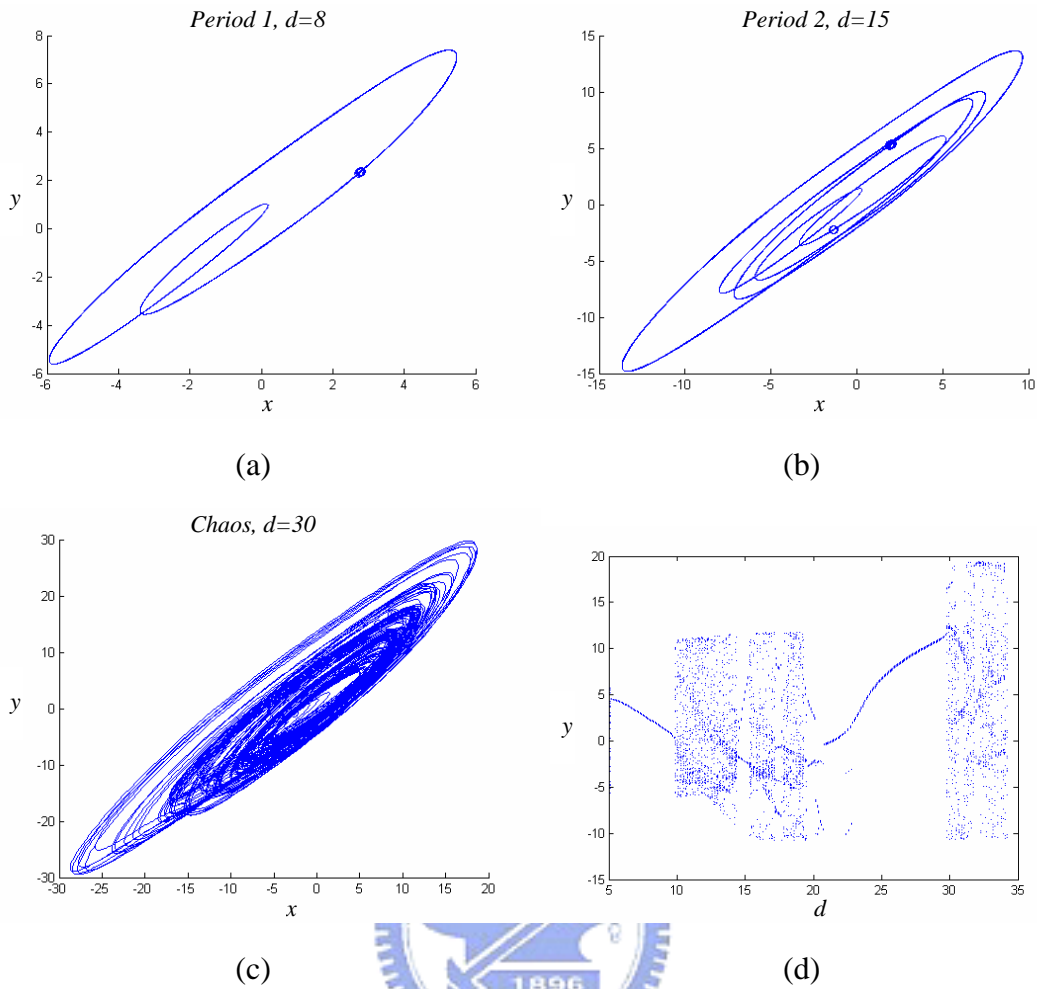
Fig. 2.12 The phase portraits and the bifurcation diagram for the nano resonator

system with order $\alpha = 0.2$ and $\beta = 1.8$.
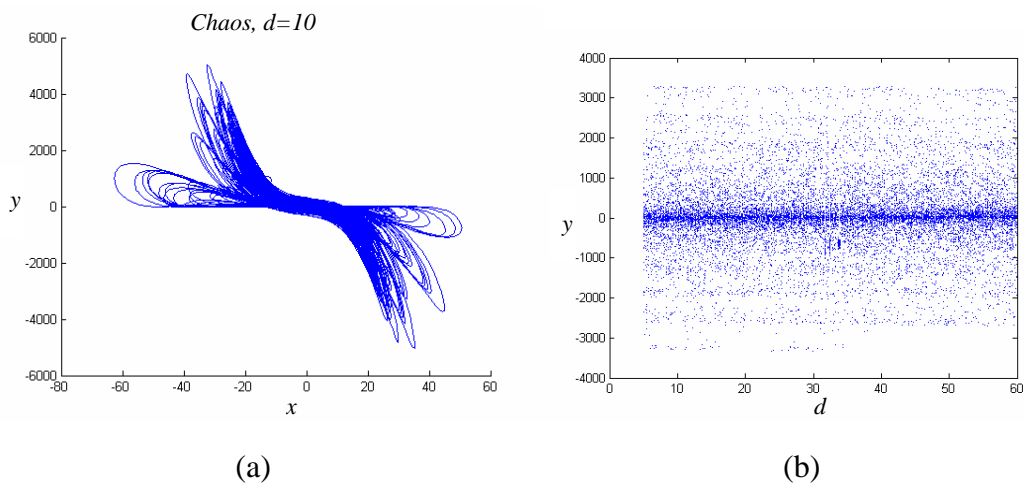
Fig. 2.13 The phase portraits and the bifurcation diagram for the nano resonator

system with order $\alpha = 1.9$ and $\beta = 0.1$.

(a)   (b)
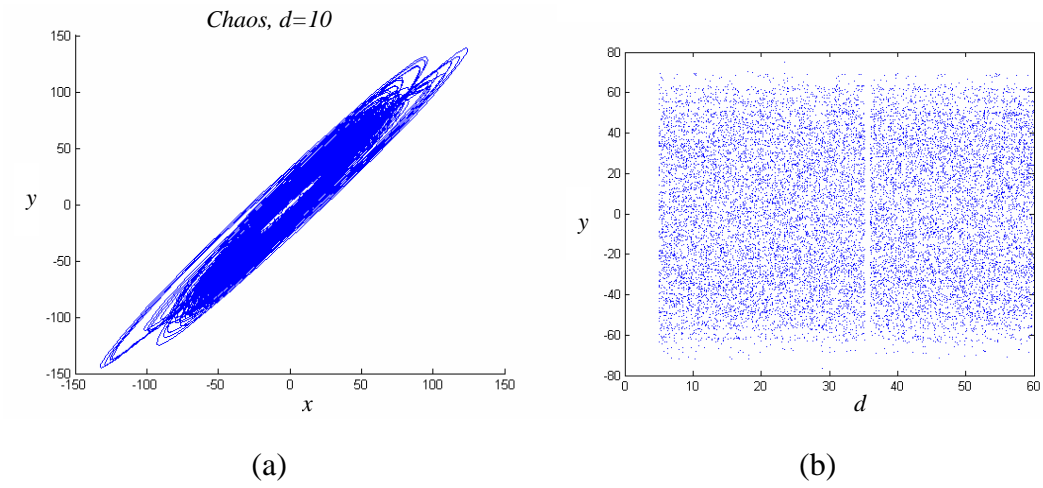
Fig. 2.14 The phase portraits and the bifurcation diagram for the nano resonator

system with order $\alpha = 0.1$ and $\beta = 1.9$.

(a)   (b)

(c)   (d)
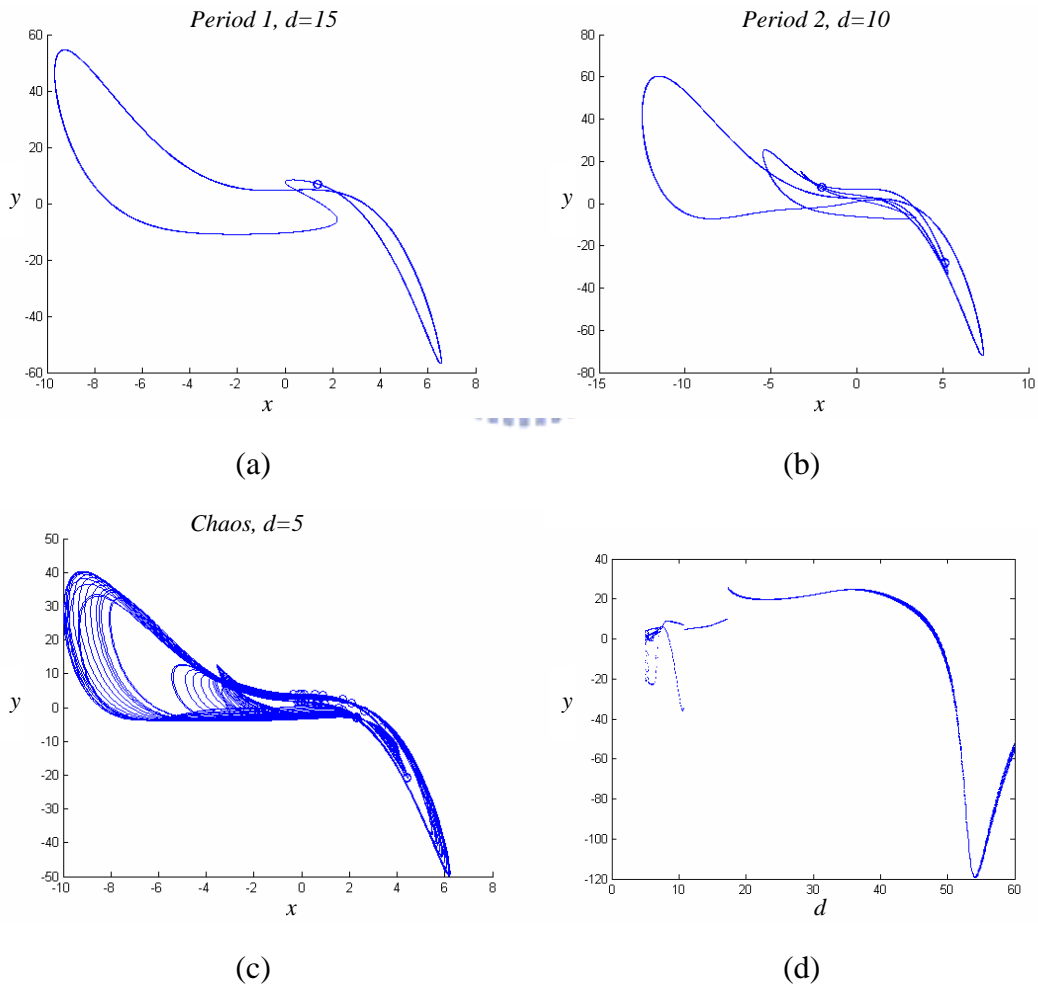
Fig. 2.15 The phase portraits and the bifurcation diagram for the nano resonator

system with order $\alpha = 1.8$ and $\beta = 0.1$.
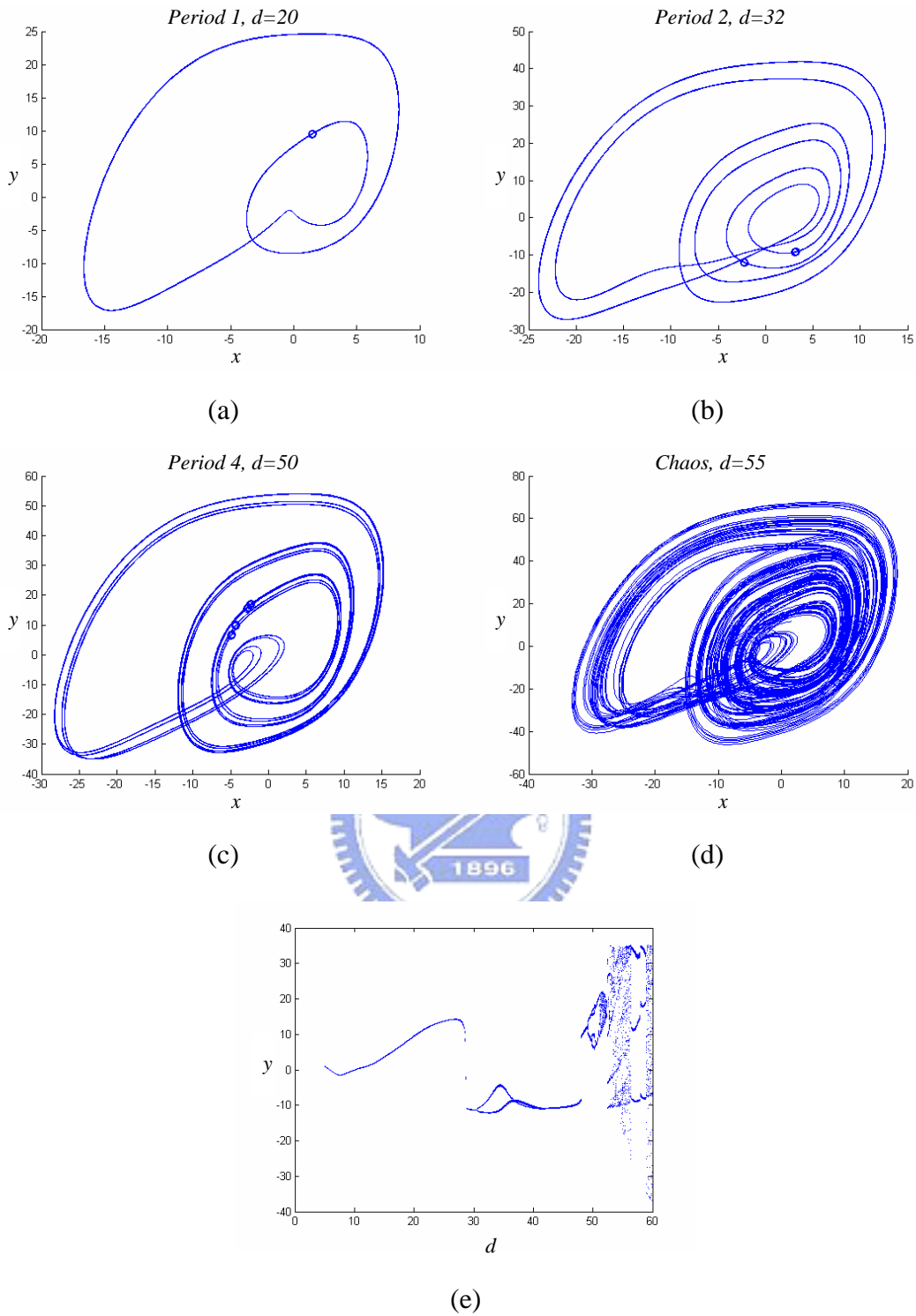
Fig. 2.16 The phase portraits and the bifurcation diagram for the nano resonator

system with order $\alpha = 0.7$ and $\beta = 1.2$.
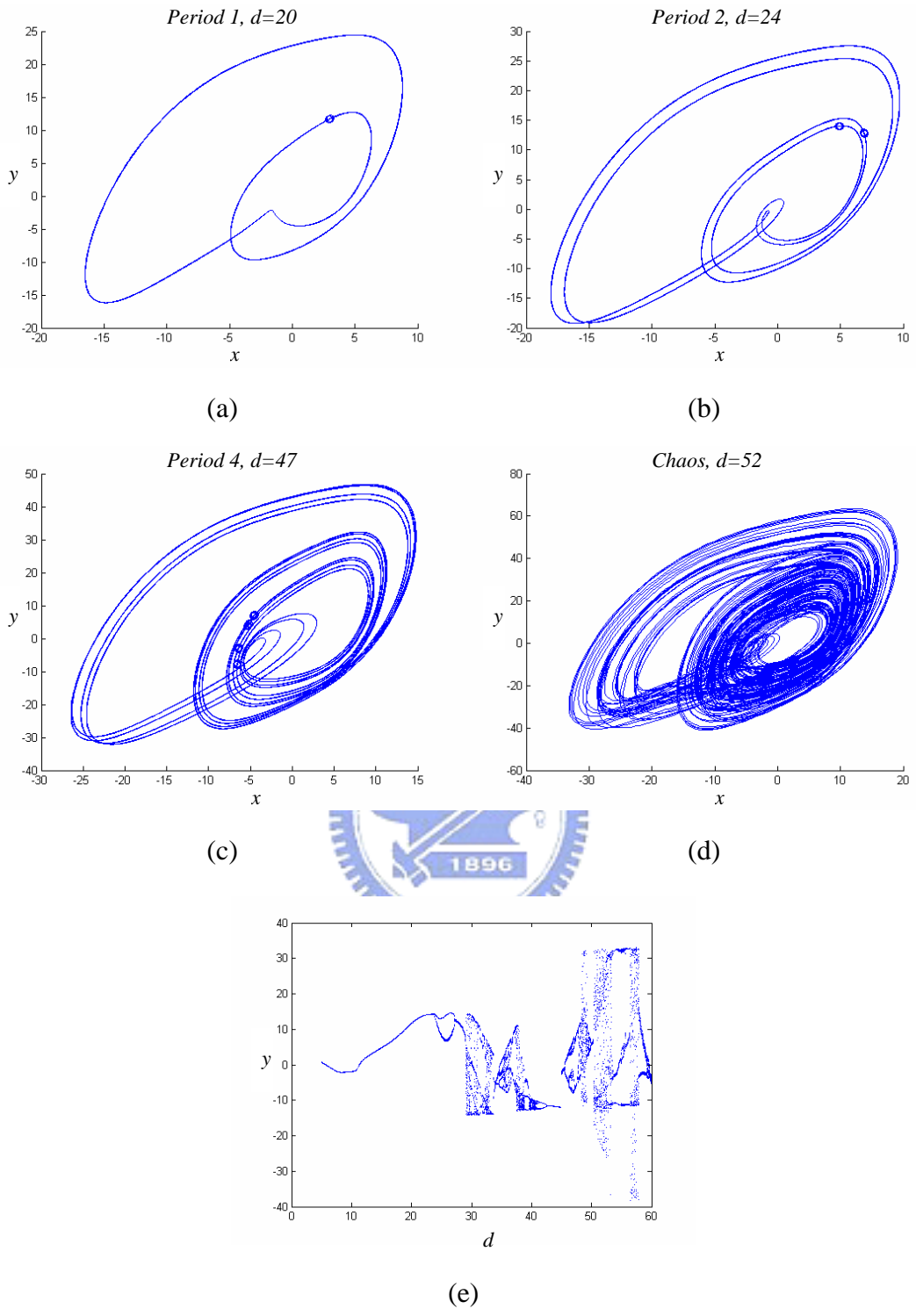
Fig. 2.17 The phase portraits and the bifurcation diagram for the nano resonator

system with order $\alpha = 0.6$ and $\beta = 1.3$.
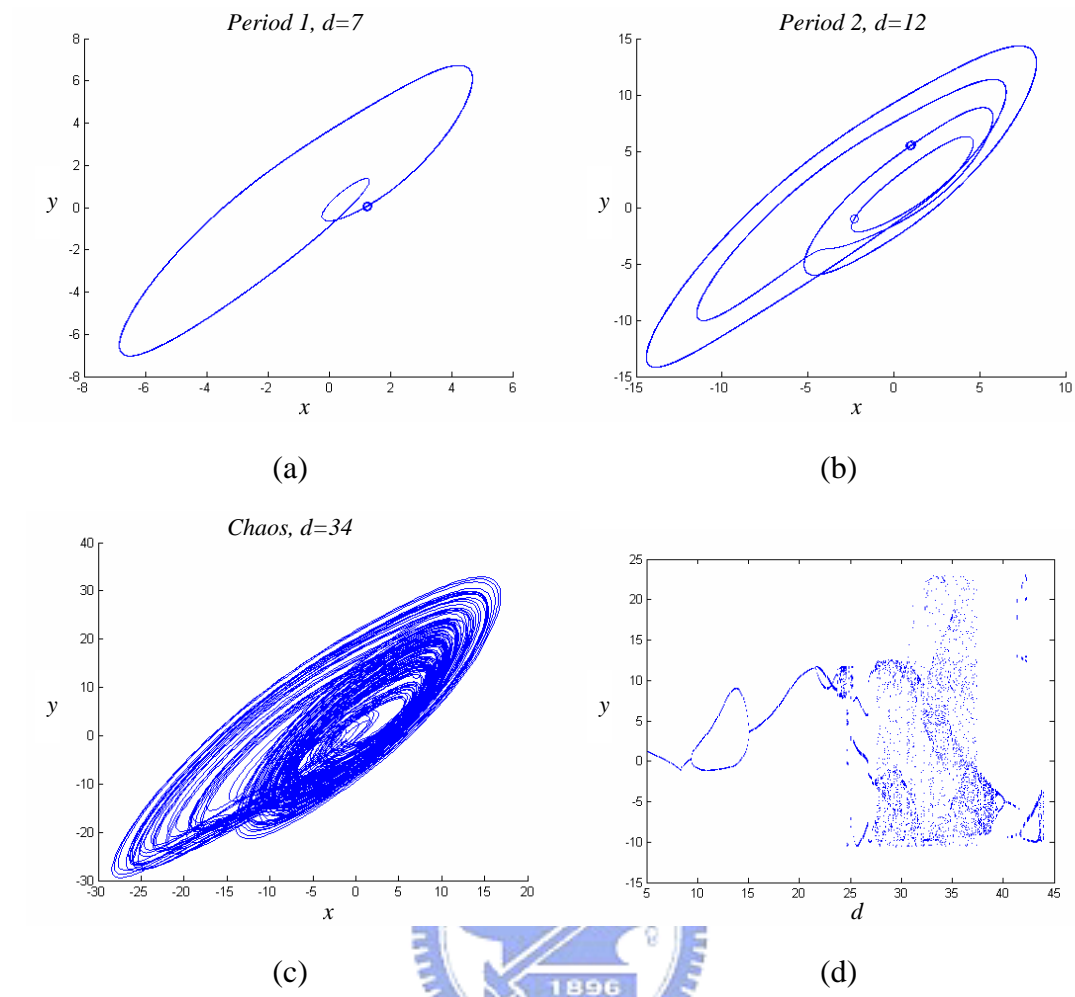
Fig. 2.18 The phase portraits and the bifurcation diagram for the nano resonator

system with order $\alpha = 0.3$ and $\beta = 1.6$.

Fig. 2.19 The phase portraits and the bifurcation diagram for the nano resonator

system with order $\alpha = 0.2$ and $\beta = 1.7$.

Chapter 3

Parameter Excited Chaos Synchronizations of Integral and Fractional Order Nano Resonator Systems

3.1 Preliminaries

In this Chapter, the chaos synchronizations of two uncoupled integral and fractional order identical chaotic nano resonator systems are obtained by replacing their corresponding parameters by the same function of chaotic state variables of a third identical chaotic system. It is named parameter excited chaos synchronization which can be successfully obtained for very low total fraction order 0.2. Numerical simulations are illustrated by phase portraits, Poincaré maps and state error plots.

3.2 Numerical Simulations for the synchronizations of Integral and fractional order chaotic nano resonator systems

It is well known that a chaotic system is very sensitive to its initial conditions, means that the behaviors of two same chaotic systems which have distinct initial conditions are totally different. In this thesis, these two chaotic fractional order nano resonator systems

$$
\begin{cases}
\dfrac{d^{\alpha} x_1}{dt^{\alpha}} = y_1 \\[2mm]
\dfrac{d^{\beta} y_1}{dt^{\beta}} = -(a + bz_1)x_1 - (a + bz_1)x_1^{3} - cy_1 + dz_1 \\[2mm]
\dfrac{dz_1}{dt} = w_1 \\[2mm]
\dfrac{dw_1}{dt} = -ez_1 - fz_1
\end{cases}
\tag{3.1}
$$

and

$$\begin{cases} \dfrac{d^{\alpha}x_2}{dt^{\alpha}} = y_2 \\[2mm] \dfrac{d^{\beta}y_2}{dt^{\beta}} = -(a+bz_1)x_1 - (a+bz_1)x_1^{\,3} - cy_2 + dz_2 \\[2mm] \dfrac{dz_2}{dt} = w_2 \\[2mm] \dfrac{dw_2}{dt} = -ez_2 - fz_2 \end{cases} \qquad (3.2)$$

where α and β are the fractional orders, are synchronized by replacing corresponding parameters by the same function of chaotic states of chaotic nano resonator system

$$\begin{cases} \dfrac{dx}{dt} = y \\[2mm] \dfrac{dy}{dt} = -(a+bz)x - (a+bz)x^{3} - cy + dz \\[2mm] \dfrac{dz}{dt} = w \\[2mm] \dfrac{dw}{dt} = -ez - fz^{3} \end{cases} \qquad (3.3)$$
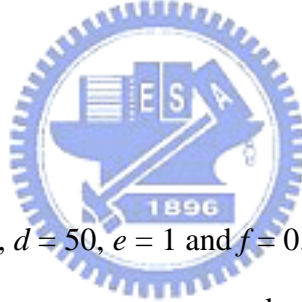
where $a = 0.2$, $b = 0.2$, $c = 0.4$, $d = 50$, $e = 1$ and $f = 0.3$ are constant parameters of the system. Define the error states as $e_1 = x_1 - x_2$ and $e_2 = y_1 - y_2$ in system (3.1) and (3.2). The synchronization scheme is to replace the corresponding parameters d, c, b or a in system (3.1) and (3.2) by the same function of chaotic states of system (3.3) such that $\|e(t)\| \to 0$ as $t \to \infty$. In following simulations, for various derivative orders α and β, we replace the system parameter d in system (3.1) and (3.2) by sin x, and by sin y, where x and y are state variables in system (3.3); replace c in system (3.1) and (3.2) by $\sin x + \sin y$, where x and y are state variables in system (3.3); replace b in system (3.1) and (3.2) by $10(\sin^2 x + \sin^2 y)$, where x and y are state variables in system (3.3) and replace a in system (3.1) and (3.2) by $10(\sin^3 x + \sin^3 y)$, where x and y are state variables in system (3.3). Simulations are performed under $\alpha = \beta = 0.1 \sim 1$ in steps of 0.1. In our numerical simulations, six parameters $a = 0.2$,

$b = 0.2$, $c = 0.4$, $d = 50$, $e = 1$ and $f = 0.3$ of system (3.3) are fixed. The initial states of system (3.3) are $x(0) = 3$, $y(0) = 4$, $z(0) = 1$ and $w(0) = 0$. The numerical simulations are carried out by MATLAB.

Case 1: The parameters $a = 0.2$, $b = 0.2$, $c = 0.4$, $e = 1$ and $f = 0.3$ of system (3.1) and (3.2) are fixed. The initial states of system (3.1) and (3.2) are $x_1(0) = 0.003$, $y_1(0) = 0.004$, $x_2(0) = 0.004$, $y_2(0) = 0.003$, $z(0) = 1$ and $w(0) = 0$. The parameter d of system (3.1) and (3.2) is replaced by the same sin x, where x is the state variable of system (3.3). All synchronizations for $\alpha = \beta = 0.1 \sim 1$ are successfully obtained. For saving space, only results for $\alpha = \beta = 0.1$, 0.4, 0.7 and 1 are shown in Fig. 3.1 ~ 3.8.

Case 2: The parameters $a = 0.2$, $b = 0.2$, $c = 0.4$, $e = 1$ and $f = 0.3$ of system (2.4) and (2.5) are fixed. The initial states of system (3.1) and (3.2) are $x_1(0) = 0.003$, $y_1(0) = 0.004$, $x_2(0) = 0.004$, $y_2(0) = 0.003$, $z(0) = 1$ and $w(0) = 0$. The parameter d of system (3.1) and (3.2) is replaced by the same sin y, where y is the state variable of system (3.3). All synchronizations for $\alpha = \beta = 0.1 \sim 1$ are successfully obtained. For saving space, only results for $\alpha = \beta = 0.1$, 0.4, 0.7 and 1 are shown in Fig. 3.9 ~ 3.16.

Case 3: The parameters $a = 0.2$, $b = 0.2$, $c = 0.4$, $e = 1$ and $f = 0.3$ of system (2.4) and (2.5) are fixed. The initial states of system (3.1) and (3.2) are $x_1(0) = 0.003$, $y_1(0) = 0.004$, $x_2(0) = 0.004$, $y_2(0) = 0.003$, $z(0) = 1$ and $w(0) = 0$. The parameter c of system (3.1) and (3.2) is replaced by the same $\sin x + \sin y$, where x and y are the state variables of system (3.3). All synchronizations for $\alpha = \beta = 0.1 \sim 0.9$ are successfully obtained. For saving space, only results for $\alpha = \beta = 0.1$, 0.4, 0.7 and 0.9 are shown in Fig. 3.17 ~ 3.24.

Case 4: The parameters $a = 0.2$, $b = 0.2$, $c = 0.4$, $e = 1$ and $f = 0.3$ of system (3.1) and (3.2) are fixed. The initial states of system (3.1) and (3.2) are

$x_1(0) = 0.003$, $y_1(0) = 0.004$, $x_2(0) = 0.004$, $y_2(0) = 0.003$, $z(0) = 1$ and $w(0) = 0$. The parameter b of system (3.1) and (3.2) is replaced by the same $10(\sin^2 x + \sin^2 y)$, where x and y are the state variables of system (3.3). All synchronizations for $\alpha = \beta = 0.1 \sim 0.9$ are successfully obtained. For saving space, only results for $\alpha = \beta = 0.1, 0.4, 0.7$ and 0.9 are shown in Fig. 3.25 ~ 3.32.

Case 5: The parameters $a = 0.2$, $b = 0.2$, $c = 0.4$, $e = 1$ and $f = 0.3$ of system (3.1) and (3.2) are fixed. The initial states of system (3.1) and (3.2) are $x_1(0) = 0.003$, $y_1(0) = 0.004$, $x_2(0) = 0.004$, $y_2(0) = 0.003$, $z(0) = 1$ and $w(0) = 0$. The parameter a of system (3.1) and (3.2) is replaced by the same $10(\sin^3 x + \sin^3 y)$, where x and y are the state variables of system (3.3). All synchronizations for $\alpha = \beta = 0.1 \sim 0.9$ are successfully obtained. For saving space, only results for $\alpha = \beta = 0.1, 0.4, 0.7$ and 0.9 are shown in Fig. 3.33 ~ 3.40.
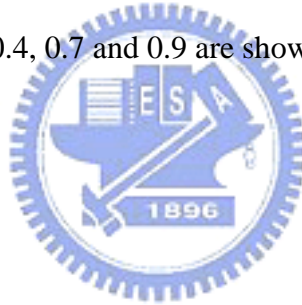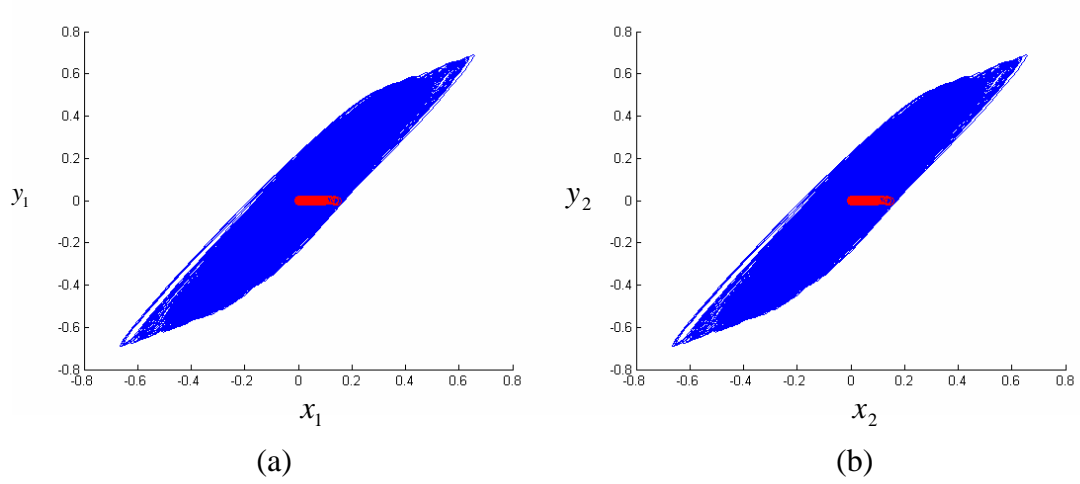
Fig. 3.1 The phase portraits of the synchronized nano resonator fractional order systems (3.1) and (3.2) with order $\alpha = \beta = 0.1$ for Case 1.
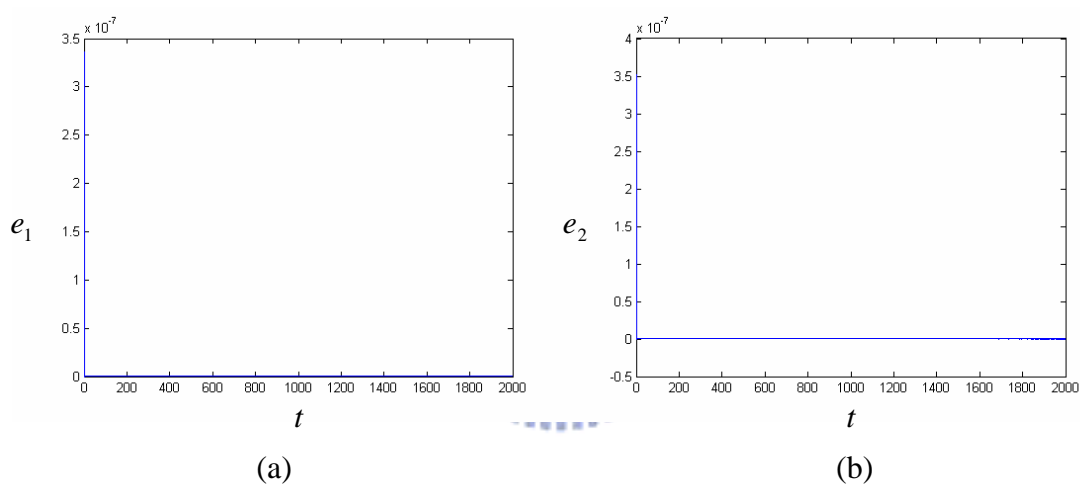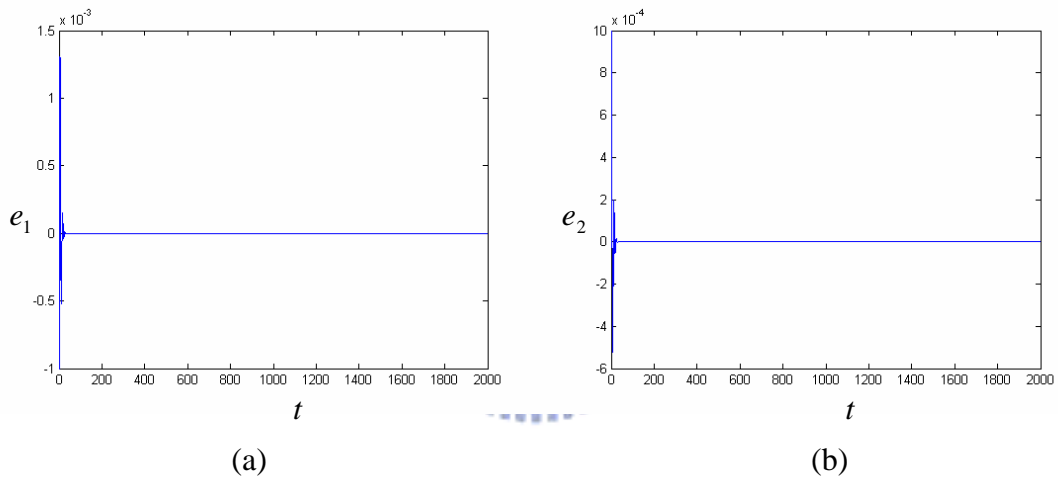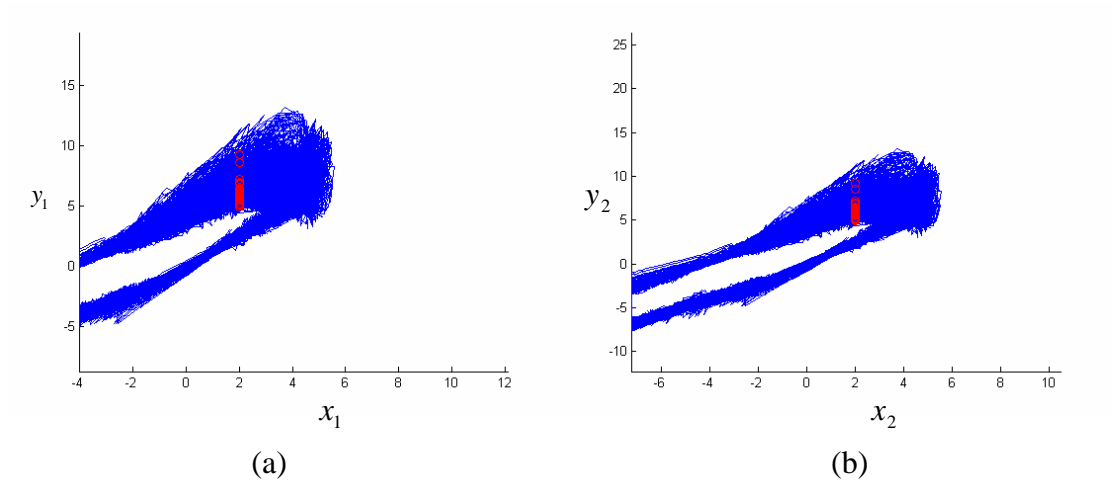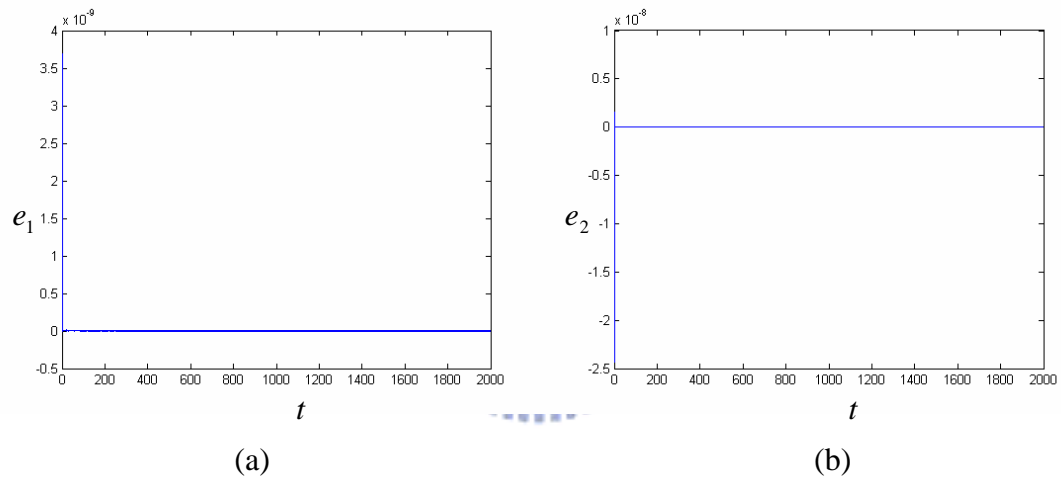

Fig. 3.2 The time histories of the errors of the states of the synchronized nano resonator fractional order systems (3.1) and (3.2) with order $\alpha = \beta = 0.1$ for Case 1.
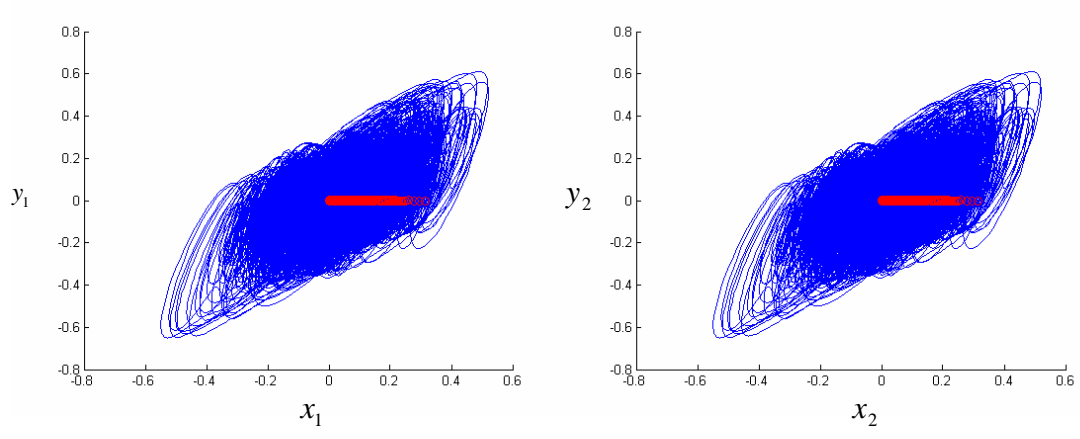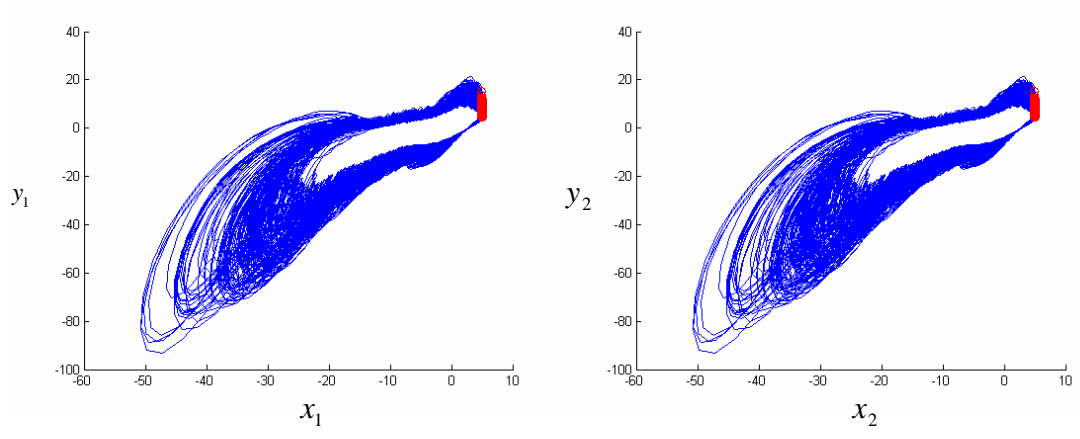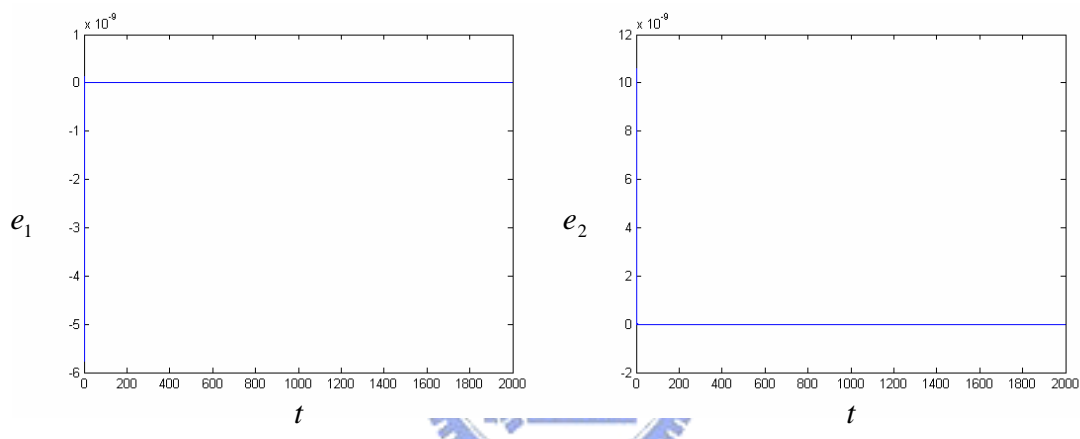
Fig. 3.3 The phase portraits of the synchronized nano resonator fractional order

systems (3.1) and (3.2) with order $\alpha = \beta = 0.4$ for Case 1.
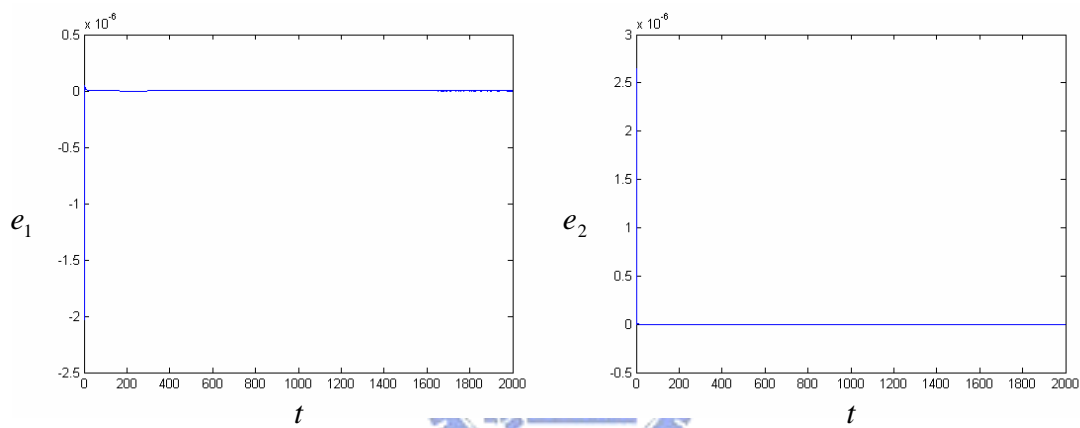
Fig. 3.4 The time histories of the errors of the states of the synchronized nano

resonator fractional order systems (3.1) and (3.2) with order $\alpha = \beta = 0.4$ for Case 1.
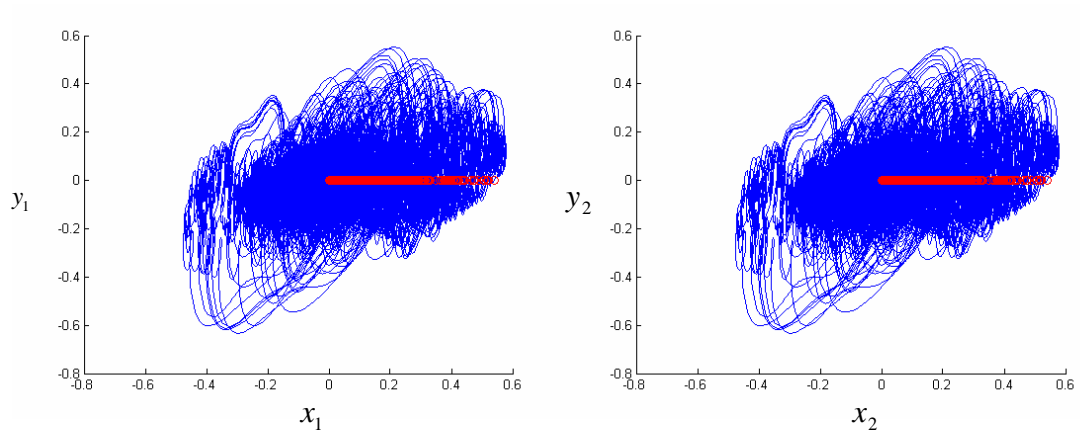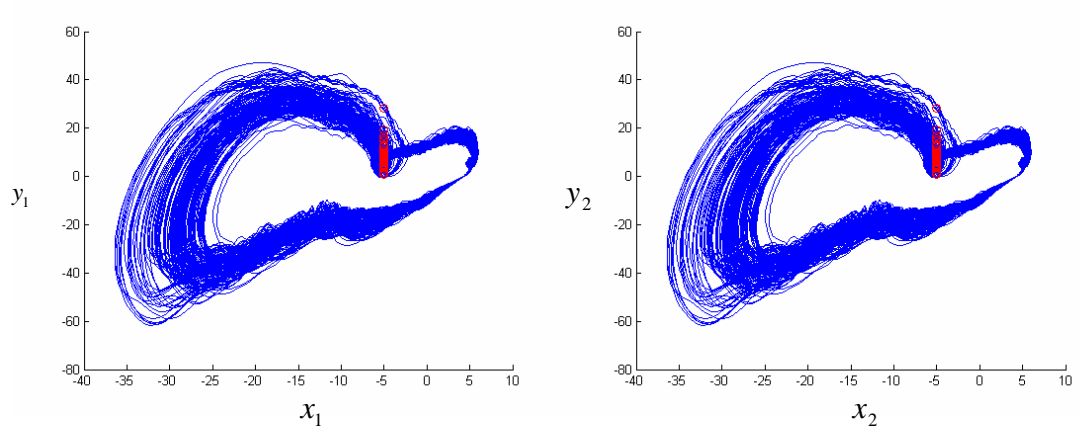
Fig. 3.5 The phase portraits of the synchronized nano resonator fractional order

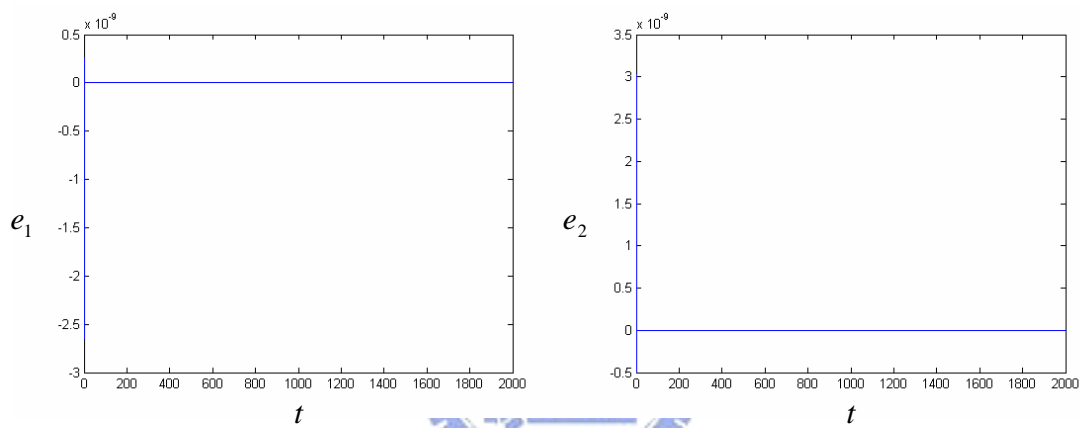systems (3.1) and (3.2) with order $\alpha = \beta = 0.7$ for Case 1.
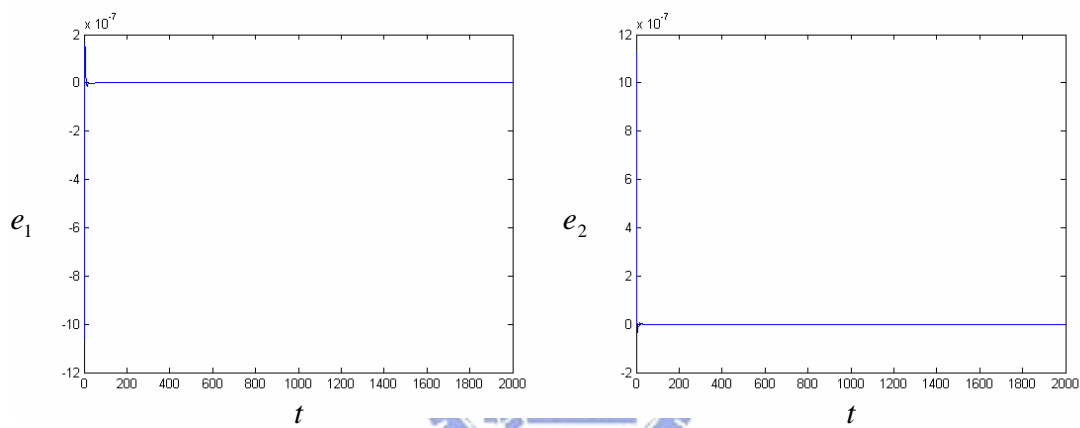
Fig. 3.6 The time histories of the errors of the states of the synchronized nano

resonator fractional order systems (3.1) and (3.2) with order $\alpha = \beta = 0.7$ for Case 1.
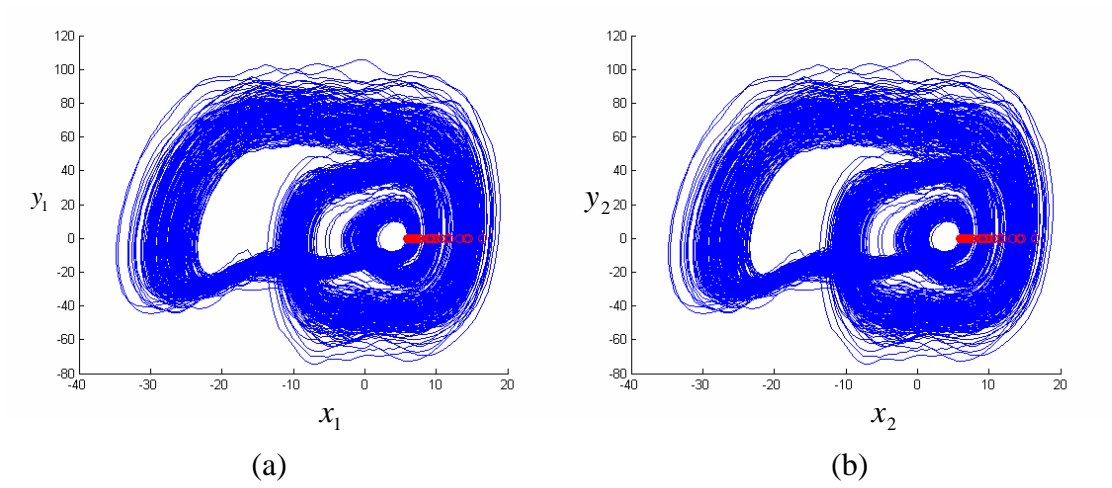
(a)   (b)
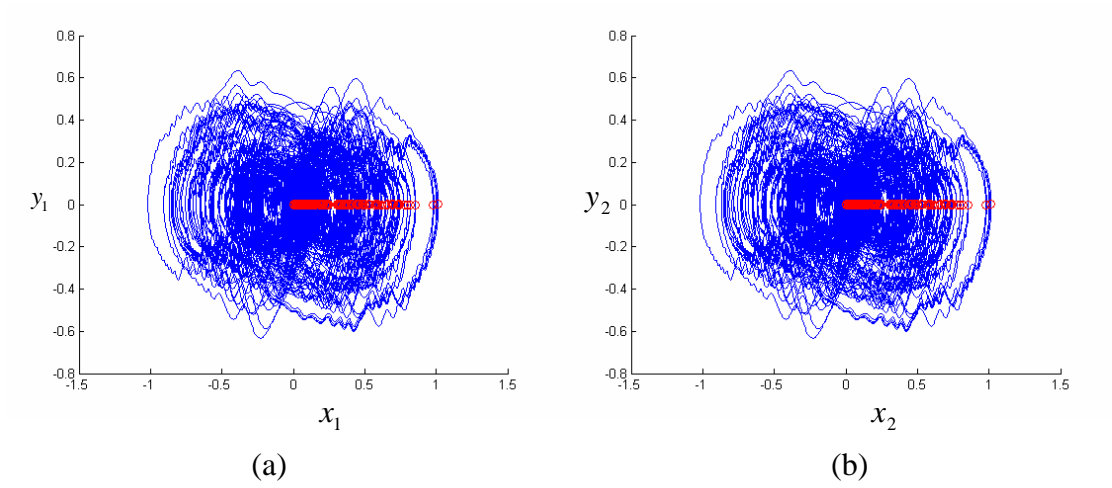
Fig. 3.7 The phase portraits of the synchronized nano resonator integral order systems

(4) and (5) with order $\alpha = \beta = 1$ for Case 1.

(a)   (b)
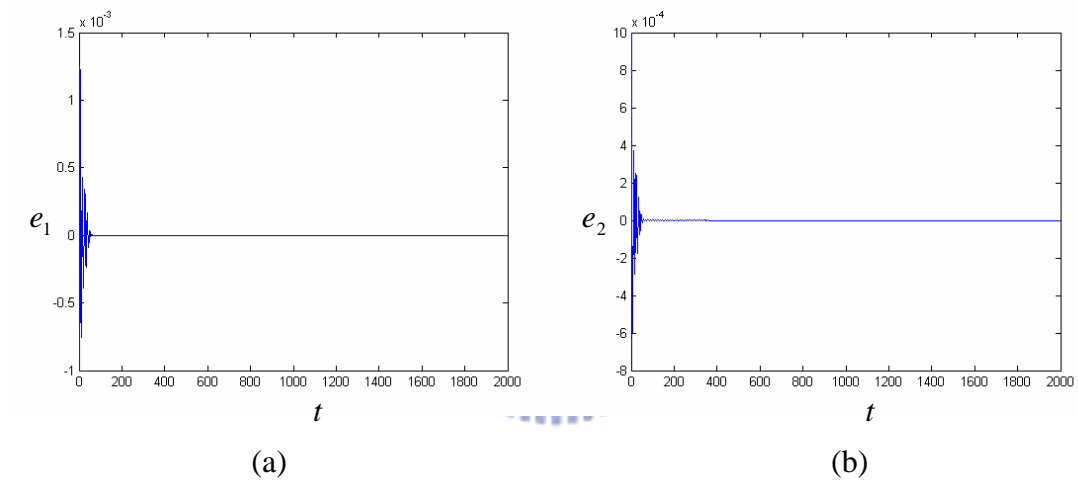
Fig. 3.8 The time histories of the errors of the states of the synchronized nano

resonator integral order systems (4) and (5) with order $\alpha = \beta = 1$ for Case 1.
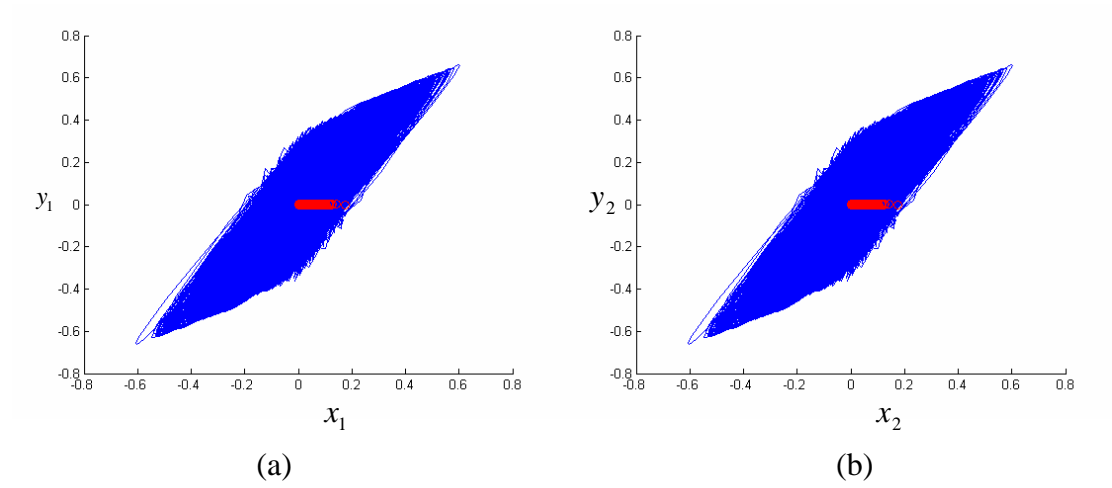
Fig. 3.9 The phase portraits of the synchronized nano resonator fractional order

systems (3.1) and (3.2) with order $\alpha = \beta = 0.1$ for Case 2.
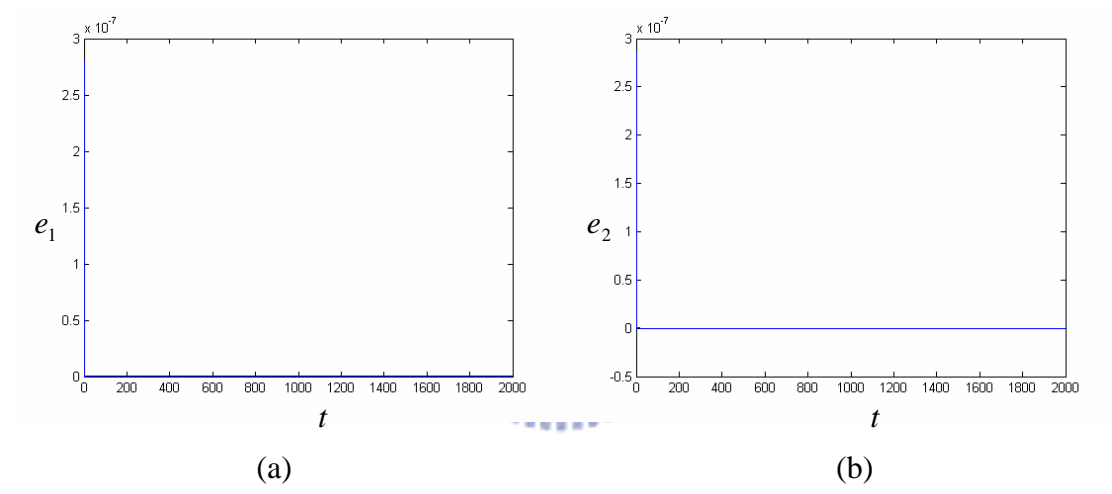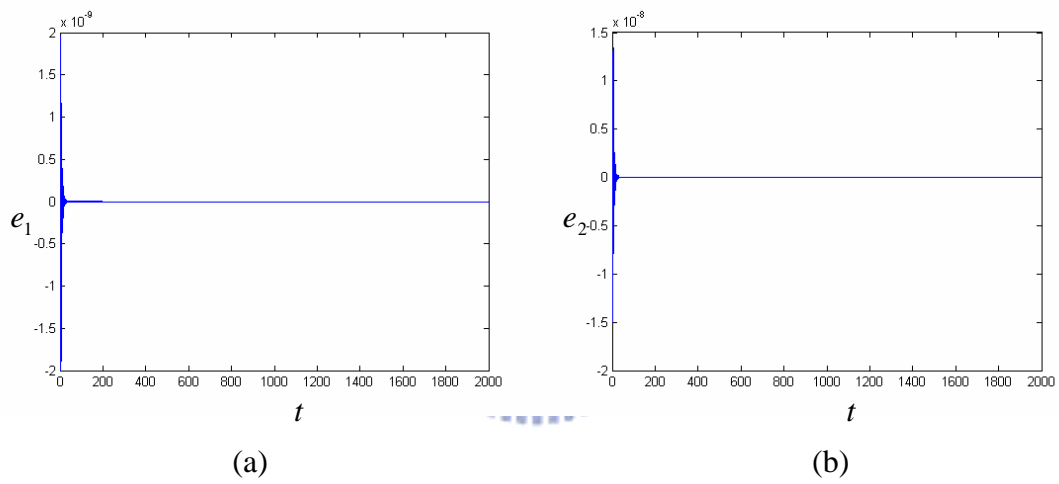

Fig. 3.10 The time histories of the errors of the states of the synchronized nano

resonator fractional order systems (3.1) and (3.2) with order $\alpha = \beta = 0.1$ for Case 2.
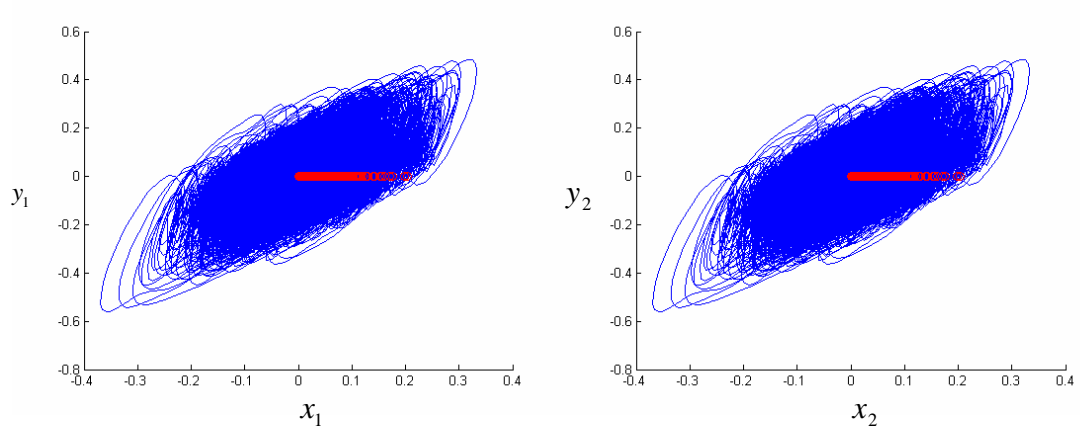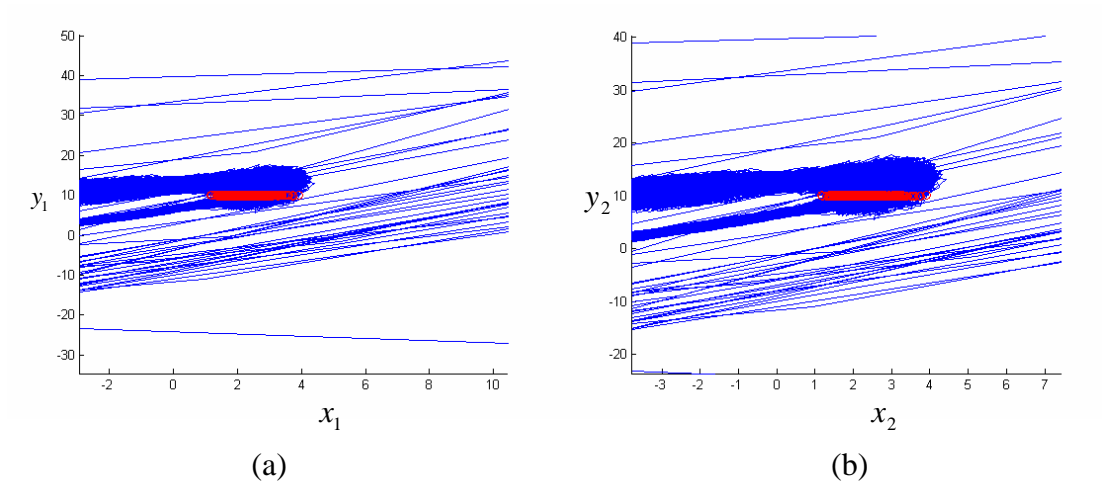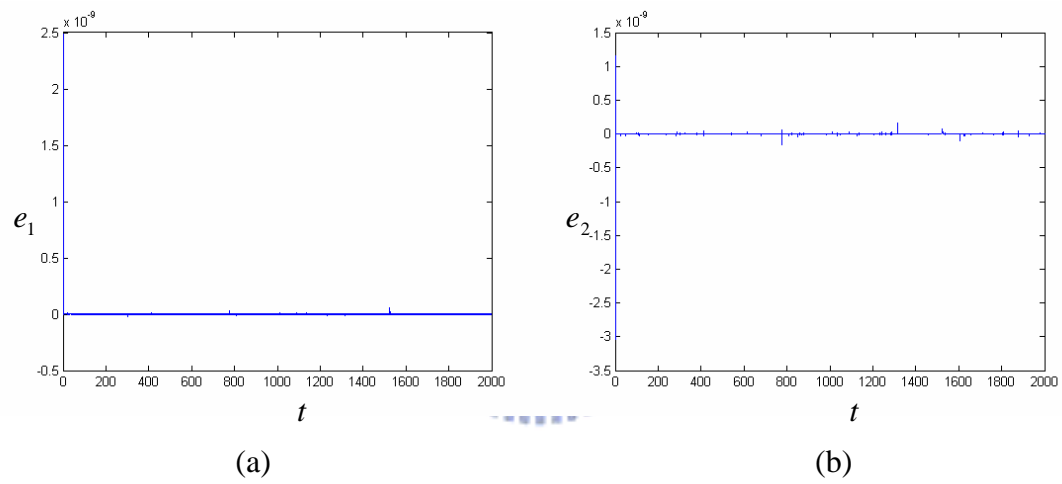
Fig. 3.11 The phase portraits of the synchronized nano resonator fractional order

systems (3.1) and (3.2) with order $\alpha = \beta = 0.4$ for Case 2.
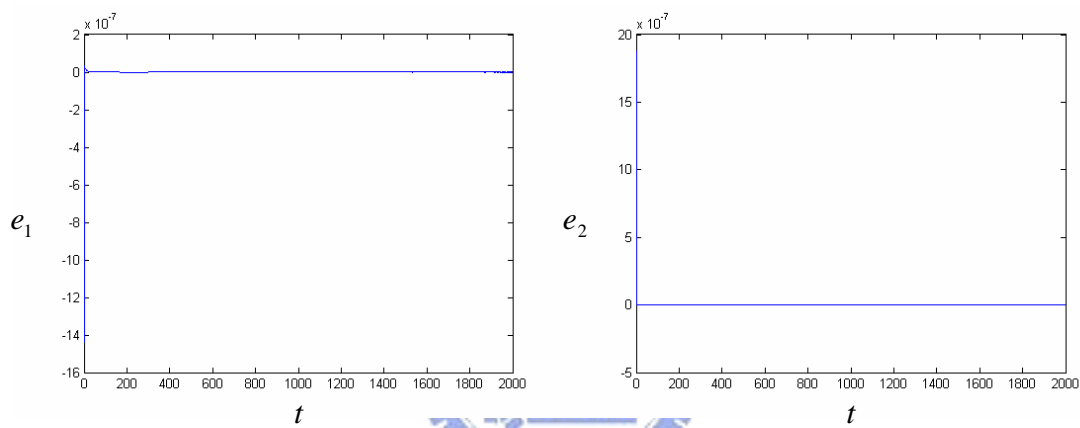
Fig. 3.12 The time histories of the errors of the states of the synchronized nano

resonator fractional order systems (3.1) and (3.2) with order $\alpha = \beta = 0.4$ for Case 2.
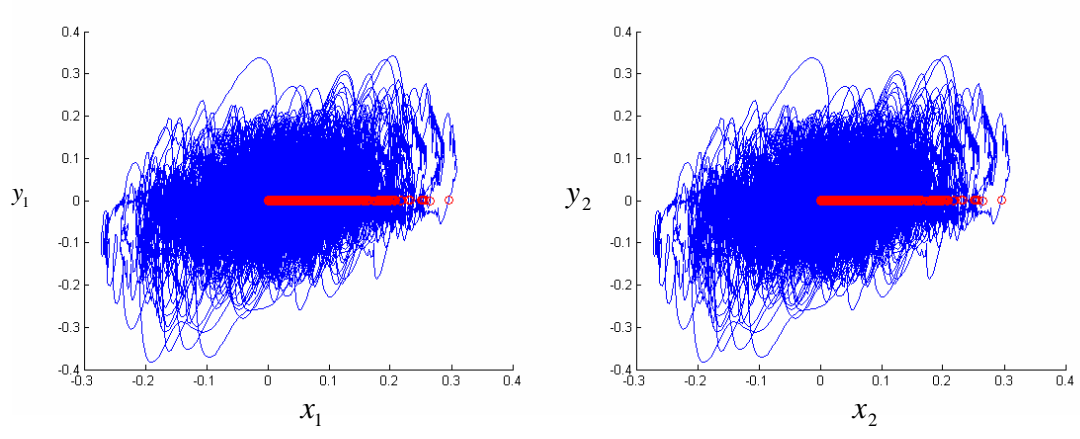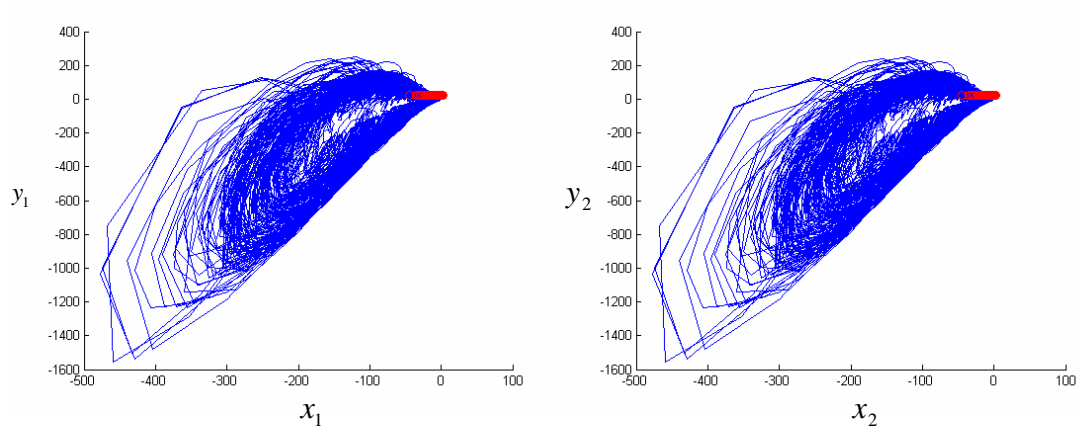
Fig. 3.13 The phase portraits of the synchronized nano resonator fractional order

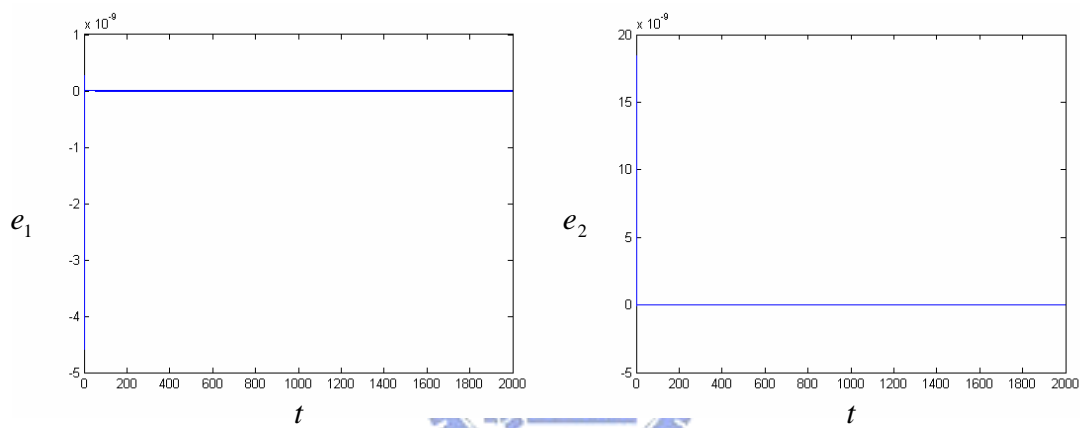systems (3.1) and (3.2) with order $\alpha = \beta = 0.7$ for Case 2.
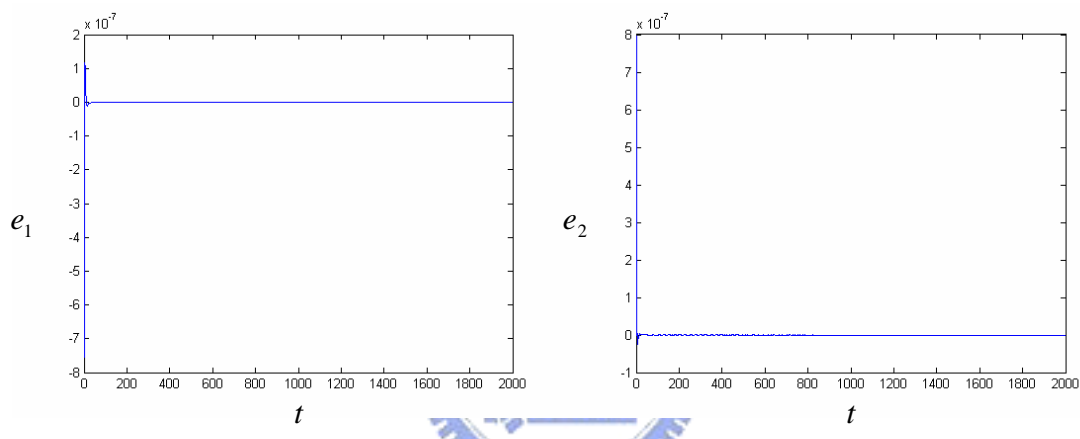
Fig. 3.14 The time histories of the errors of the states of the synchronized nano

resonator fractional order systems (3.1) and (3.2) with order $\alpha = \beta = 0.7$ for Case 2.
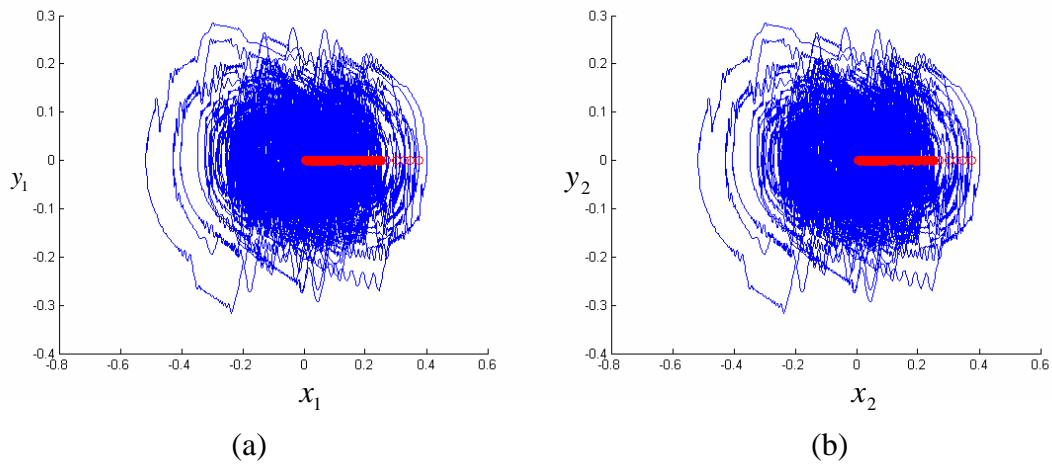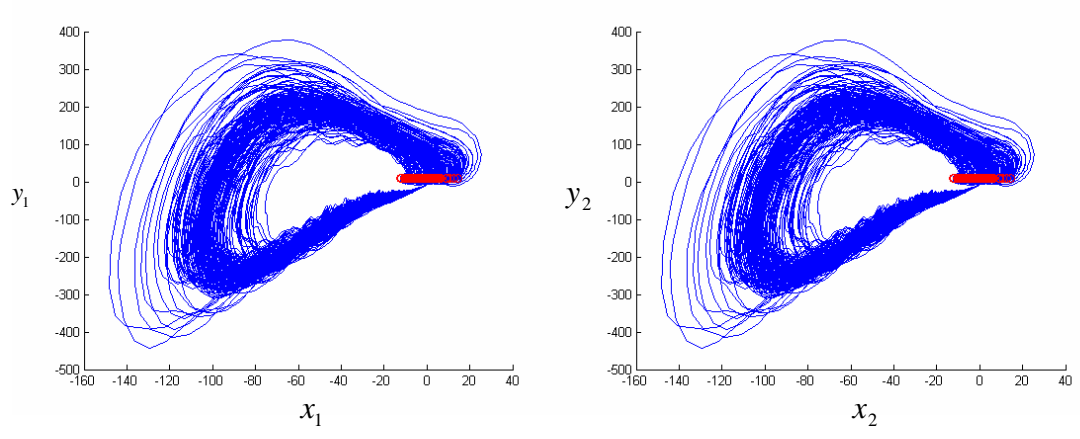
Fig. 3.15 The phase portraits of the synchronized nano resonator integral order

systems (4) and (5) with order $\alpha = \beta = 1$ for Case 2.

Fig. 3.16 The time histories of the errors of the states of the synchronized nano

resonator integral order systems (4) and (5) with order $\alpha = \beta = 1$ for Case 2.

Fig. 3.17 The phase portraits of the synchronized nano resonator fractional order systems (3.1) and (3.2) with order $\alpha = \beta = 0.1$ for Case 3.
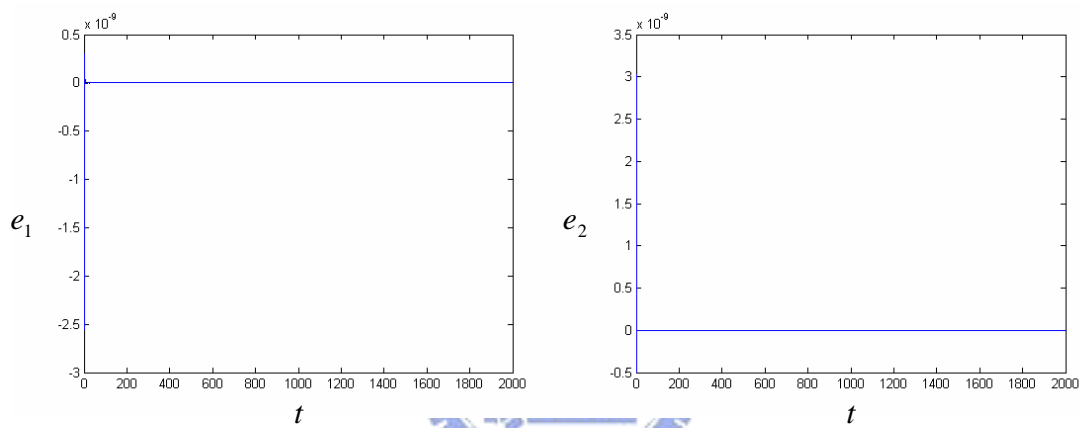

Fig. 3.18 The time histories of the errors of the states of the synchronized nano resonator fractional order systems (3.1) and (3.2) with order $\alpha = \beta = 0.1$ for Case 3.
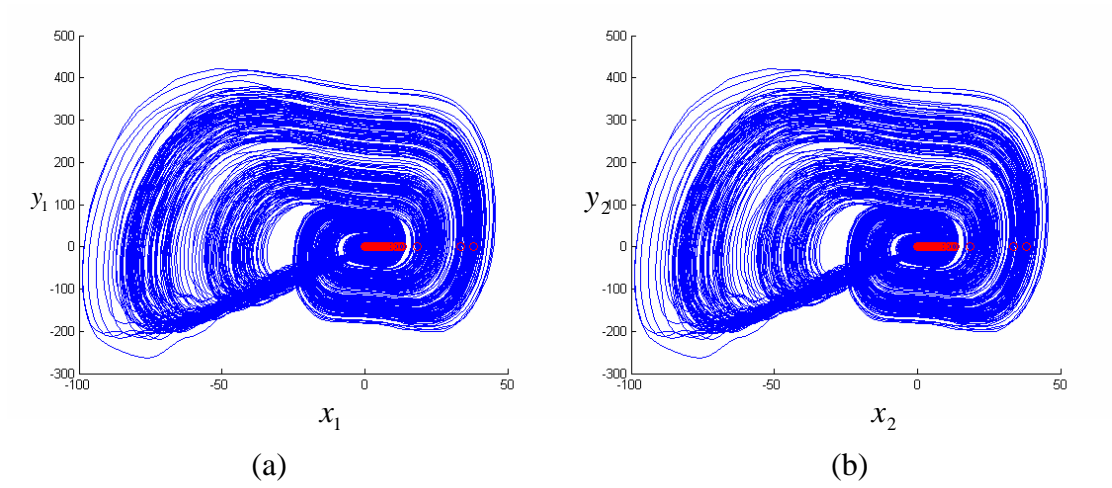
Fig. 3.19 The phase portraits of the synchronized nano resonator fractional order

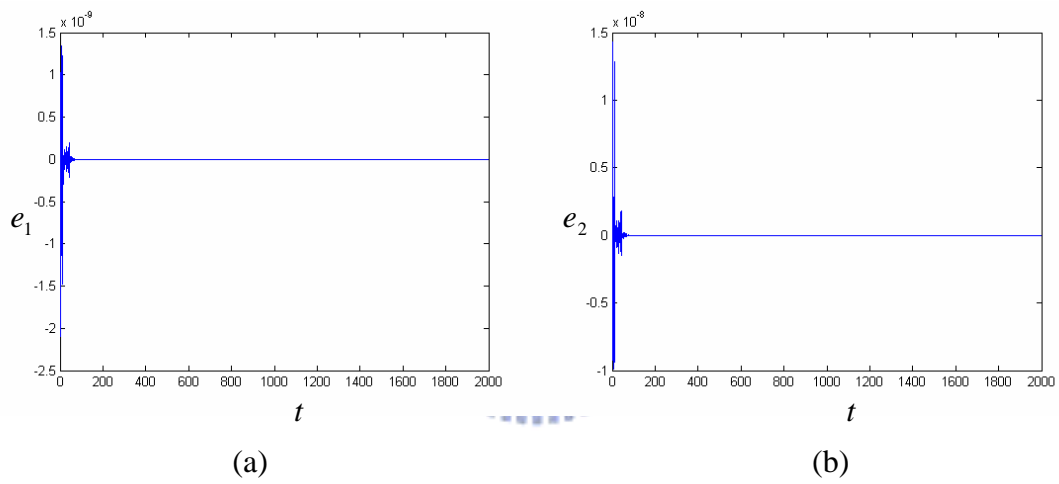systems (3.1) and (3.2) with order $\alpha = \beta = 0.4$ for Case 3.

Fig. 3.20 The time histories of the errors of the states of the synchronized nano

resonator fractional order systems (3.1) and (3.2) with order $\alpha = \beta = 0.4$ for Case 3.

Fig. 3.21 The phase portraits of the synchronized nano resonator fractional order

systems (3.1) and (3.2) with order $\alpha = \beta = 0.7$ for Case 3.

Fig. 3.22 The time histories of the errors of the states of the synchronized nano

resonator fractional order systems (3.1) and (3.2) with order $\alpha = \beta = 0.7$ for Case 3.
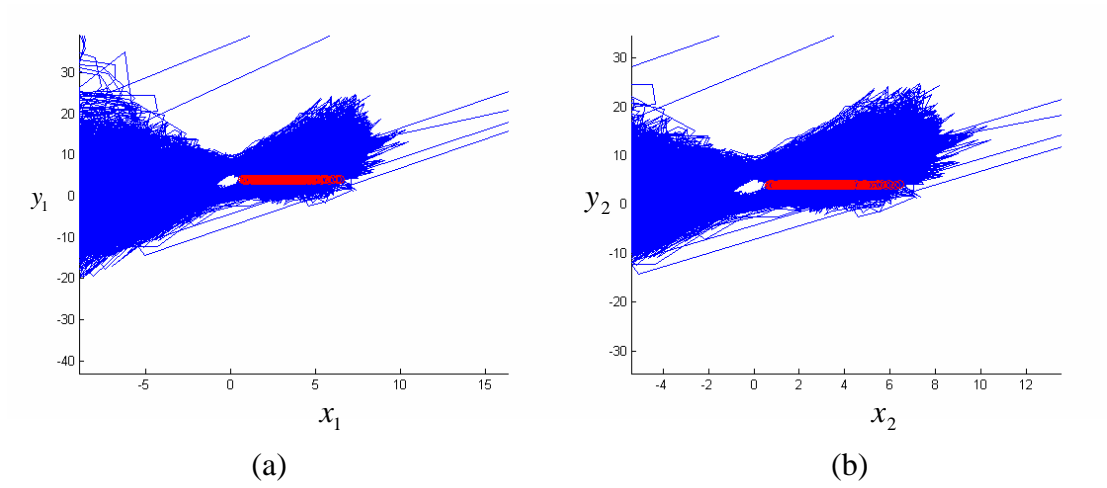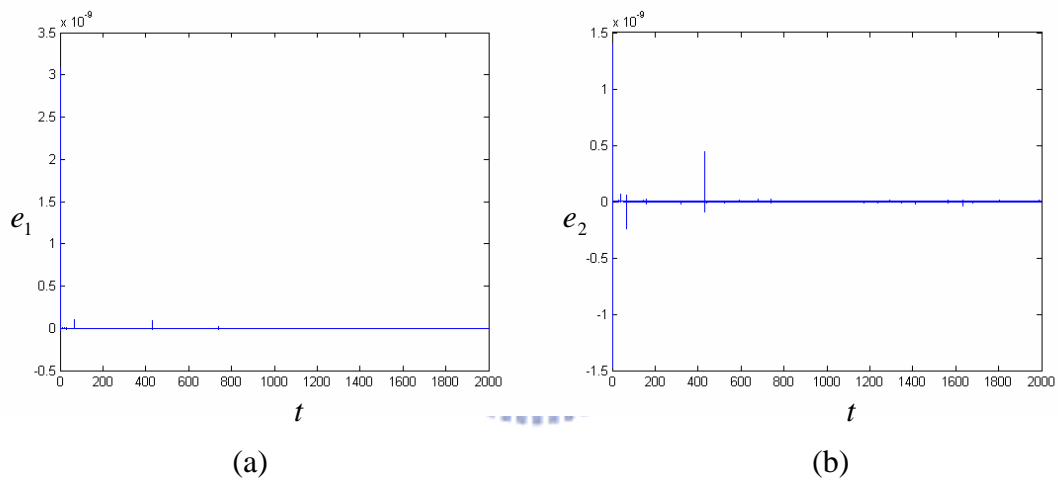
(a)   (b)

Fig. 3.23 The phase portraits of the synchronized nano resonator fractional order

systems (3.1) and (3.2) with order $\alpha = \beta = 0.9$ for Case 3.

(a)   (b)

Fig. 3.24 The time histories of the errors of the states of the synchronized nano

resonator fractional order systems (3.1) and (3.2) with order $\alpha = \beta = 0.9$ for Case 3.
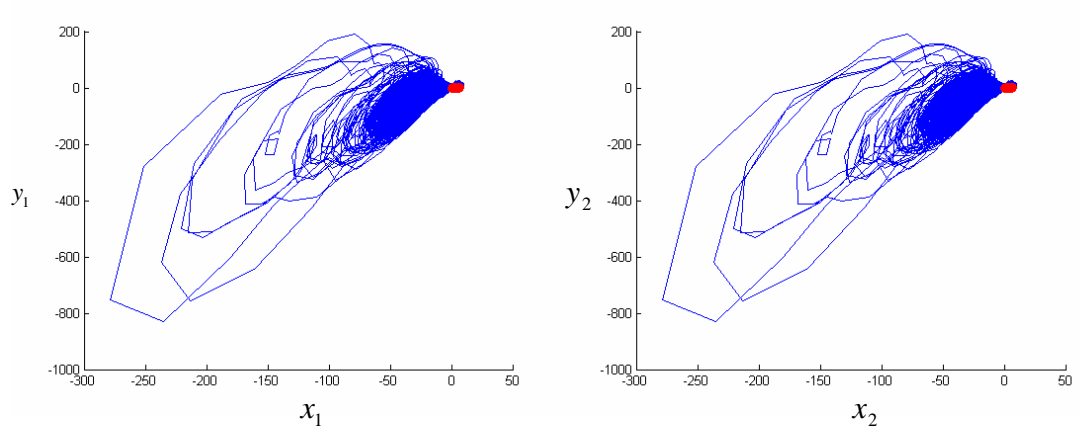
Fig. 3.25 The phase portraits of the synchronized nano resonator fractional order

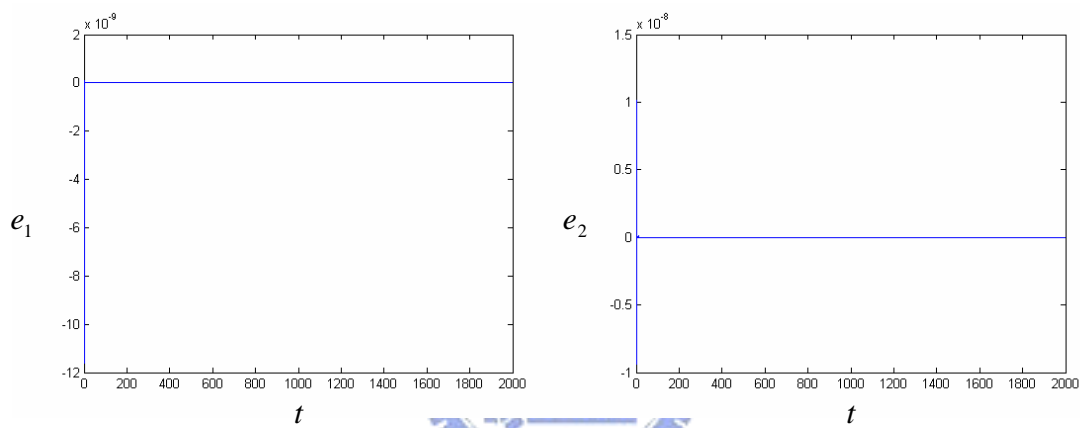systems (3.1) and (3.2) with order $\alpha = \beta = 0.1$ for Case 4.

Fig. 3.26 The time histories of the errors of the states of the synchronized nano

resonator fractional order systems (3.1) and (3.2) with order $\alpha = \beta = 0.1$ for Case 4.
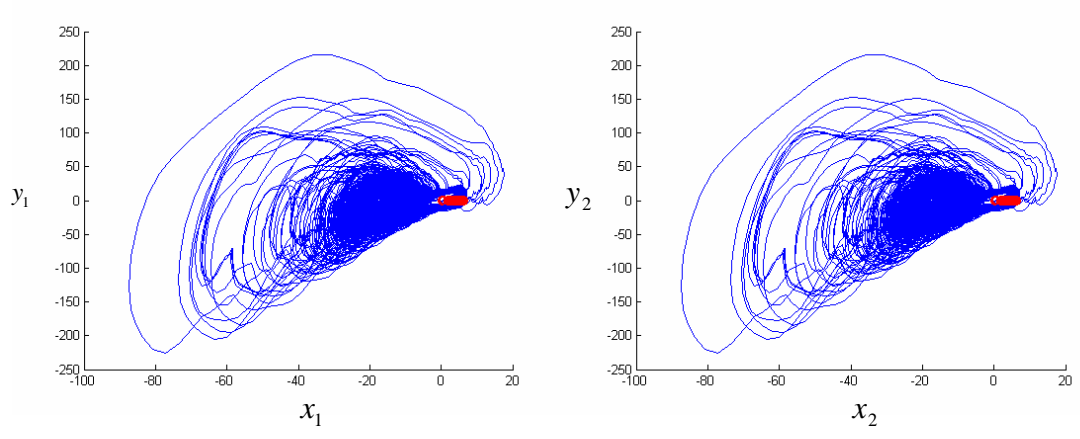
Fig. 3.27 The phase portraits of the synchronized nano resonator fractional order

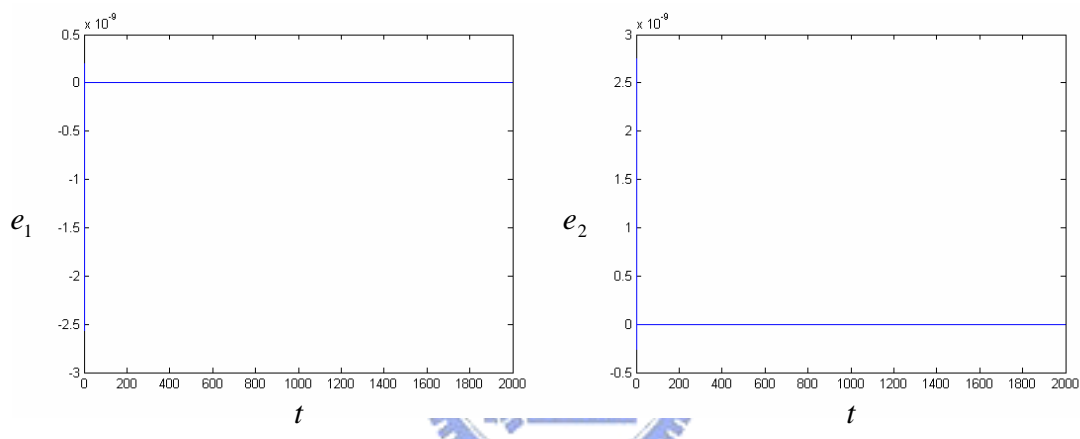systems (3.1) and (3.2) with order $\alpha = \beta = 0.4$ for Case 4.

Fig. 3.28 The time histories of the errors of the states of the synchronized nano

resonator fractional order systems (3.1) and (3.2) with order $\alpha = \beta = 0.4$ for Case 4.

Fig. 3.29 The phase portraits of the synchronized nano resonator fractional order

systems (3.1) and (3.2) with order $\alpha = \beta = 0.7$ for Case 4.

Fig. 3.30 The time histories of the errors of the states of the synchronized nano

resonator fractional order systems (3.1) and (3.2) with order $\alpha = \beta = 0.7$ for Case 4.
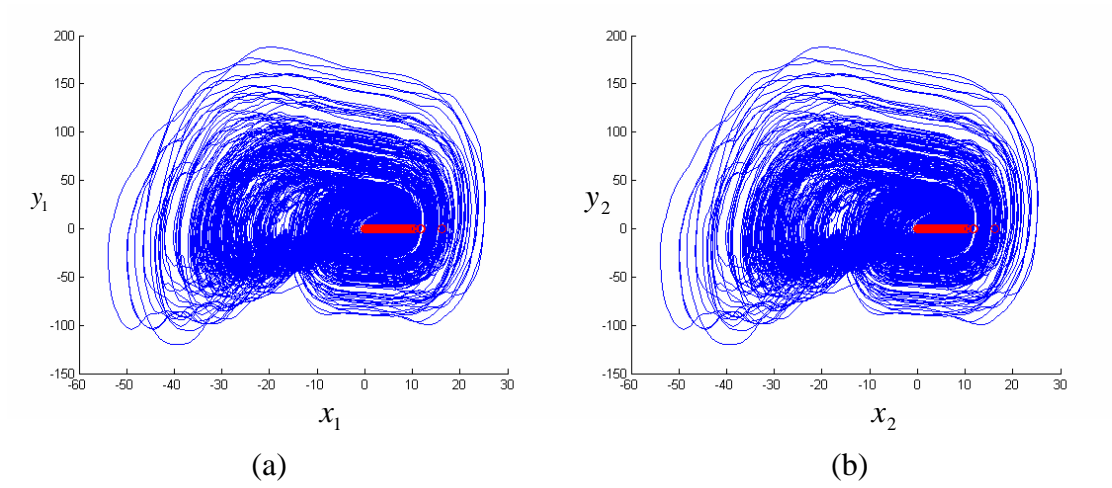
(a)   (b)

Fig. 3.31 The phase portraits of the synchronized nano resonator fractional order

systems (3.1) and (3.2) with order $\alpha = \beta = 0.9$ for Case 4.

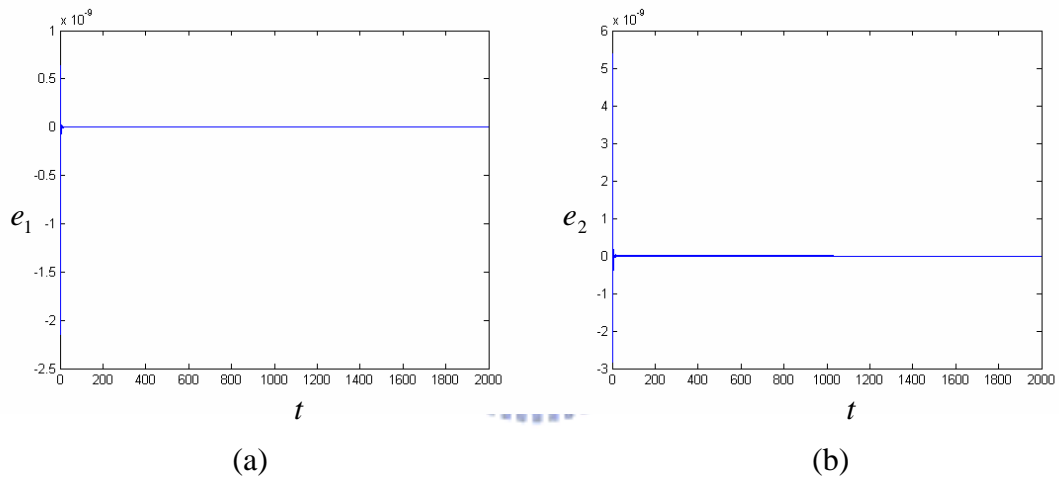(a)   (b)

Fig. 3.32 The time histories of the errors of the states of the synchronized nano

resonator fractional order systems (3.1) and (3.2) with order $\alpha = \beta = 0.9$ for Case 4.

Fig. 3.33 The phase portraits of the synchronized nano resonator fractional order

systems (3.1) and (3.2) with order $\alpha = \beta = 0.1$ for Case 5.

Fig. 3.34 The time histories of the errors of the states of the synchronized nano

resonator fractional order systems (3.1) and (3.2) with order $\alpha = \beta = 0.1$ for Case 5.

Fig. 3.35 The phase portraits of the synchronized nano resonator fractional order

systems (3.1) and (3.2) with order $\alpha = \beta = 0.4$ for Case 5.

Fig. 3.36 The time histories of the errors of the states of the synchronized nano

resonator fractional order systems (3.1) and (3.2) with order $\alpha = \beta = 0.4$ for Case 5.

Fig. 3.37 The phase portraits of the synchronized nano resonator fractional order

systems (3.1) and (3.2) with order $\alpha = \beta = 0.7$ for Case 5.

Fig. 3.38 The time histories of the errors of the states of the synchronized nano

resonator fractional order systems (3.1) and (3.2) with order $\alpha = \beta = 0.7$ for Case 5.

(a)　　　　　　　　　　　(b)

Fig. 3.39 The phase portraits of the synchronized nano resonator fractional order

systems (3.1) and (3.2) with order $\alpha = \beta = 0.9$ for Case 5.

(a)　　　　　　　　　　　(b)

Fig. 3.40 The time histories of the errors of the states of the synchronized nano

resonator fractional order systems (3.1) and (3.2) with order $\alpha = \beta = 0.9$ for Case 5.

Chapter 4

Anti-Control of Chaos of Fractional Order Nano Resonator Systems

4.1 Preliminaries

Anti-control of chaos of fractional order chaotic nano resonator system has been studied in this Chapter. By addition of an external term, we can obtain anti-control of chaos, i.e. changing state from regular to chaos. The addition of constant term k and of nonlinear term $kz|z|$ are used where z is the third state variable of the system. The results are illustrated by bifurcation diagrams.

4.2 Numerical Simulations for the Anti-Control of Chaos of fractional order chaotic nano resonator systems

Creating chaos is called anti-control of chaos at times [95]. The problem of anti-control of chaos is interesting, nontraditional, and indeed very challenging. In this section, two methods of anti-control, such as addition of a linear term k and a nonlinear term $kz|z|$, are proposed, which can excite the existing of chaos of the originally non-chaotic system. The results are demonstrated by numerical results, i.e. bifurcation diagrams.

First, we add an external linear input k to the second equation of (2.9). Thus Eq. (2.9) becomes

$$\begin{cases} \dfrac{d^{\alpha}x}{dt^{\alpha}} = y \\[2mm] \dfrac{d^{\beta}y}{dt^{\beta}} = -(a+bz)x - (a+bz)x^3 - cy + dz + k \\[2mm] \dfrac{dz}{dt} = w \\[2mm] \dfrac{dw}{dt} = -ez - fz \end{cases} \qquad (4.1)$$

The numerical results, i.e. bifurcation diagrams are shown in Fig. 6-1~6-7.

Second, we add an external nonlinear input $kz|z|$ to the second equation of (2.9).

Thus Eq. (2.9) becomes

$$\begin{cases} \dfrac{d^{\alpha}x}{dt^{\alpha}} = y \\[2mm] \dfrac{d^{\beta}y}{dt^{\beta}} = -(a+bz)x - (a+bz)x^3 - cy + dz + kz|z| \\[2mm] \dfrac{dz}{dt} = w \\[2mm] \dfrac{dw}{dt} = -ez - fz \end{cases} \qquad (4.2)$$
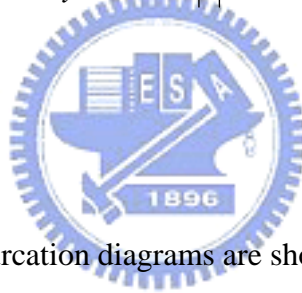
The numerical results, i.e. bifurcation diagrams are shown in Fig. 6-8~6-16.

We vary the derivative orders α, β, the system parameter d and the external input term k, the other system parameters are fixed. The system parameter d is chosen that making the behavior of system (2.9) preserve periodic phenomena. Changing the external input term k from zero upwards, the chaotic behavior is increased. Simulations are performed under $\alpha + \beta = 2$, $\alpha + \beta = 1.9$ where α, β are not integers. In our numerical simulations, five parameters $a = 0.2$, $b = 0.2$, $c = 0.4$, $e = 1$ and $f = 0.3$ are fixed, d and k is varied. The initial states of the nano resonator system are $x(0) = 0.003$, $y(0) = 0.004$, $z(0) = 1$ and $w(0) = 0$.
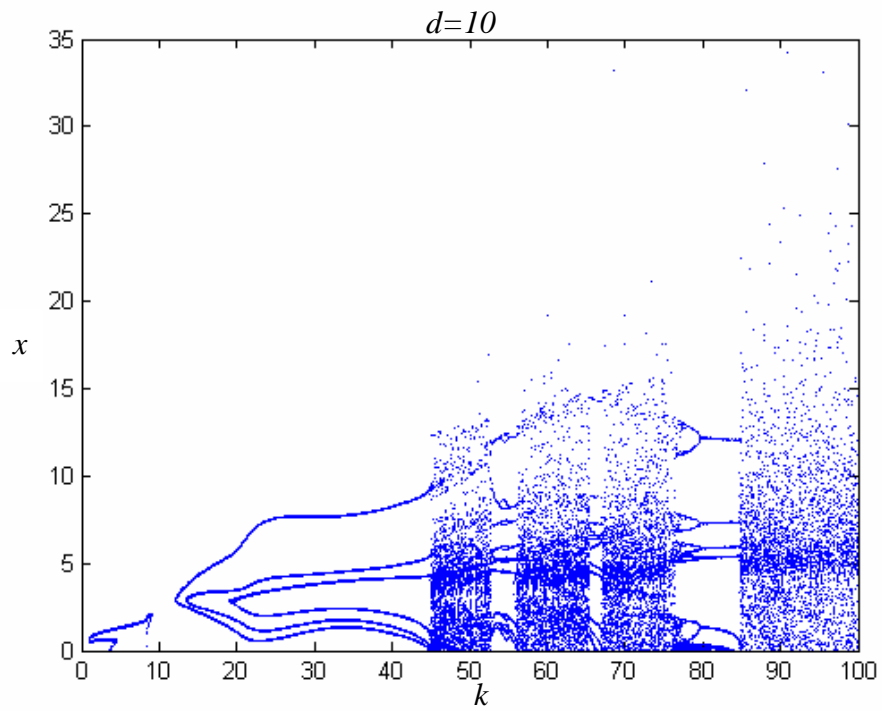
Fig. 4.1 The bifurcation diagram for the system (4.1) with order $\alpha = 0.2$ and

$\beta = 1.7$.
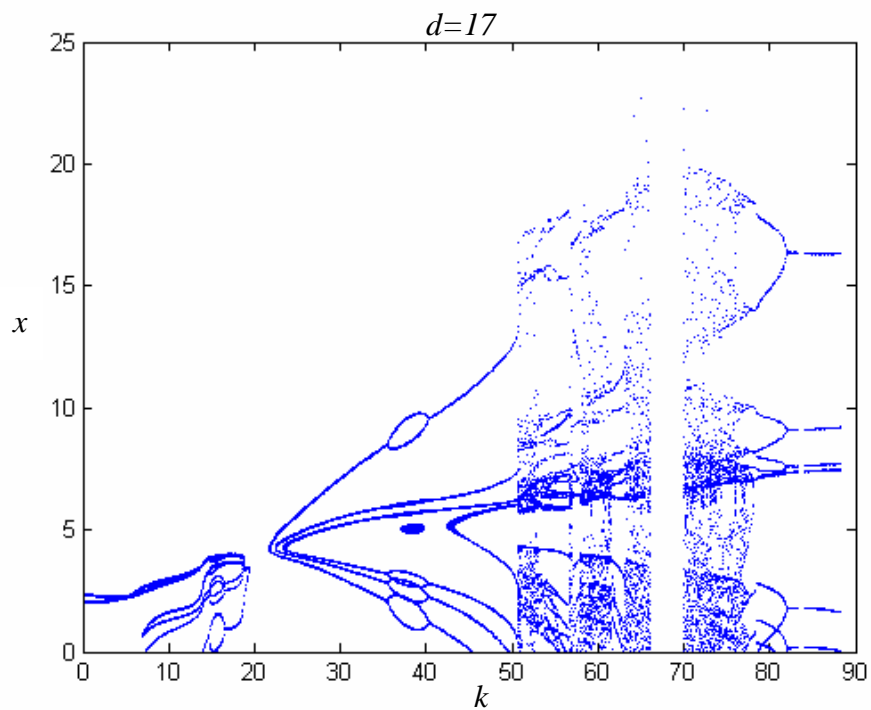
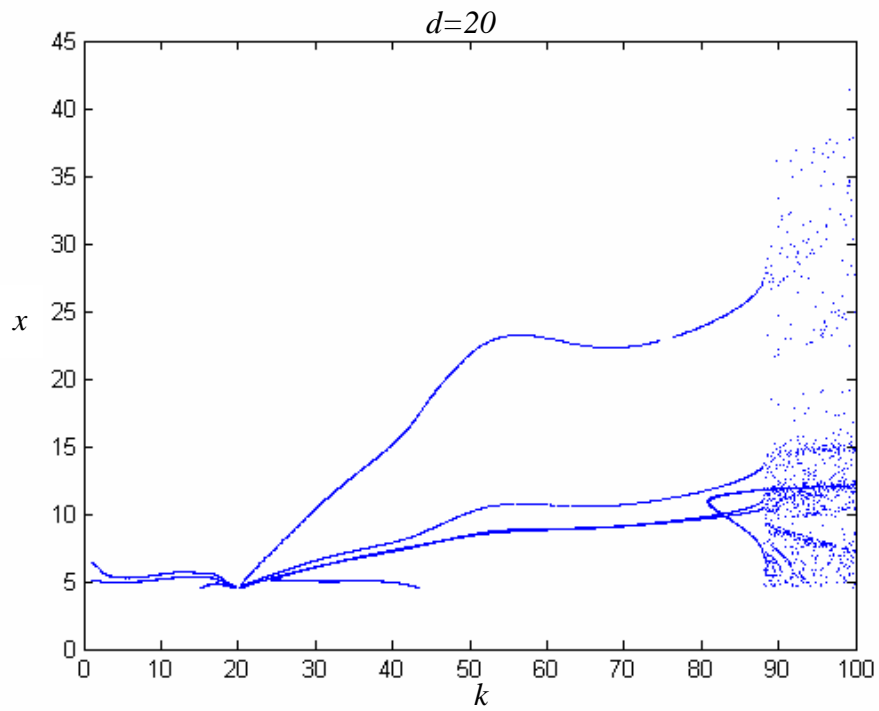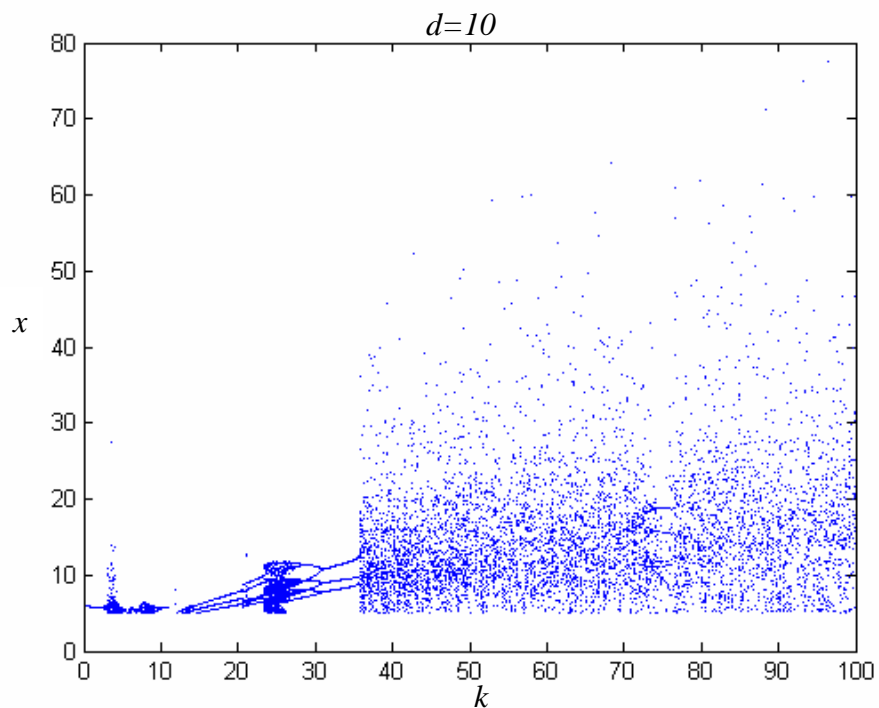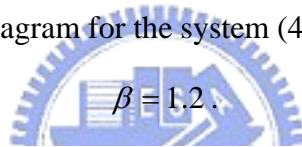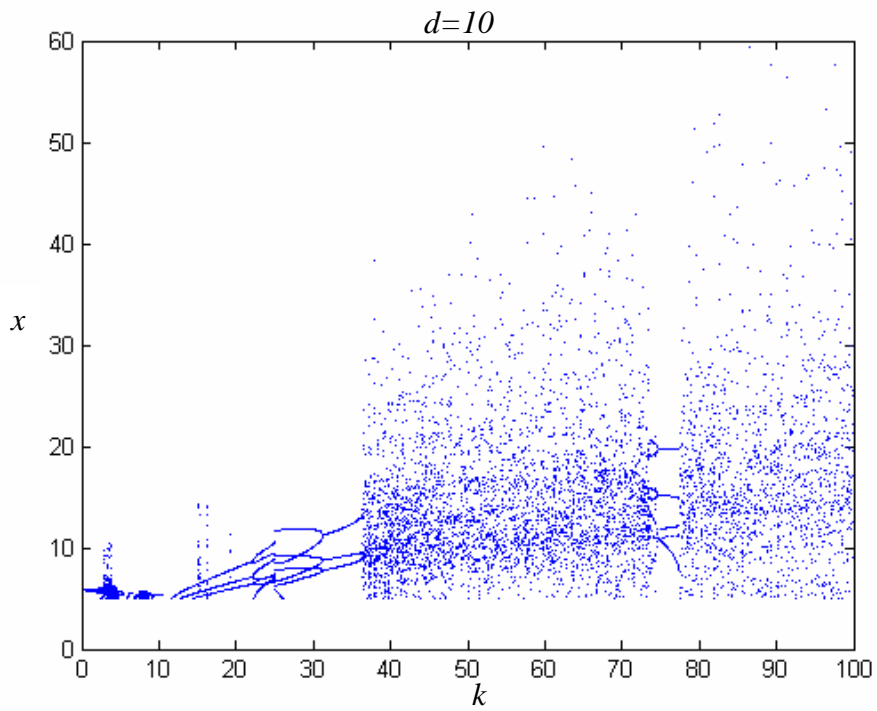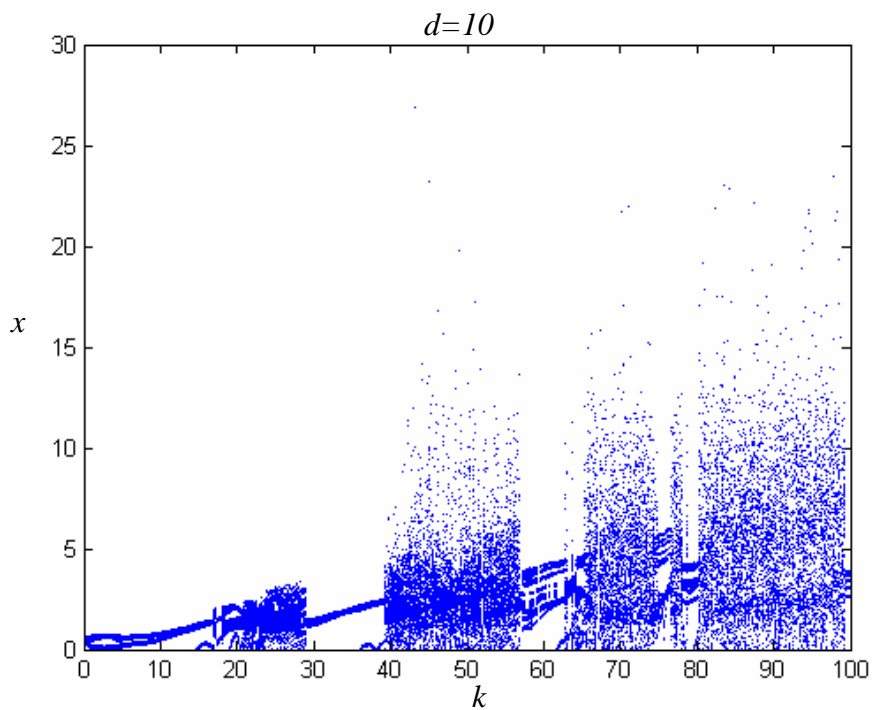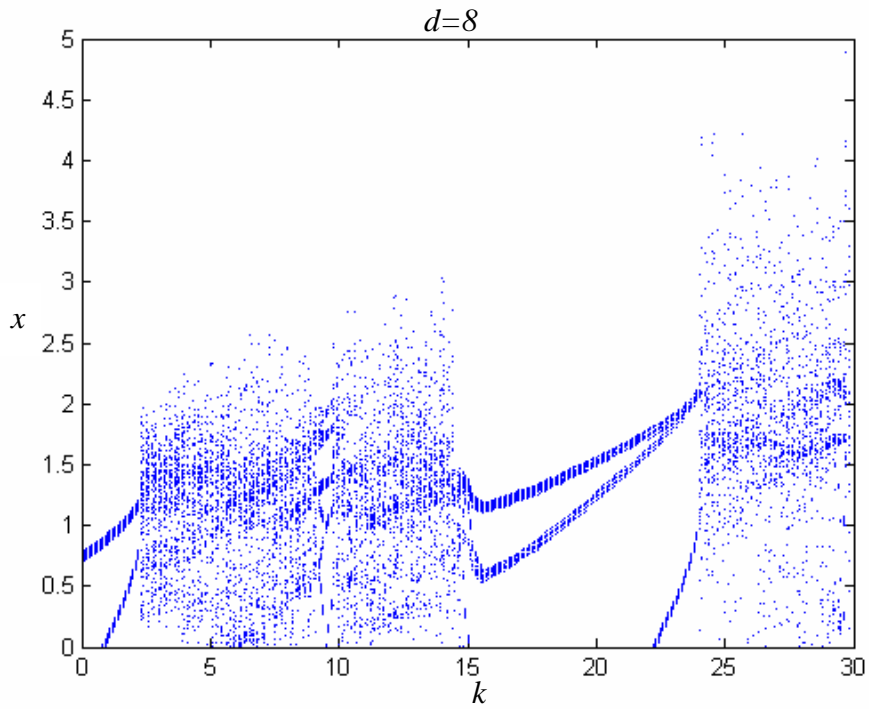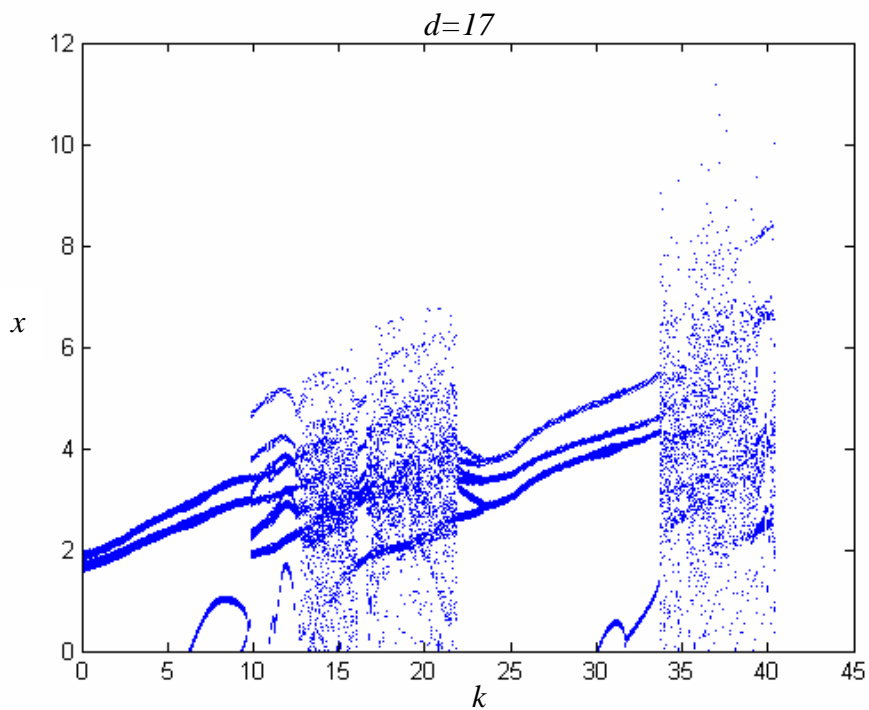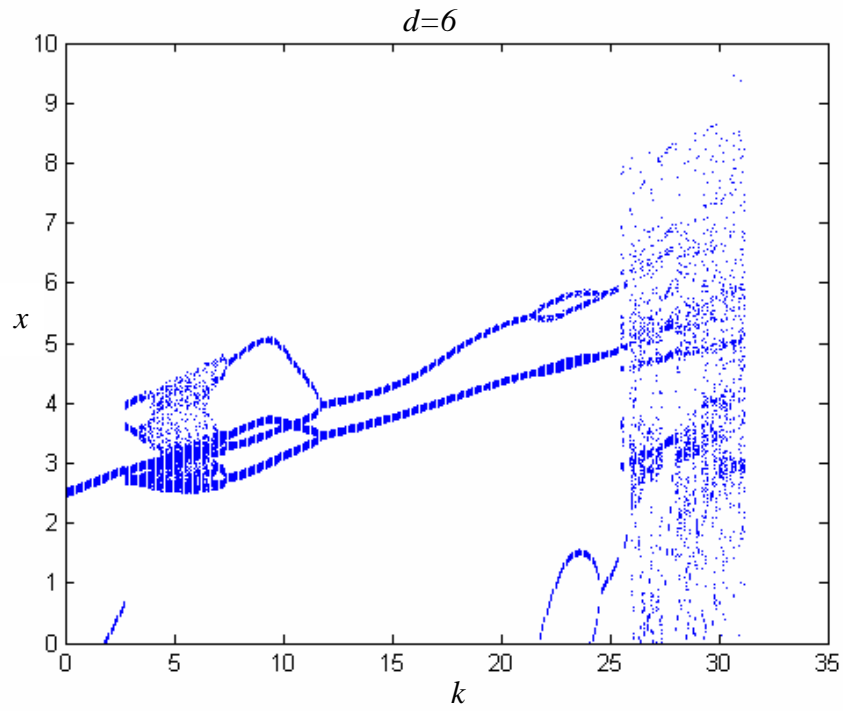Fig. 4.2 The bifurcation diagram for the system (4.1) with order $\alpha = 0.3$ and

$\beta = 1.6$.

d=6
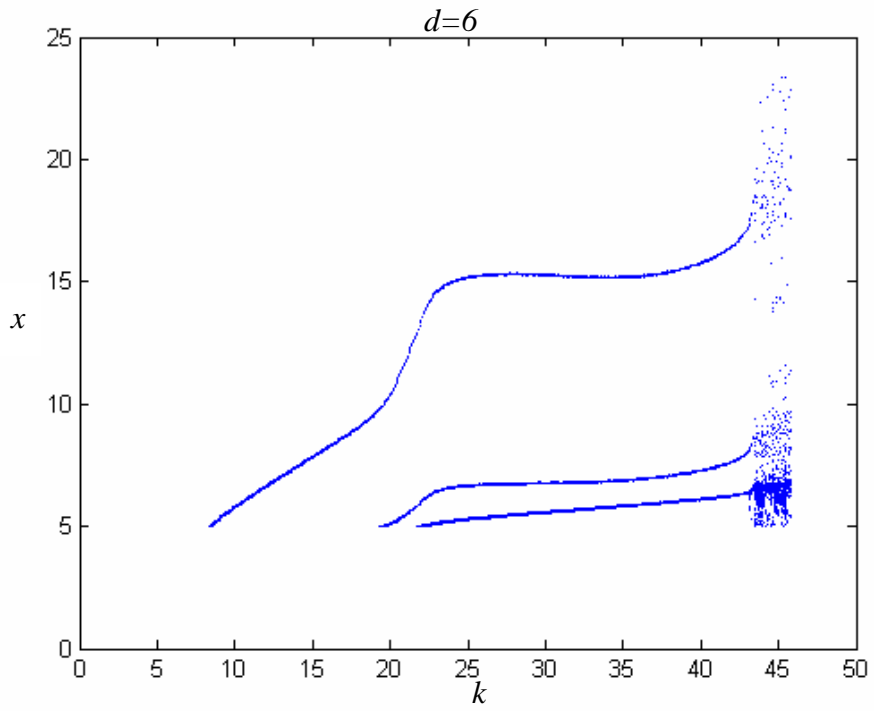
Fig. 4.3 The bifurcation diagram for the system (4.1) with order $\alpha = 0.5$ and $\beta = 1.5$.
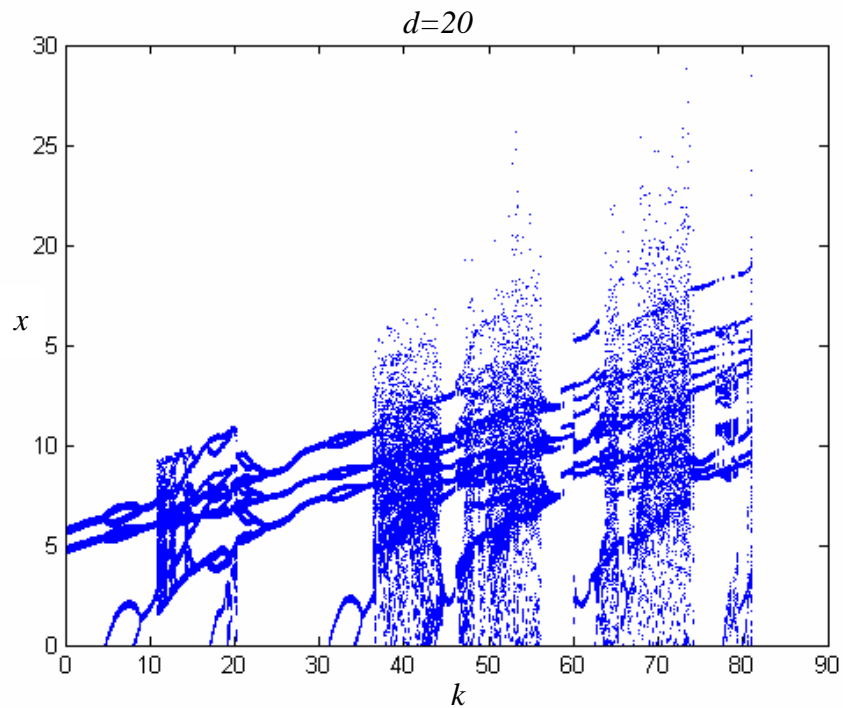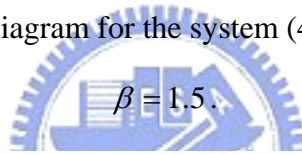

d=20
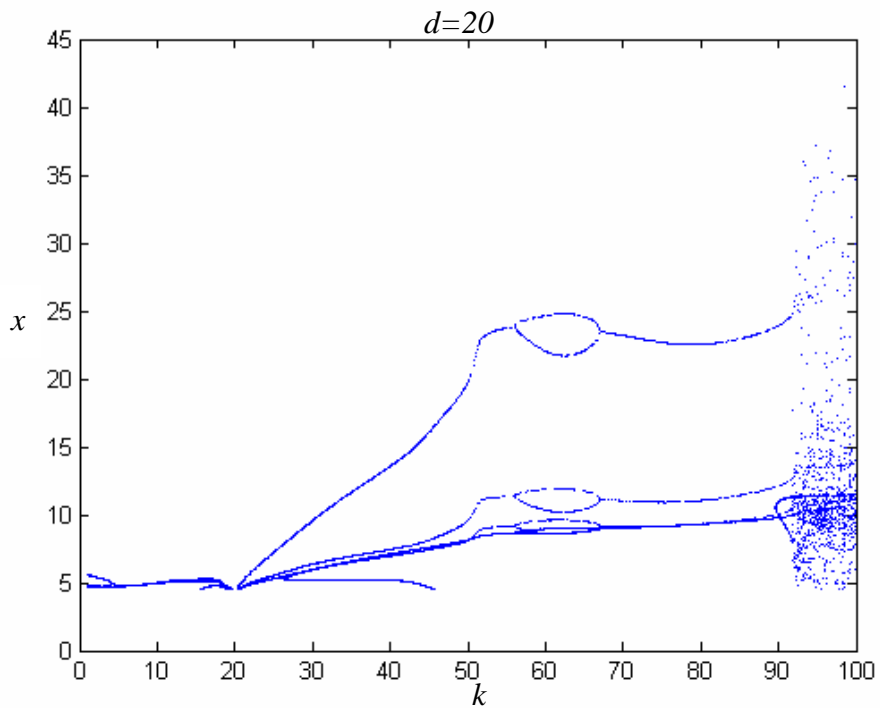
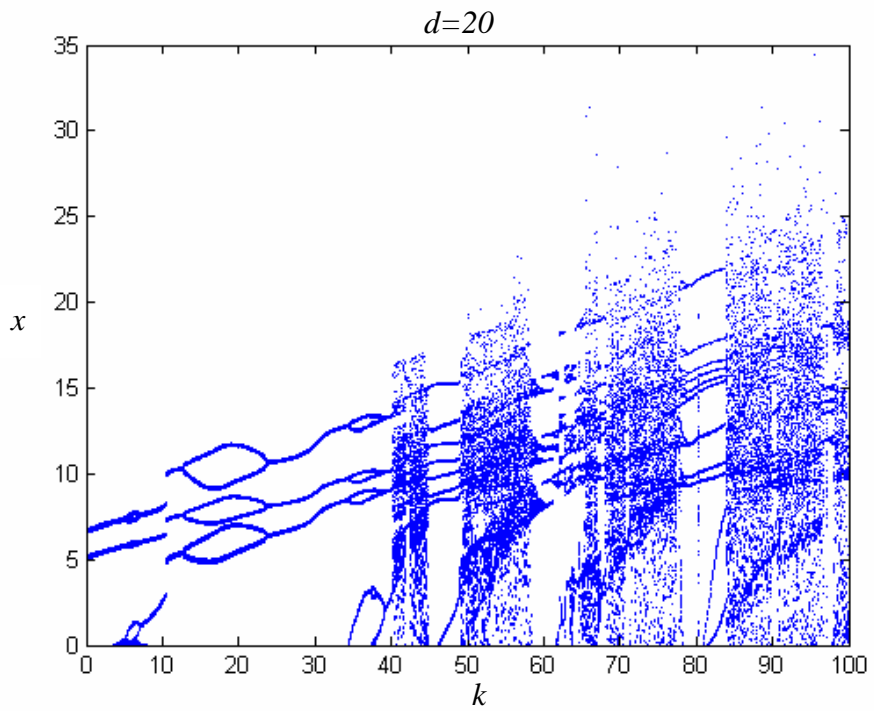Fig. 4.4 The bifurcation diagram for the system (4.1) with order $\alpha = 0.6$ and $\beta = 1.3$.

Fig. 4.5 The bifurcation diagram for the system (4.1) with order $\alpha = 0.7$ and

$\beta = 1.2$.

Fig. 4.6 The bifurcation diagram for the system (4.1) with order $\alpha = 0.9$ and

$\beta = 1.1$.

Fig. 4.7 The bifurcation diagram for the system (4.1) with order $\alpha = 1.1$ and

$\beta = 0.9$.

Fig. 4.8 The bifurcation diagram for the system (4.2) with order $\alpha = 0.2$ and

$\beta = 1.7$.

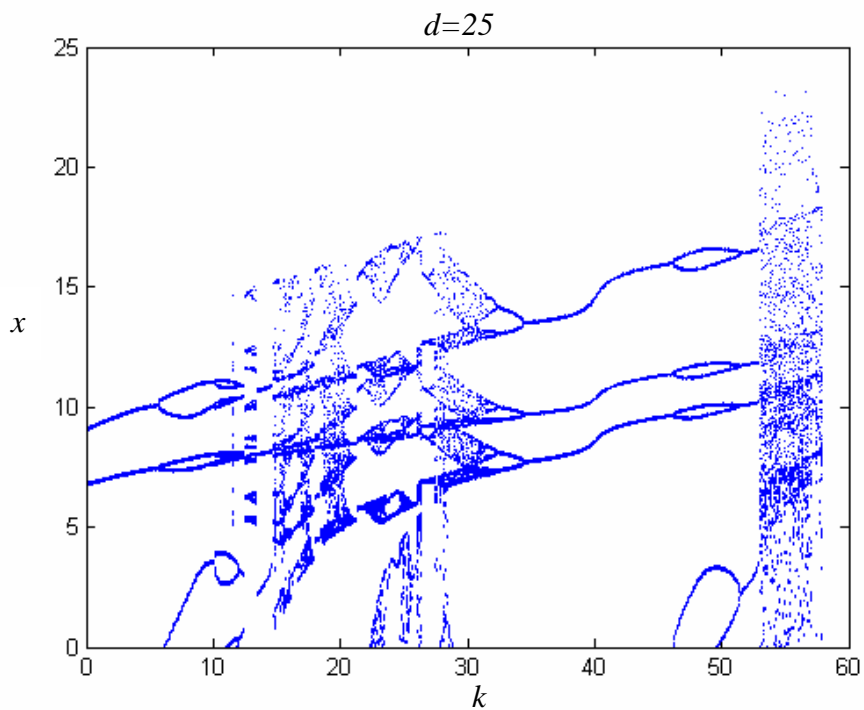Fig. 4.9 The bifurcation diagram for the system (4.2) with order $\alpha = 0.2$ and $\beta = 1.8$.
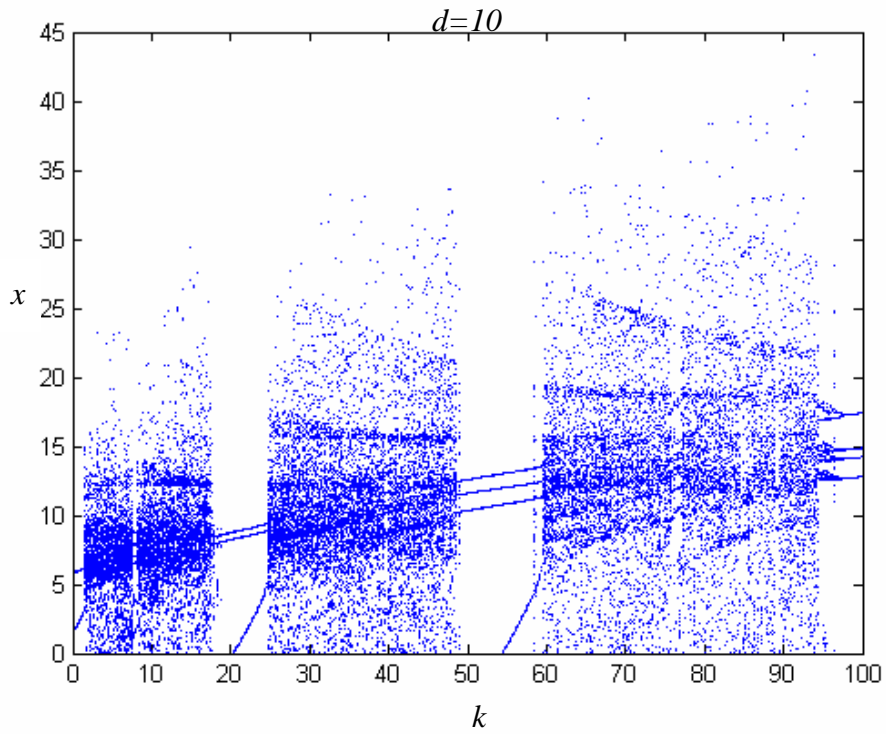

Fig. 4.10 The bifurcation diagram for the system (4.2) with order $\alpha = 0.3$ and $\beta = 1.6$.

Fig. 4.11 The bifurcation diagram for the system (4.2) with order $\alpha = 0.5$ and $\beta = 1.5$.

Fig. 4.12 The bifurcation diagram for the system (4.2) with order $\alpha = 0.6$ and $\beta = 1.3$.

Fig. 4.13 The bifurcation diagram for the system (4.2) with order $\alpha = 0.7$ and

$\beta = 1.2$.

Fig. 4.14 The bifurcation diagram for the system (4.2) with order $\alpha = 0.8$ and

$\beta = 1.2$.

Fig. 4.15 The bifurcation diagram for the system (4.2) with order $\alpha = 1.1$ and $\beta = 0.9$.
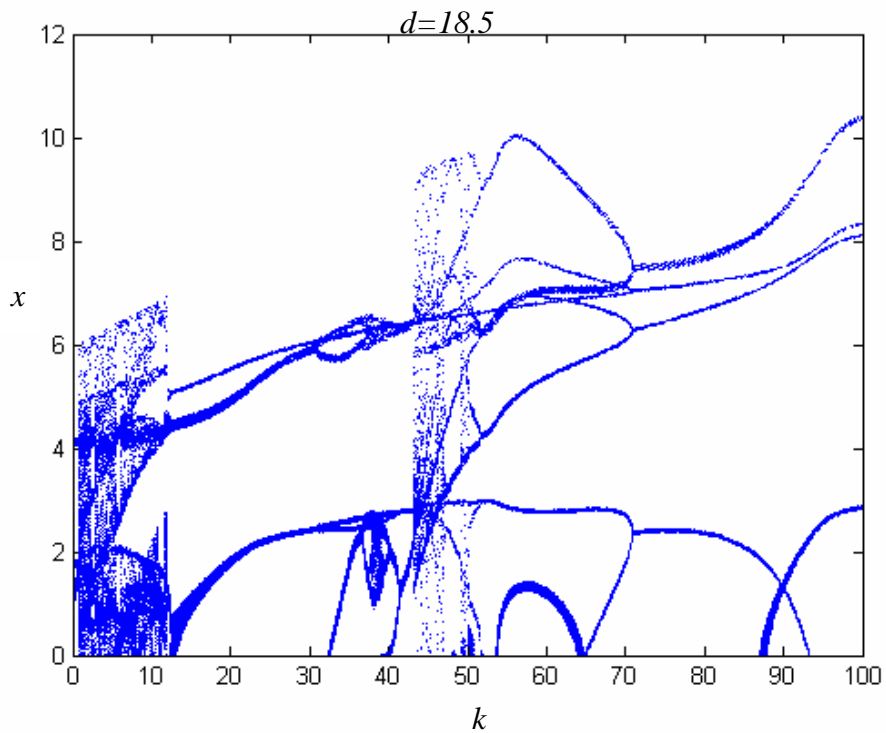

Fig. 4.16 The bifurcation diagram for the system (4.2) with order $\alpha = 1.8$ and $\beta = 0.2$.

Chapter 5

Parameter Excited Anti-Control of Chaos of Fractional Order Nano Resonator Systems

5.1 Preliminaries

Parameter excited anti-control of chaos of fractional order chaotic nano resonator system is studied in this Chapter. By replacing the system parameter with a function of chaotic state variables of a modified van der Pol system, we can obtain anti-control of chaos. It is named parameter excited anti-control of chaos which can be successfully obtained for very low total fraction order 0.2. Numerical simulations are illustrated by phase portraits, Poincaré maps and bifurcation diagrams.

5.2 A Modified Van der Pol System

The equation of a van der Pol oscillator driven by a periodic force can be written as

$$\ddot{x} + \varphi x + a\dot{x}(x^2 - 1) - b \sin \omega t = 0 \tag{5.1}$$

In Eq. (5.1), the linear term stands for a conservative harmonic force which determines the intrinsic oscillation frequency. The self-sustaining mechanism which is responsible for the perpetual oscillation rests on the nonlinear term. Energy exchange with the external agent depends on the magnitude of displacement $|x|$ and on the sign of velocity $\dot{x}$. During a complete cycle of oscillation, the energy is dissipated if displacement $x(t)$ is large than one, and that energy is fed-in if $|x| < 1$. The time-dependent term stands for the external driving force with amplitude b and frequency ω. Eq. (5.1) can be rewritten as two first order equations:

$$\begin{cases} \dot{x} = y \\ \dot{y} = -\varphi x + a(1 - x^2)y + b \sin \omega t \end{cases} \tag{5.2}$$

The modified van der Pol system studied in this thesis is

$$\begin{cases} \dfrac{dx_2}{dt} = y_2 \\[2mm] \dfrac{dy_2}{dt} = -x_2 + a(1 - x_2{}^2)y_2 + bz_2 \\[2mm] \dfrac{dz_2}{dt} = w_2 \\[2mm] \dfrac{dw_2}{dt} = -cz_2 - dz_2{}^3 \end{cases} \qquad (5.3)$$

can be separated into two parts:

$$\begin{cases} \dfrac{dx}{dt} = y \\[2mm] \dfrac{dy}{dt} = -x + a(1 - x^2)y + bz \end{cases} \qquad (5.4)$$

and

$$\begin{cases} \dfrac{dz}{dt} = w \\[2mm] \dfrac{dw}{dt} = -cz - dz^3 \end{cases} \qquad (5.5)$$

In Eq. (5.2), replaceing $\sin \omega t$ by z which is the periodic time function solution of the nonlinear oscillator (5.5), we obtain system (5.4). In Eq. (5.5) if $d = 0$, z is a sinusoidal function of time. Now $d \neq 0$, z is a periodic motion of time but not a sinusoidal function of time. As a result, system (5.4) can be considered as a nonautonomous system with two states, while system (5.3) consisting of Eq. (5.4) and Eq. (5.5) can be considered as an autonomous system with four states.

5.3 Numerical Simulations for the Parameter Excited Anti-Control of Chaos of Fractional Order Chaotic Nano Resonator Systems

In this section, the method of anti-control, such as replacing the parameter d of system (2.9) by a nonlinear term $ky_2 + d$ where y_2 is a state of system (5.3), is proposed:

$$\begin{cases} \dfrac{d^{\alpha} x_1}{dt^{\alpha}} = y_1 \\[2mm] \dfrac{d^{\beta} y_1}{dt^{\beta}} = -(a + b z_1) x_1 - (a + b z_1) x_1^{3} - c y_1 + (k y_2 + d) z_1 \\[2mm] \dfrac{d z_1}{dt} = w_1 \\[2mm] \dfrac{d w_1}{dt} = -e z_1 - f z_1 \end{cases} \qquad (5.6)$$

which can chaotize originally non-chaotic system. The results are shown by numerical simulations, i.e. phase portraits, Poincaré maps and bifurcation diagrams shown in Fig. 5.1 ~ 5.9.

We vary the derivative orders α, β and the gain k, the other system parameters are fixed. From the bifurcation diagrams, changing the gain k from zero upwards increases the wandering range of chaotic state variables. Simulations are performed under $\alpha = \beta = 0.1 \sim 0.9$. In system (9), six parameters $a = 0.2$, $b = 0.2$, $c = 0.4$, $d = 10$, $e = 1$ and $f = 0.3$ are fixed, k is from 0 to 5. In system (12), four parameters $a = 5$, $b = 1$, $c = 1$ and $d = 0.0001$ are fixed and the system behavior is chaotic. The initial states of the nano resonator system are $x(0) = 0.003$, $y(0) = 0.004$, $z(0) = 1$ and $w(0) = 0$.
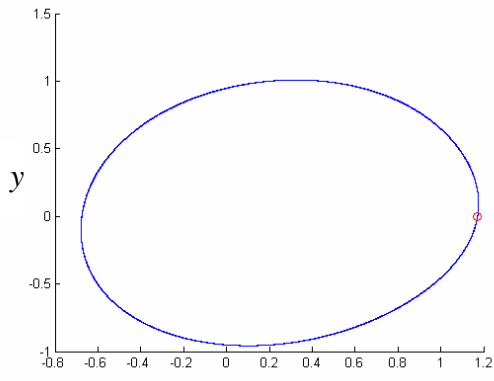
(a)
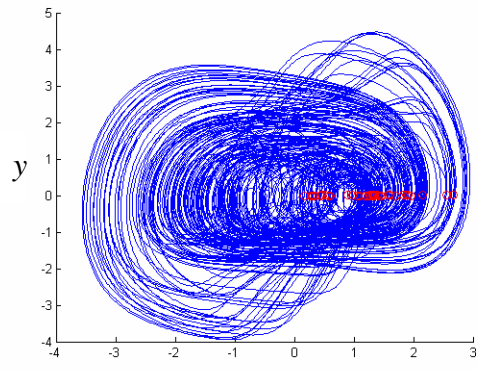
(b)
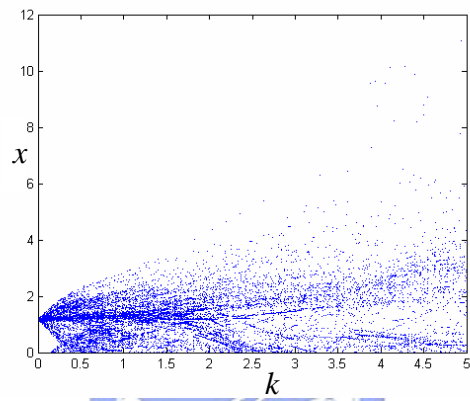
(c)

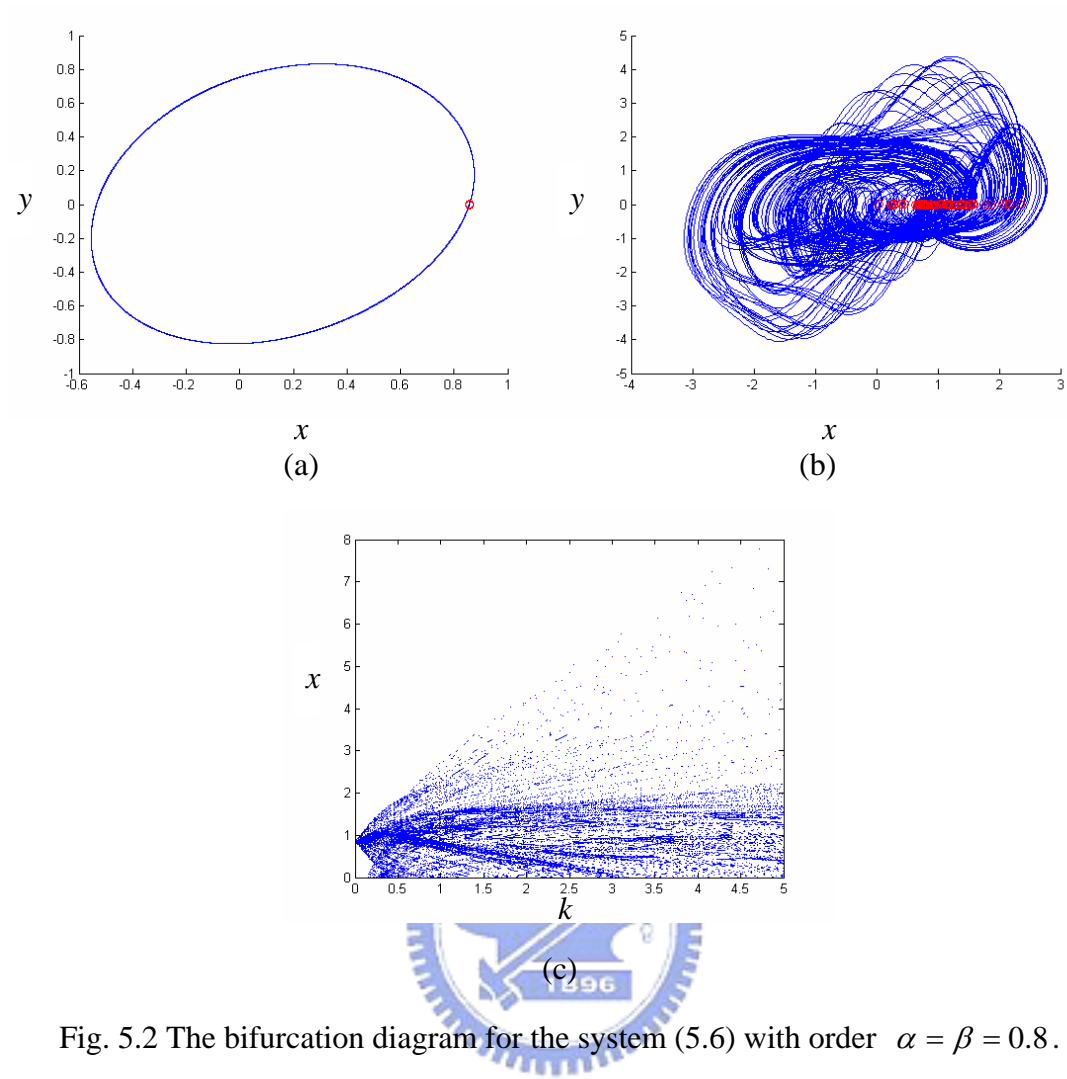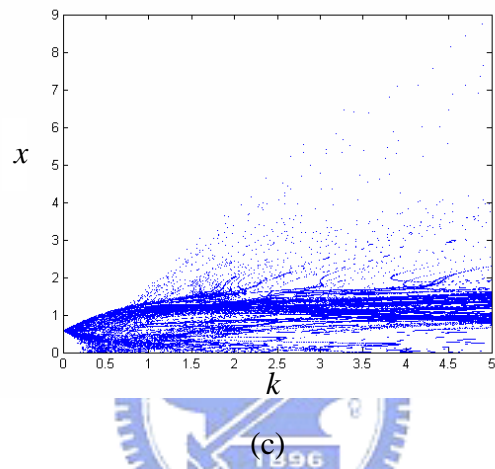Fig. 5.1 The bifurcation diagram for the system (5.6) with order $\alpha = \beta = 0.9$.

(a)

(b)

(c)

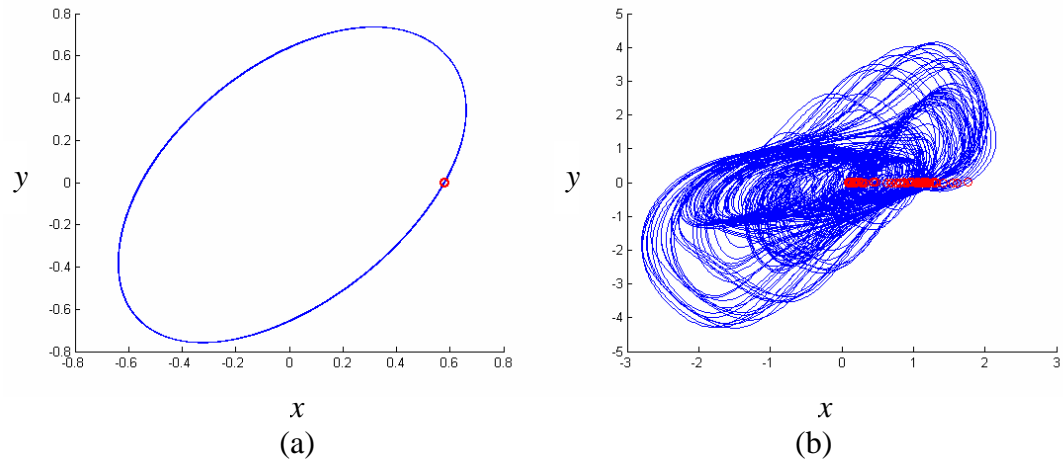Fig. 5.2 The bifurcation diagram for the system (5.6) with order $\alpha = \beta = 0.8$.

(a)

(b)

(c)

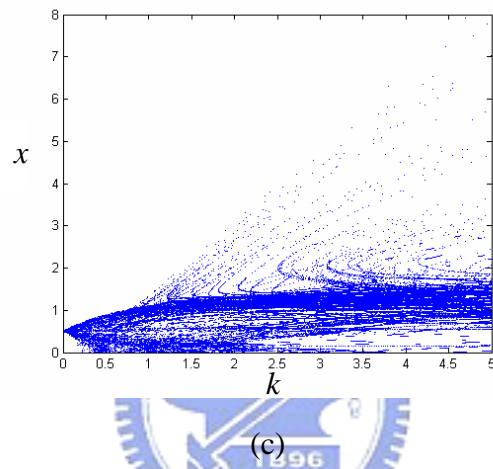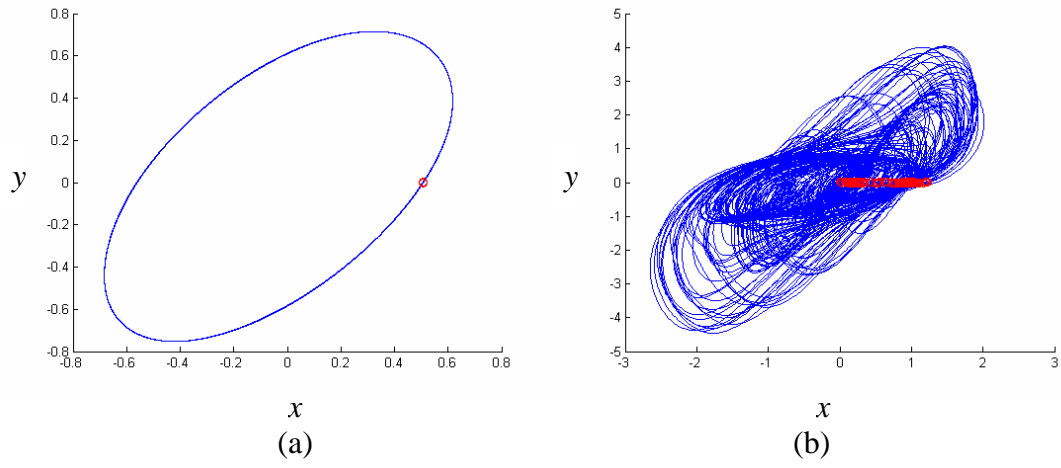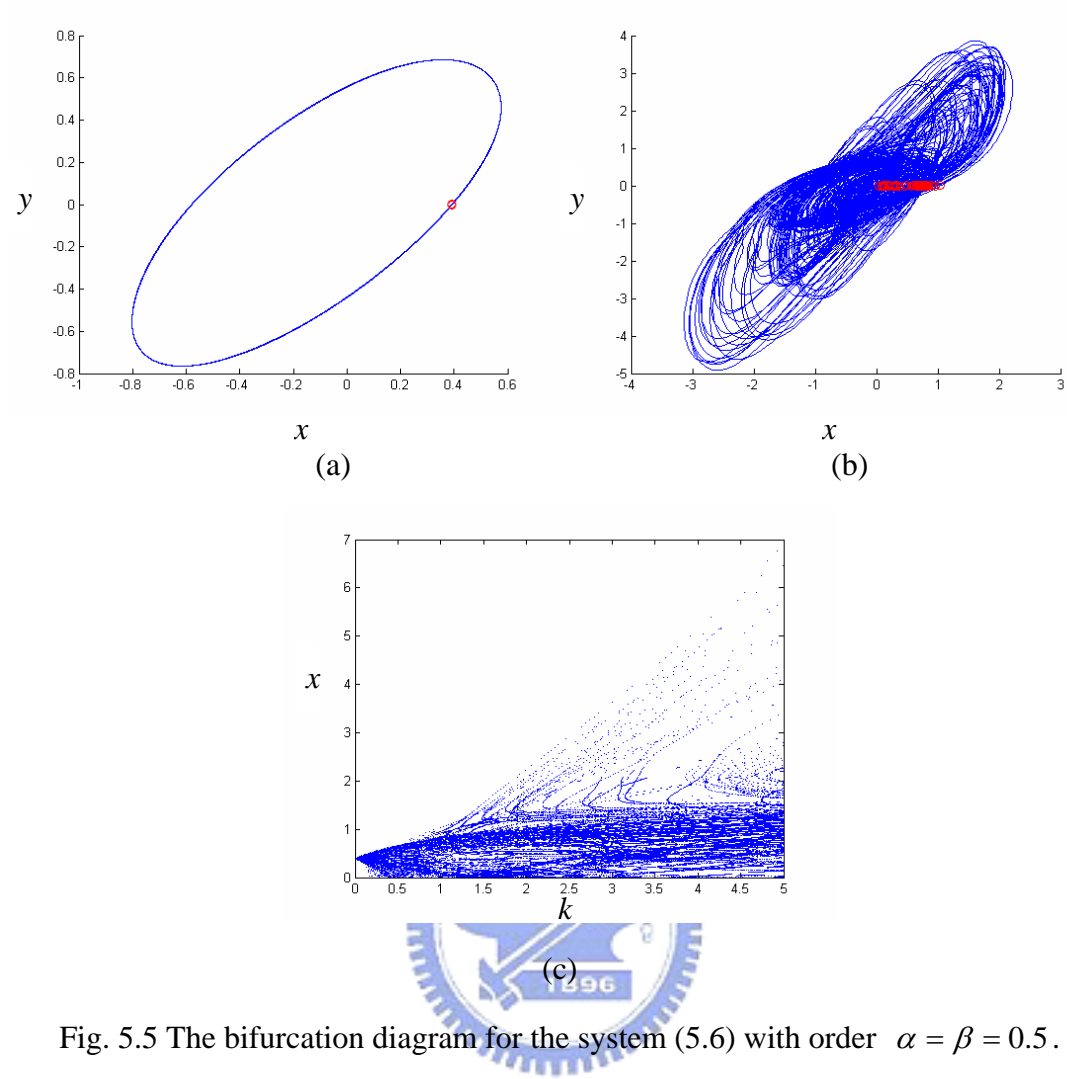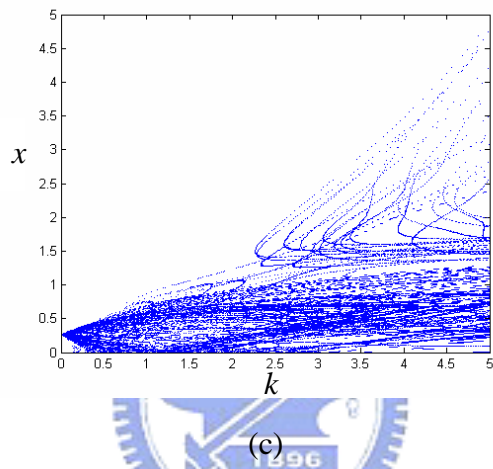Fig. 5.3 The bifurcation diagram for the system (5.6) with order $\alpha = \beta = 0.7$.

(a)

(b)

(c)

Fig. 5.4 The bifurcation diagram for the system (5.6) with order $\alpha = \beta = 0.6$.

(a)

(b)

(c)

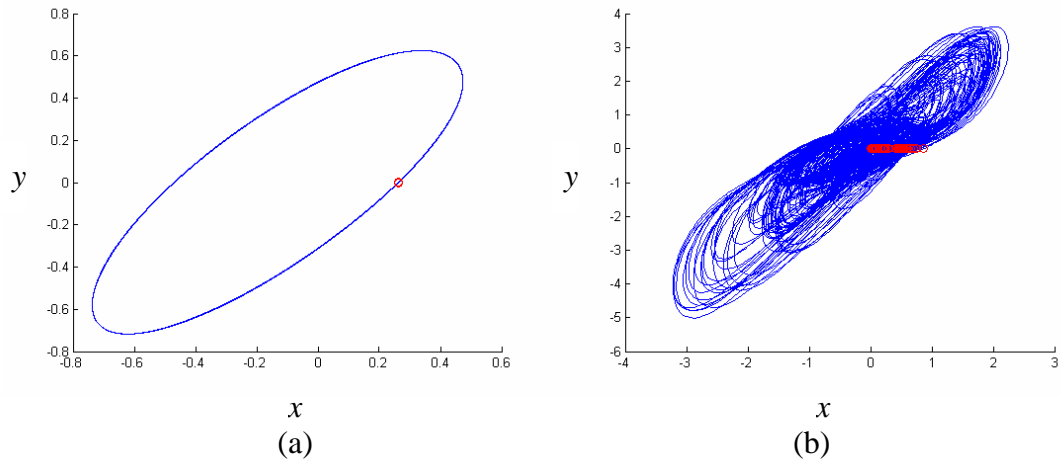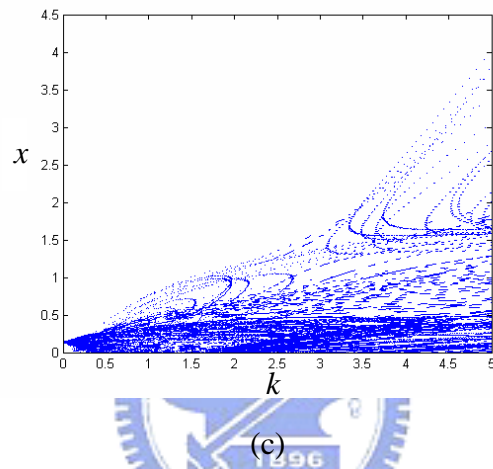Fig. 5.5 The bifurcation diagram for the system (5.6) with order $\alpha = \beta = 0.5$.

(a)   (b)

(c)

Fig. 5.6 The bifurcation diagram for the system (5.6) with order $\alpha = \beta = 0.4$.
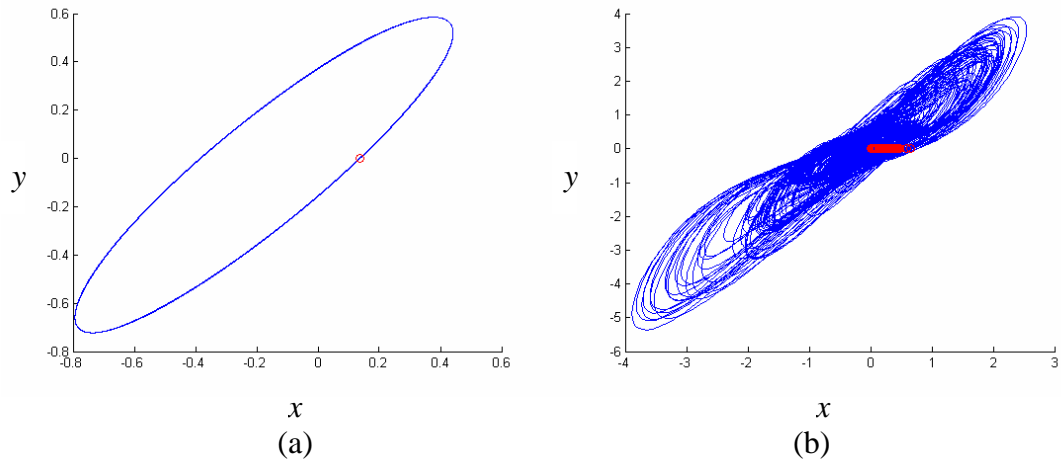
(a)

(b)

(c)

Fig. 5.7 The bifurcation diagram for the system (5.6) with order $\alpha = \beta = 0.3$.
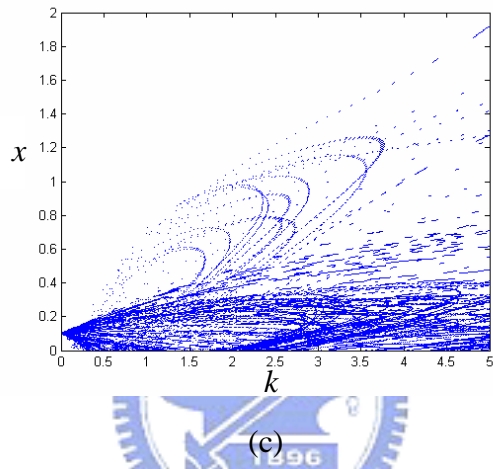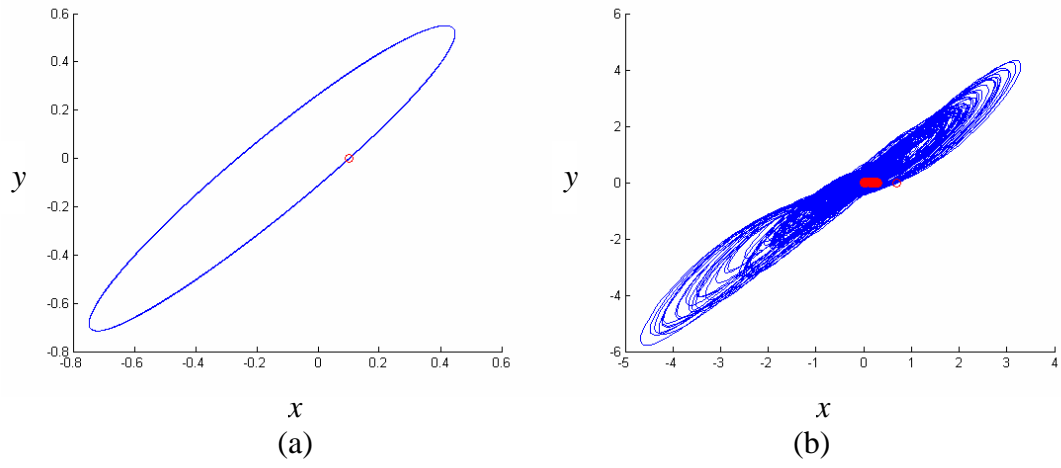
(a)

(b)

(c)

Fig. 5.8 The bifurcation diagram for the system (5.6) with order $\alpha = \beta = 0.2$.
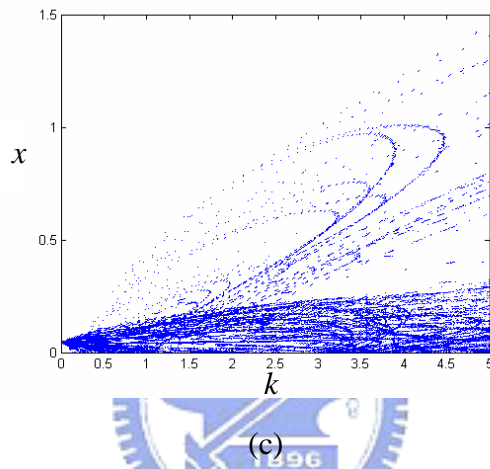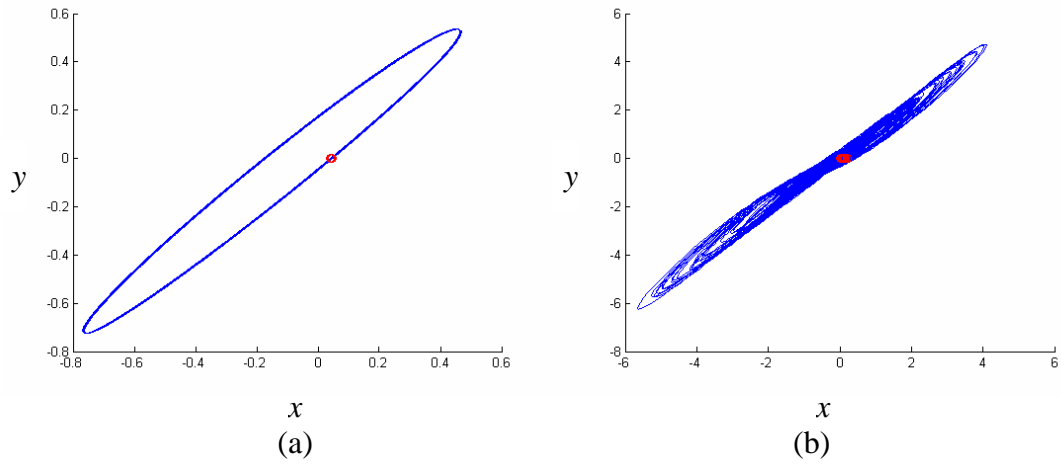
(a)

(b)

(c)

Fig. 5.9 The bifurcation diagram for the system (5.6) with order $\alpha = \beta = 0.1$.

Chapter 6

Conclusions

In this thesis, the chaotic behaviors of a nonautonomous nonlinear nano resonator system are investigated by means of phase portraits, Poincaré maps and bifurcation diagrams. The total orders of the system for the existence of chaos are 1.9 and 2.0.

Parameter excited chaos synchronizations of uncoupled integral and fractional order nano resonator systems are obtained by replacing their corresponding parameters by the same function of chaotic state variables of a third identical chaotic system. Numerical simulations for integral and fractional order nano resonator systems are given for order $1 \sim 0.1$. It is found that this approach is very effective even for very low total fractional order 0.2. An interesting phenomenon is found that the lower the total fractional order is, the faster the synchronization is accomplished.

Anti-control of chaos of fractional order nano resonator systems is studied. Three methods of anti-control, such as addition of a constant term k, a nonlinear term $kz|z|$ and replacing a system parameter by a function of chaotic state variables of a modified van der Pol system, are proposed, which can excite the existing of chaos of the originally non-chaotic system. The results are demonstrated by numerical results, i.e. bifurcation diagrams. The chaotic motion of the system has been obtained easily by choosing suitable feedback gains. It is found that those three methods are succeeded in exciting chaos of fractional order nano resonator system from periodic one for very low total fractional order 0.2.